In:
Synaptic Organization of the Brain
G.M. Shepherd, ed.
Oxford University Press, 2004

6

RETINA

PETER STERLING AND JONATHAN B. DEMB

The *retina* is a thin sheet of neural tissue lining the posterior hemisphere of the eye ball. It is actually part of the brain itself (≈0.5%), evaginating from the lateral wall of the neural tube during embryonic development. The *optic stalk* grows out from the brain toward the ectoderm, inducing it to form an optical system (cornea, pupil, lens), which projects a physical image of the world onto the retina. The retina's task is to convert this optical image into a "neural image" for transmission down the optic nerve to a multitude of centers for further analysis. The task is complex—which is reflected in the synaptic organization.

The transformation from optical to neural image involves three stages: (*1*) transduction of the image by *photoreceptors*; (*2*) transmission of these signals by excitatory chemical synapses to *bipolar neurons*; and (*3*) further transmission by excitatory chemical synapses to *ganglion cells*. Ganglion cell axons collect in the optic nerve and project forward to the brain. At each synaptic stage there are specialized laterally connecting neurons called *horizontal* and *amacrine* cells. These modify (largely by inhibitory chemical synapses) forward transmission across the synaptic layers. These elements are shown schematically in Fig. 6.1.

A closer look at this apparently simple design (three interconnected layers and five broad classes of neuron) reveals additional complexity (Figs. 6.2 and 6.3). Each neuron class is represented by several or many specific *types*. Each cell type is distinguished from others in its class by its characteristic morphology, connections, neurochemistry, and function (Rodieck and Brening, 1983; Sterling, 1983). This diversity, amounting to some 80 cellular types (Kolb et al., 1981; Sterling, 1983; Vaney, 1990; Masland, 2001), was puzzling at first, but a broad explanation has gradually emerged: it is impossible to encode all the information in an optical image using a single neural image. Therefore, the retina uses different cell types to create parallel circuits for simultaneous transmission of *multiple neural images* to the brain. The retina also creates separate circuits for different light levels—daylight, twilight, and starlight—but these share certain circuit components and use the same final pathways to the brain (Smith et al., 1986).

This chapter describes key cell types and their interconnection in parallel circuits. It also discusses how the functional architecture of a circuit depends on the functional architecture of its synapses. Finally, it suggests how the flow of visual information

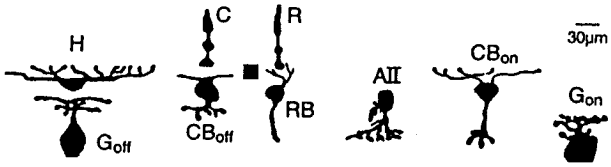

Fig. 6.1. Neuronal elements of the mammalian retina (same scale as diagrams for other regions). Symbols are defined in legend for Fig 6.2.

shifts between circuits that are specialized for different light levels and how the circuits are switched. The chapter focuses on mammalian retina because that is where the combined knowledge of circuitry and cell physiology is best known. Early efforts centered on cat, so specific measurements, counts, etc. cited here refer to cat central retina. However, efforts have broadened to include rabbit, guinea pig, rat, mouse, monkey, and human. These demonstrate strongly conserved patterns in the circuitry, as well as special adaptations, and some of both are mentioned.

NEURONAL ELEMENTS

INPUT ELEMENTS: RECEPTORS

Photoreceptors are elongated (Fig. 6.4). The distal tip points toward the back of the eye, away from the light, and is embedded in folds of melanotic epithelium. The outer

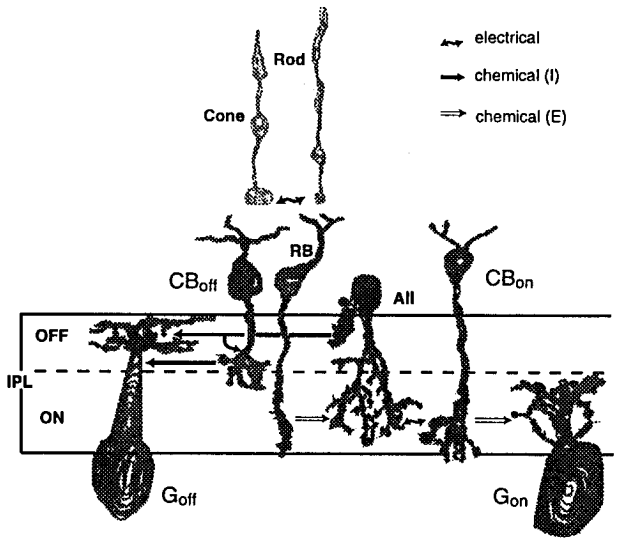

Fig. 6.2. Neuronal elements, scale enlarged in the vertical axis, to show more clearly the cell morphology and layers. Inputs: rod and cone photoreceptors. Principal neurons: ON and OFF ganglion cells (G_{on}, G_{off}). Intrinsic neurons: rod bipolar (RB) and cone bipolar (CB) neurons; horizontal (H), and amacrine neurons (A). IPL, inner plexiform layer. AII designates a specific type of amacrine cell that serves the starlight circuit (see text).

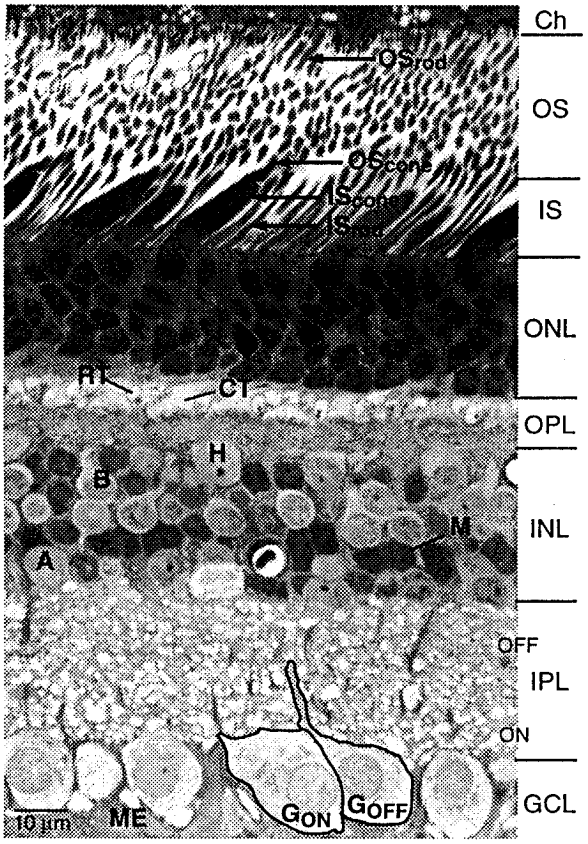

Fig. 6.3. Radial section through monkey retina about 5 mm (≈25 degrees) from the fovea. Here, cone and rod inner segments are easily distinguished from each other, as are their terminals in the outer plexiform layer. Pigmented cells of the choroid layer (Ch) attach the active form of vitamin A (aldehyde) to opsin and return it to the outer segment. Pigment cells also phagocytose membrane discs, shed daily from the outer segment tips. Abbreviations: OS, outer segments; IS, inner segments; ONL, outer nuclear layer; CT, cone terminal; RT, rod terminal; OPL, outer plexiform layer; INL, inner nuclear layer; IPL, inner plexiform layer; GCL, ganglion cell layer; B, bipolar cell; M, Müller cell; H, horizontal cell; A, amacrine cells; ME, Müller end feet; G_{ON}, ON ganglion cell; G_{OFF}, OFF ganglion cell. [Light micrograph from N. Vardi.]

segment contains about 900 membranous discs, stacked perpendicular to the cell's long axis (Fig. 6.4B). The disc surface is densely packed with molecules of the photopigment rhodopsin, at nearly 60,000 per disc (reviewed in Pugh and Lamb, 1993). The inner segment is filled with mitochondria. These fuel the ion pumps essential for transduction and raise the refractive index, thereby creating a wave-guide that traps photons and funnels them to the outer segment (Enoch, 1981).

The region of the photoreceptor, between the inner segment and the soma, contains the usual machinery for protein synthesis and packaging. Because the soma is stouter than the inner segment (which packs densely with its neighbors), the somas pile up

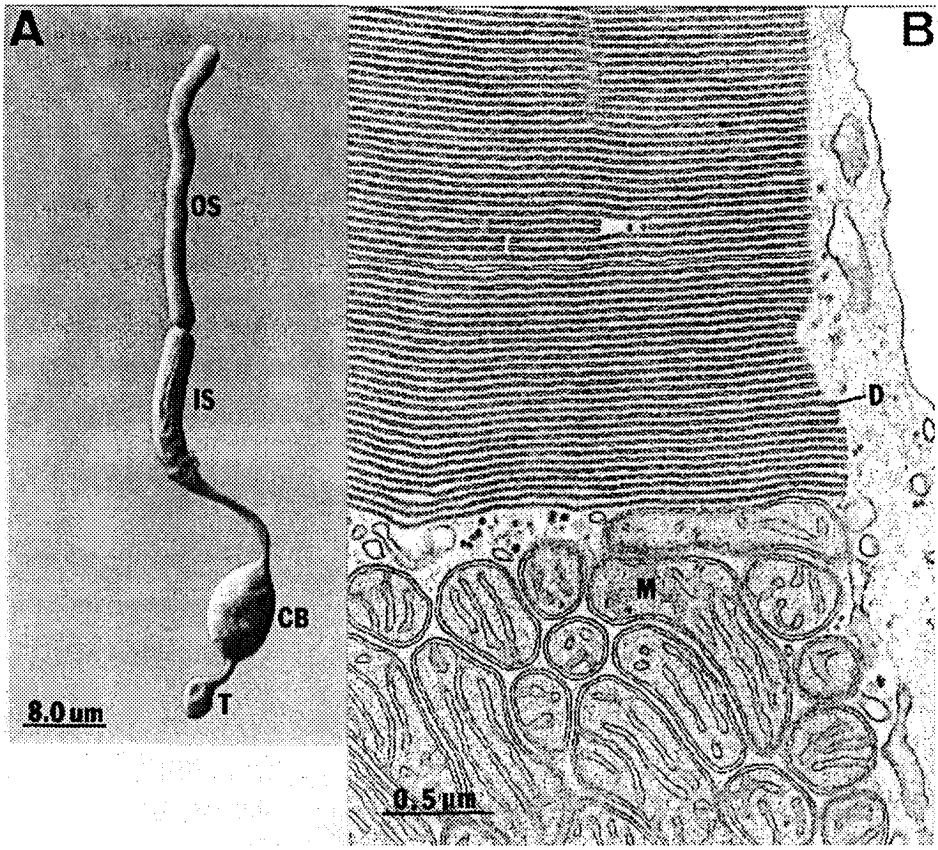

Fig. 6.4. **A:** Isolated rod photoreceptor (rabbit) showing the cell's distinct regions. Light micrograph. **B:** Radial section through rod outer/inner segment junction (salamander) showing regularly spaced membraneous discs (D) and densely packed mitochondria (M). Abbreviations: CB, cell body; T, terminal. [Electron micrographs from Townes-Anderson et al., 1985, 1988, with permission.]

in tiers (outer nuclear layer; see Fig. 6.3). The photoreceptor axon is generally short, 50 μm or less, except those in the fovea, where extremely dense packing of cones leaves no room for connections to the second- and third-order neurons. A foveal cone axon can be as long as 500 μm (Polyak, 1941; Schein, 1988; Hsu et al., 1998). The photoreceptor axon ends, without branching, in a single, highly specialized synapse that contains one or more synaptic "ribbons" (see Figs. 6.4 and 6.13).

Intensity Range. Light intensity in the natural environment varies over a range of about 10^{10}, and we can see over this entire range. Two types of receptor divide the range: rods for night and cones for day. In mammals both have a narrow outer segment: 1- to 2-μm diameter for the rod and 3- to 5-μm diameter for the cone. This ensures a small cytoplasmic volume, which is essential to a rapid response time, and this is suited to the rapid image motion generated by rapid movements of the organism. By comparison, the

rod of sluggish amphibians has a 5-fold greater diameter (25-fold greater volume) and partly as a consequence is 10-fold slower (Pugh and Lamb, 1993). So, if our photoreceptors were large, sports such as baseball or tennis would be out of the question.

A narrow outer segment limits the number of photons that a receptor can collect within an "integration time." A rod integrates photon signals over about 300 ms (Yau, 1994), yet starlight presents it with only 1 photon per 10 minutes! So even when the light is 2000 times brighter, there is still only 1 photon per rod per integration time. Thus, from dusk to dimmest starlight the rod detects single photons and needs to transmit only a *binary signal*: 0 or 1 photon. The task of transmitting this irreducibly simple message shapes the circuit design at all stages proximal to the outer segment. For example, the rod axon is extremely thin (0.25 μm diameter), and the synaptic terminal is small, with a single ribbon synapse (see Figs. 6.4 and 6.13).

A cone integrates photon signals over about 50 ms. During this interval, twilight (with color just barely discernible) delivers about 10^2 photons per cone, and bright sun delivers about 10^5 photons per cone (Schnapf et al., 1990). Thus, a cone integrates many photons to give a *graded signal* with good temporal resolution. The cone, having much more information to transmit than a rod, employs a thicker axon (1.6 μm diameter) and a larger terminal with many ribbon synapses (see Fig. 6.13). At dusk, as light intensity drops below cone threshold (marked by loss of color perception), the rod is collecting up to 10^2 photons per integration time. Thus, over a modest range (2 log units of intensity), the rod produces a graded signal that fills in for the failing cone. This graded rod signal for twilight is routed differently from the binary signal for starlight (see Circuits, later).

Spectral Sensitivity. Mammals have a single type of rod (peak sensitivity at $\approx$500 nm). This makes sense because at night photons are too sparse to be worth segregating by wavelength. But in daylight, there are plenty of photons, so most mammals gain extra information by using two cone types with different spectral sensitivity (Barlow, 1982). Most cones (at least 90%) are tuned to middle wavelengths (peak at $\approx$550 nm), termed "M" or *green* (reviewed in Jacobs, 1993). A few are tuned to short wavelengths (peak at $\approx$450 nm), termed "S" or *blue*. Because S cones can be distinguished by morphology and by antibody labeling, we know that they form a sparse but regular mosaic (de Monasterio et al., 1981; Szél et al., 1988; Ahnelt et al. 1990; Curcio et al., 1991). These anatomical methods confirm psychophysical maps of punctate sensitivity to S cone stimuli (Williams et al., 1981). S cones connect via a selective circuit to a special type of ganglion cell (see Circuits, later).

Old World primates (including humans) are special in being "trichromatic," meaning that there is an additional cone type tuned to long wavelengths (peak at $\approx$570 nm), termed "L" or *red*. The M and L cone pigments are nearly identical except for a few critical amino acids in the transmembrane region, so antibodies have not yet distinguished them (Neitz et al., 1991). Spectral sensitivity mapped for cone populations in situ shows M and L cones in monkey and human to distribute randomly in clusters. M and L cones in humans distribute differently across an individual retina and differ greatly between individuals—with surprisingly little effect on color vision (Roorda and Williams, 1999; Brainard et al., 2000; Neitz et al., 2002). How these cones connect to ganglion cells is naturally of great interest and is presently

controversial (Dacey, 1996; Calkins and Sterling, 1999; Martin et al., 2001; Reid and Shapley, 2002).

Some animals using three cone pigments, such as fish, turtles, and birds, may express up to seven types of cone! This trick is accomplished by fitting the inner segment with an oil droplet of specific color/absorbance (red, yellow/ultraviolet [UV]). These serve as filters to limit the spectral composition of the light entering the outer segment (e.g., Ohtsuka, 1985). Also, evolution tunes cone pigments to match the environment's spectral content. For example, Lake Baikal is very clear and deep, but longer wavelengths fail to penetrate at greater depths. Consequently, fish species at greater depths shift their cone pigments down the spectrum (Bowmaker et al., 1994). Equally wonderful in its vision capability is the kestrel (a falcon), which has a cone type tuned to UV (≈350 nm). Soaring high with this receptor, it can identify the urine trails of its prey (meadow vole), which in sunlight fluoresce UV (Viitala et al., 1995).

INTRINSIC ELEMENTS FOR FORWARD TRANSMISSION: BIPOLAR AND AII CELLS

Bipolar Cells. Bipolar somas occupy the middle region of the inner nuclear layer (see Fig. 6.3). Their dendrites ascend to collect synapses from photoreceptors. One bipolar type collects only from rods, and most other types collect only from cones. However, one bipolar type in rodent retina receives chemical synaptic input directly from both rods and cones (Soucy et al., 1998; Hack et al., 1999; Tsukamoto et al., 2001). Bipolar axons descend to the inner plexiform layer where they provide ribbon synapses, each directed at a pair of postsynaptic processes, termed a *dyad* (see later; Dowling and Boycott, 1966).

The rod bipolar soma (7 μm diameter) is located high in the outer nuclear layer (Fig. 6.5). The narrow, candelabra-like, dendritic arbor penetrates the stratum of cone terminals to reach the overlying rod terminals where it collects signals from 20 rods in cat, 15–45 in human, and up to 80 rods or more in rabbit (Boycott and Dowling, 1969; Dacheux and Raviola, 1986; Young and Vaney, 1991). The rod bipolar axon descends without branching to the deepest stratum of the inner plexiform layer where it contacts not ganglion cells, but a third-order, intrinsic neuron, termed the *AII* amacrine cell (see Fig. 6.2; Kolb and Famiglietti, 1974; McGuire et al., 1984; Freed et al., 1987; Strettoi et al., 1990; Wässle et al., 1991). The cat rod bipolar terminal employs 30 ribbon synapses, with little variation within or between animals (McGuire et al., 1984; Rao and Sterling, 1991).

The cone bipolar somas are also small (≈8 μm), and the dendritic fields are narrow (≈15 μm; Fig. 6.6). The dendritic arbor typically collects signals from 5–10 overlying cone terminals without skipping any (Cohen and Sterling, 1990a,b; Boycott and Wässle, 1991; Calkins and Sterling, 1996). An exception is the S cone bipolar cell, which *does* skip overlying M and L cones to contact S cones exclusively (Mariani, 1984; Kouyama and Marshak, 1992). The S cone bipolar cell has been defined clearly in monkey and probably corresponds to the wide-field cone bipolar in cat and other mammals that also skips certain cones (e.g., type b_5, Fig. 6.6). Cone bipolar axons descend to the inner plexiform layer, where each type selects a particular stratum and contacts both amacrine and ganglion cells (Fig. 6.6). Cone bipolar teminals employ 30–130 ribbon synapses, depending on cell type (Cohen and Sterling, 1990b; Calkins et al., 1994; Tsukamoto et al., 2001).

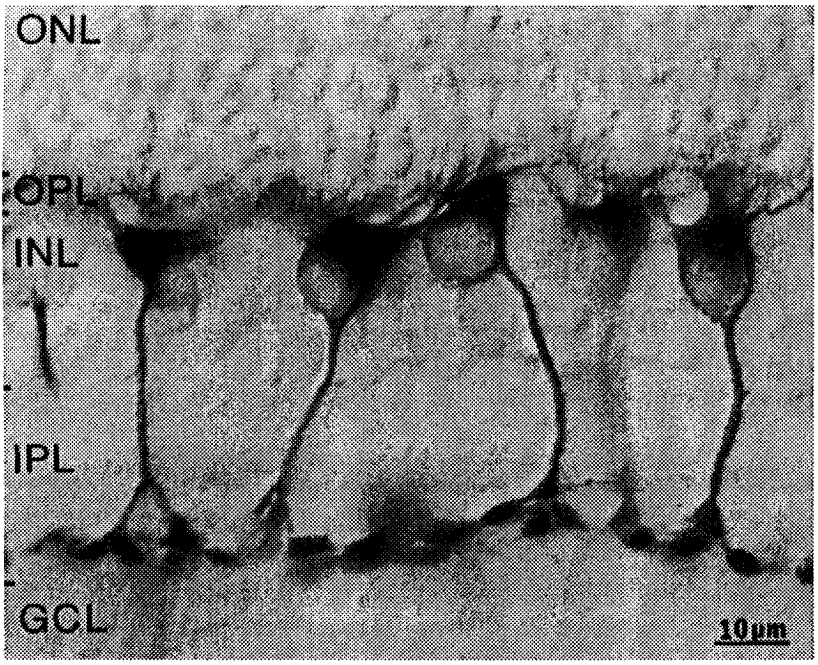

Fig. 6.5. Rod bipolar array (rabbit) immunostained for protein kinase C. Dendrites of adjacent cells overlap modestly in OPL, but axon terminals simply "tile" the deepest level of the IPL without overlap. [Light micrograph from Young and Vaney, 1991, with permission.]

ON vs. OFF Bipolar Types. It was discovered early that some bipolar cells are excited (i.e., depolarized) by light onset, whereas others are excited by light offset (Werblin and Dowling, 1969; Kaneko, 1970). How the cone synapse manages to drive these cells in opposite directions is explained later (see Fig. 6.15). Here we note that the two categories of axon terminate at different levels: OFF axons arborize in the upper half of the inner plexiform layer, and ON axons arborize in the lower half (see Fig. 6.2). Within these OFF and ON regions, multiple types segregate in different strata (see Fig. 6.6; Kolb et al., 1981; Cohen and Sterling, 1990b; Boycott and Wässle, 1991; Euler et al., 1996). It was unexpected that ON and OFF bipolar cells would comprise so many types (≈4 or 5 types for each category). Because all types (except for the S cone bipolar cell) collect from the same cones, their spatial and spectral inputs are identical. Therefore, one surmises that they carry different *temporal* components of the cone signal. Indeed, two types of ON bipolar cell do differ temporally, some depolarizing sustainedly to steady illumination, and others depolarizing transiently (Saito et al., 1985; Dacey et al., 2000; Euler and Masland, 2000).

AII Cell. The AII soma in the amacrine cell layer sends a thick stalk to the ON level of the inner plexiform layer where it arborizes richly to collect chemical synapses from rod bipolar terminals (see Fig. 6.2; Kolb and Famiglietti, 1974; Vaney, 1985; Sterling et al., 1988; Strettoi et al., 1990; Mills and Massey, 1999). This arbor also forms nu-

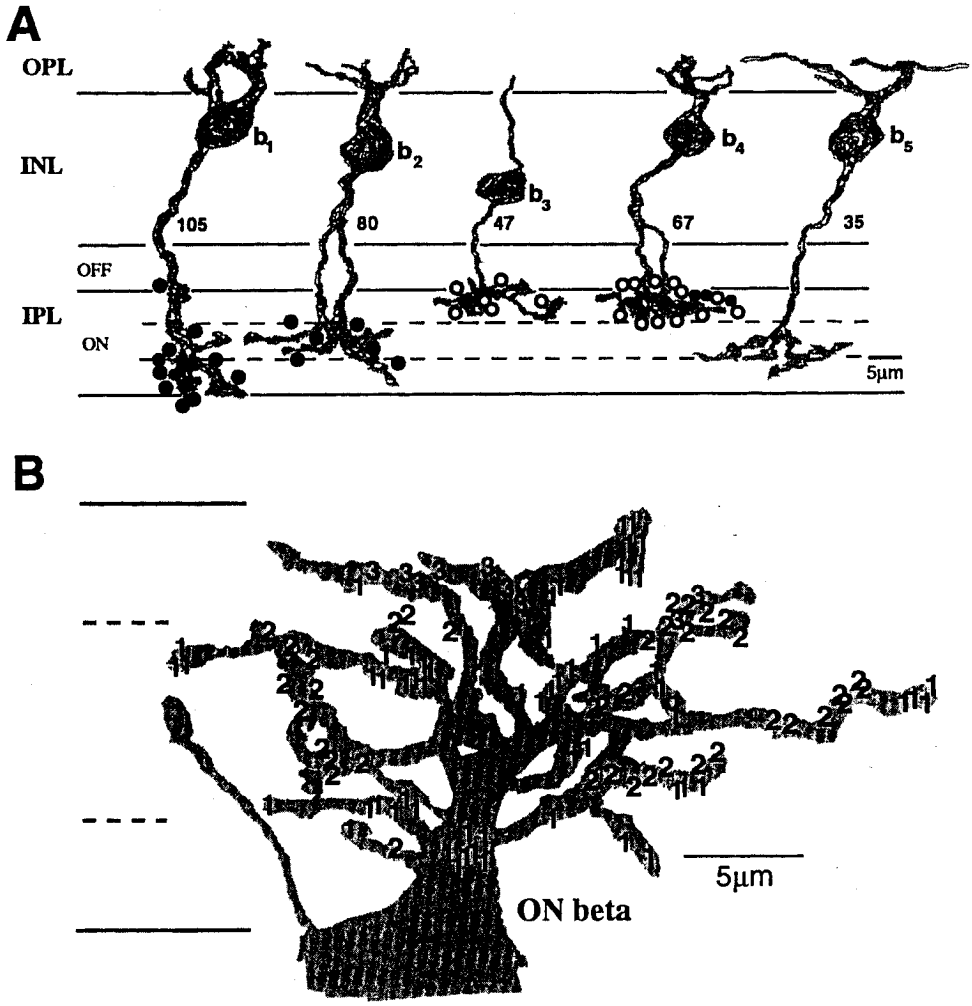

Fig. 6.6. **A:** Multiple types of ON cone bipolar cell with axons in the ON region of the IPL. Each type expresses a different number of ribbon outputs (noted at the right of each axon) and a different pattern of gap junctions (filled circles, CB–AII; open circles, CB–CB). Types b_1 – b_4 collect from all the overlying cones without skipping any; type b_5 ignores the immediately overlying cones and reaches widely to collect from outlying cones. [Reconstructions from Cohen and Sterling, 1990a,b.] **B:** ON beta ganglion cell arborizes among all types of ON cone bipolar axon, but collects ribbon synapses from only three types (b_1, b_2, b_3) in the proportion 80:40:20. [From Cohen and Sterling, 1992, with permission.]

merous, large gap junctions with the axon terminals of ON cone bipolar cells. When these gap junctions are in a conducting state, rod bipolar excitation spreads from AII into the cone bipolar terminals, evoking their transmitter release onto ganglion cells (see Fig. 6.21). The AII also forms "lobular appendages" at the OFF level of the inner plexiform layer. These structures, which are jammed with mitochondria and synaptic

vesicles, provide inhibitory chemical synapses to OFF bipolar terminals and OFF ganglion cell dendrites (McGuire et al., 1984; Kolb and Nelson, 1993). This wiring explains how a single type of rod bipolar cell can simultaneously excite the ON and inhibit the OFF ganglion cells (Mastronarde, 1983; Sterling, 1983).

OUTPUT ELEMENTS: GANGLION CELLS

Ganglion cell bodies form the innermost cellular layer of the retina (see Figs. 6.2 and 6.3). Their dendrites penetrate the inner plexiform layer to collect excitatory synapses from bipolar axons and both excitatory and inhibitory synapses from amacrine cells. Ganglion cell axons enter the optic nerve and extend to the brain. The domestic cat optic nerve contains about 160,000 axons (260,000 for its wild progenitor; Williams et al., 1993b); the human nerve contains about 1.2 million axons, and the macaque optic nerve contains about 1.8 million axons (Potts et al., 1972). Because the number of fibers in the optic nerve can vary 10-fold, it does not seem to be a physical "bottleneck" for information outflow as was commonly thought. Thus, the reason that many cones converge onto a single ganglion cell is not to reduce the number of transmission channels in the nerve but rather for deeper reasons to which we shall return.

Ganglion cell somas look pretty much alike (see Fig. 6.3), but Golgi impregnations revealed the dendritic arbors to be remarkably diverse—on the order of 20 types (e.g., Polyak, 1941; Boycott and Dowling, 1969; Cajal, 1972; Boycott and Wässle, 1974; Kolb et al., 1981). Now that one can record data from a ganglion cell *in vitro* and render its dendritic arbor visible by injecting dye, we realize that each morphological type has a distinctive physiology. For example, the ganglion cell with a planar, "loopy" dendritic arbor responds selectively to stimuli moving in a particular direction (see Fig. 6.11C; Amthor et al., 1989a). This specific structure–function correspondence was first shown in rabbit but also holds for cat, and probably also for primate (Berson et al., 1998, 1999; Isayama et al., 2000). Thus, a ganglion cell type carrying a particular sort of information can (like a gene) be conserved across species.

Each type of ganglion cell distributes to a particular brain region, which uses the special information carried by that cell. Thus, the nucleus of the optic tract, which controls optokinetic eye movements, collects from the directionally selective ganglion cell (Pu and Amthor, 1990). And the suprachiasmatic nucleus, which uses light to reset circadian rhythms, collects from another type that branches over extremely wide areas. This ganglion cell type is unusual because it expresses its own visual pigment, melanopsin, and thus monitors light levels independently of the rods and cones (Berson et al., 2002; Hattar et al., 2002). Still other types of motion-selective ganglion cell project to the superior colliculus—which uses the information to orient the head and eyes (Rodieck and Watanabe, 1993; Berson et al., 1998, 1999; Isayama et al., 2000). Such subcortical "house-keeping" centers use about 40% of the cat's ganglion cells. But these cells have small somas ($\approx$10 μm) and fine axons (0.3 μm diameter), so they occupy less than 5% of the optic nerve cross section. Similar *numbers* of house-keeping ganglion cells are required in primates, but their *proportion* of all ganglion cells is much smaller—due to the high density of midget cells (see later; Rodieck et al., 1993).

The key region for mammalian visual processing is the striate cortex, which receives its main thalamic input from the dorsal lateral geniculate nucleus. Thus, it is to this nucleus that most ganglion cells project (60% in cat; 90% in monkey). Two major

classes of ganglion cell in cat are geniculate-bound: "beta" and "alpha" cells (Fig. 6.7) (Boycott and Wässle, 1974;, Wässle et al., 1981a,c; Stein et al., 1996). The beta cell has a narrow, bushy dendritic tree and a sustained (tonic) discharge of action potentials to a maintained stimulus (Figs. 6.2 and 6.7). The alpha cell has a wider, sparser dendritic tree and a transient (phasic) discharge (Cleland and Levick, 1974; Stone and Fukuda, 1974; Saito, 1983). The beta and alpha cells are each of two types, one with dendrites in the ON strata of the inner plexiform layer and the other with dendrites in the OFF strata (Fig. 6.7) (Famiglietti and Kolb, 1976). The former are excited by light onset; the latter are excited by light offset (Fig. 6.7) (Nelson et al., 1978). Thus, they are termed ON beta, OFF beta, ON alpha, and OFF alpha.

The primate retina expresses a similar division into ON and OFF versions of narrow-field, tonic cells and wider-field, phasic cells (e.g., de Monasterio, 1978). The narrow-field types are termed *midget cells* because in central retina the dendritic arbor collects from a midget bipolar cell with input from a single cone (Polyak, 1941; Kolb and Dekorver, 1991; Calkins et al., 1994), but more peripherally the arbor broadens to collect from many midget bipolar axons (Watanabe and Rodieck, 1989; Dacey, 1993; Goodchild et al., 1996b). Midget cells are also termed "P" cells because they project to the lateral geniculate's parvocellular layers. The wider-field cells are morphologically diverse (Polyak, 1941; Boycott and Dowling, 1969). Some are termed *parasol* because of their broad, flat dendritic arbors. These are also termed "M" cells because they project to the geniculate magnocellular layers (Perry et al., 1984; Watanabe and Rodieck, 1989). However, other types of wide-field ganglion cell probably also project to the magnocellular layers, so the term *M cell* probably includes diverse types (e.g., Kaplan and Shapley, 1982; Shapley and Perry, 1986).

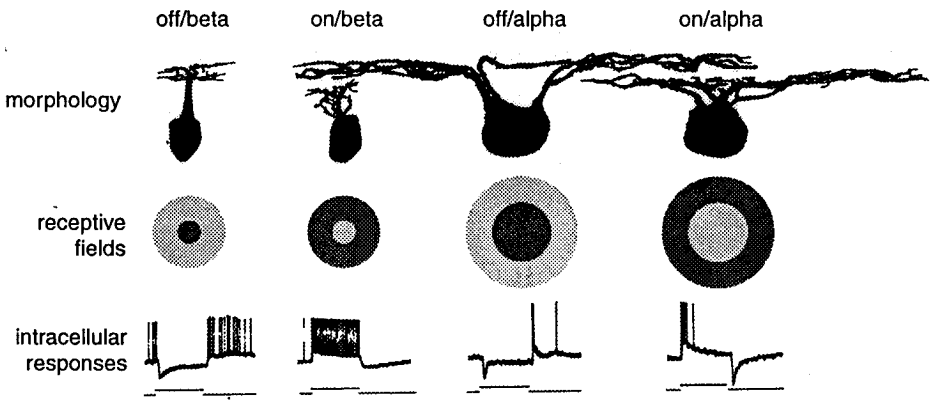

Fig. 6.7. Form and function of cat ganglion cells. Beta cells have a narrow dendritic field, and alpha cells, a broad one (top row, vertical views). Cells are maximally excited by stimuli covering the whole dendritic field, corresponding to the *receptive* field "center" and maximally supressed by stimuli filling the outer annulus, termed the receptive field "surround" (middle row, tangential views). ON cells, excited by *in*creased intensity on the center, arborize deep in the inner plexiform layer; OFF cells, excited by *de*creased intensity on the center, arborize superficially. Beta cells give a transient plus sustained response; alpha cells give mainly a transient response. [Intracellular recordings from Saito, 1983.]

Over a decade of intense description, physiologists divided ganglion cells into different functional categories: Y (brisk-transient), X (brisk-sustained), and W (other, including edge-detector, directionally sensitive, etc.). Simultaneously, morphologists categorized ganglion cells by dendritic branching patterns: alpha (planar-radiate), beta (3-D-bushy), and gamma (other, including planar-sparse, planar-loopy, etc.). It was quickly appreciated that functional categories might map onto the morphological ones, but to prove this directly by recording followed by tracer injection required almost another decade (e.g., Saito, 1983). This correspondence of structure to function in ganglion cells is now firmly established as a principle of retinal organization, and consequently a type can be named for its function (e.g., directionally sensitive; see Fig. 6.11C) or its morphology without any confusion (see Fig. 6.7). However, when a category is named for its central projection, such as M or P, one must remember that several types can project to the same locus. Thus, one expects multiple types of M and P cell (Amthor et al., 1989a,b; Dacey and Lee, 1994).

INTRINSIC ELEMENTS FOR LATERAL TRANSMISSION: HORIZONTAL AND AMACRINE CELLS

Horizontal Cells. Horizontal cell somas form the upper tier of the inner nuclear layer (see Fig. 6.3), and the processes connect exclusively within the outer plexiform layer. Collecting widely from receptors, their main task is to average the signals and feed negatively back onto receptor terminals and forward onto bipolar dendrites. Horizontal cells couple to each other electrically. The strength of this coupling changes with adaptive state and is modulated by dopamine secreted by certain cells in the amacrine layer (reviewed in Weiler et al., 2000).

Two types of horizontal cell in diurnal mammals connect with cones (Fig. 6.8). One has thick dendrites, a wide field and couples strongly to its neighbors; the other has thin dendrites, a narrow field and couples weakly (Mills and Massey, 1994; Peichl and Gonzalez-Soriano, 1994; Vaney, 1994a; Sandmann et al., 1996). Generally, each type connects to all the cone terminals in its dendritic field. However, in primate the large-field cell avoids S cones, and the narrow-field cell connects especially strongly to them (Dacey, et al., 1996; Goodchild et al., 1996a; see also Sandmann et al., 1996). Within this general framework are some quite spectacular morphological variations whose functions remain mysterious (see, e.g., Müller and Peichl, 1993).

One of the two types of horizontal cell connects with rods. It does so by emitting a fine axon that in cat meanders for several millimeters and then breaks into an elaborate arbor that contacts several thousand rods (see Fig. 6.8). This axon also couples to its neighbors and thus pools signals from tens of thousands of rods (Vaney, 1993). This is not the usual sort of axon because it lacks action potentials; further, cone input to the dendrites does not reach the rod axon arbor, so it must be electrically isolated from the soma (Nelson, 1977). On the other hand, the horizontal cell soma *does* receive strong rod signals (e.g., Steinberg, 1969; Nelson, 1977; Lankeet et al., 1996), which must therefore come via rod-to-cone gap junctions (Raviola and Gilula, 1973; Kolb, 1977; Smith et al., 1986). Thus, the soma serves metabolically two processes with utterly different connections. It does not seem to matter which type of horizontal cell produces the axon, because in cat and rabbit it is the wide-field cell and in primate it is the narrow-field cell (reviewed in Sandmann et al., 1996).

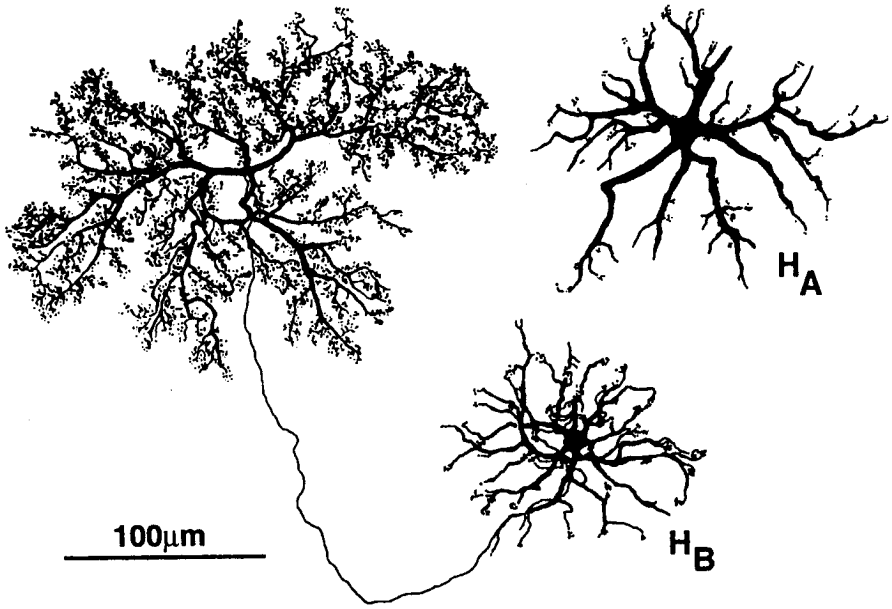

Fig. 6.8. Two types of horizontal cell from cat retina as seen in tangential view following Golgi impregnation. Dendrites of types A and B both connect with cones; axon arbor of type B connects with about 3000 rods. [From Kolb, 1974, with permission.]

Amacrine Cells. Amacrine somas form the lower tier of the inner nuclear layer and are also numerous in the ganglion cell layer, where they are called *displaced.* Amacrine cells connect exclusively within the inner plexiform layer (plus some synapses in the ganglion cell fiber layer) and are diverse in the extreme; there are about 40 types (Kolb et al., 1981; MacNeil and Masland, 1998; Vaney, 1990). Given such diversity, attempts to generalize are likely to be inadequate, but consider the following:

1. The AII amacrine, being narrow-field, distributes densely and thus constitutes about 20% of the amacrine layer cells (see Fig. 6.2). As noted, the AII collects purely from rod bipolars and serves a feedforward link in the rod's starlight pathway.
2. Certain narrow-field amacrines collect purely from cone bipolar terminals. These amacrines feed back reciprocally onto the bipolar terminal and forward onto the ganglion cell (see Fig. 6.14). These types, which exist as both ON and OFF forms, must distribute densely to tile the plane (Polyak, 1941; Kolb et al., 1981). This pattern of connection may reflect lateral inhibition across a small spatial scale covering tens of microns rather than hundreds as for the horizontal cells.
3. Certain medium-field amacrines collect from cone bipolars and arborize intimately with dendrites of certain ganglion cell types. For example, the starburst amacrine cell associates with other members of its own type to form a loopy pattern that in rabbit associates with dendrites of the direction-selective ganglion cell

(Fig. 6.9A; Tauchi and Masland, 1984; Vaney et al., 1989a; Famiglietti, 1992a), and in cat, the alpha ganglion cell (Vardi et al., 1989). The starburst cell is also present in primate, where it probably associates with the co-planar arbors of parasol ganglion cells (Rodieck, 1989; Jacoby et al., 1996). There are separate starburst populations for the ON and OFF levels of the inner plexiform layer. The starburst cell responds phasically to glutamatergic bipolar input (kainate receptors; Linn et al., 1991) and releases a pulse of acetylcholine onto the ganglion cells (Masland et al., 1984; Massey and Redburn, 1985). The acetylcholine, binding to nicotinic receptors, excites ganglion cells (e.g., Schmidt et al., 1987; Kaneda et al., 1995). Thus, the starburst circuit probably boosts ganglion cell transient responses, enhancing sensitivity to motion. Several studies suggest that the starburst cell fires action potentials (Bloomfield, 1992; Jensen, 1995; Cohen, 2001), but other studies report purely passive responses (Taylor and Wässle, 1995; Zhou and Fain, 1995; Peters and Masland, 1996).

4. Certain types of wide-field amacrine connect exclusively to rod bipolar cells (cat A17; Nelson and Kolb, 1985; rabbit S1, S2, Vaney, 1986; Sandell and Masland, 1986; Li et al., 2002), but other wide-field types arborize in strata supplied only by cone bipolar terminals. The "dendritic" fields reach about 500 to 1000 μm—probably near the electrotonic limit for fine, passive cables (see Fig. 6.9C; Dacey, 1989a, 1990; Famiglietti, 1992b). However, the proximal region of each dendrite sprouts a fine axon that travels centrifugally for at least 3 mm (Fig. 6.9B). Such a cell resembles a wagon wheel, with the dendritic field for a hub and the axons as radiating spokes (Fig. 6.9C). These axons conduct full action potentials (Dacheux and Raviola, 1995; Freed et al., 1996; Stafford and Dacey, 1997), which appear to travel centrifugally (Cook and Werblin, 1994). Long-range amacrine cells mediate the inhibition and excitation of certain ganglion cells evoked by stimuli millimeters beyond the conventional receptive field (e.g., McIlwain, 1966; Derrington et al., 1979; Cook et al., 1998; Demb et al., 1999; Taylor, 1999).

Interplexiform Cells. These cells have somas in the amacrine layer but send processes to both outer and inner plexiform layers (Cajal, 1972). The interplexiform cell receives synapses only on its inner processes but provides synaptic outputs in both the inner and outer plexiform layers. In cat, it forms chemical synapses upon both rod bipolar and cone bipolar dendrites (Kolb and West, 1977; Nakamura et al., 1980; McGuire et al., 1984; Cohen and Sterling, 1990b), and in fish it contacts horizontal cells (Dowling, 1986). Some authors refer to the interplexiform as a "sixth cell class," but it seems equally reasonable to consider it as one more extraordinary type of amacrine cell.

The interplexiform cell in New World monkey and fish contains dopamine (Dowling, 1986). In cat, the dopaminergic amacrine cell also sends sporadic processes to the outer plexiform layer (Oyster et al., 1985). Because dopamine regulates horizontal cell coupling (Piccolino et al., 1984; Teranishi et al., 1984; Hampson et al., 1992; reviewed in Weiler et al., 2000), which shapes the inhibitory surround of cones and bipolar cells (see Fig. 6.17), the dopamine cell may adjust the surround's depth and extent to ambient image statistics. Cat and rabbit interplexiform cells use γ-aminobutyric acid (GABA) and contact bipolar dendrites, so they probably have a different function.

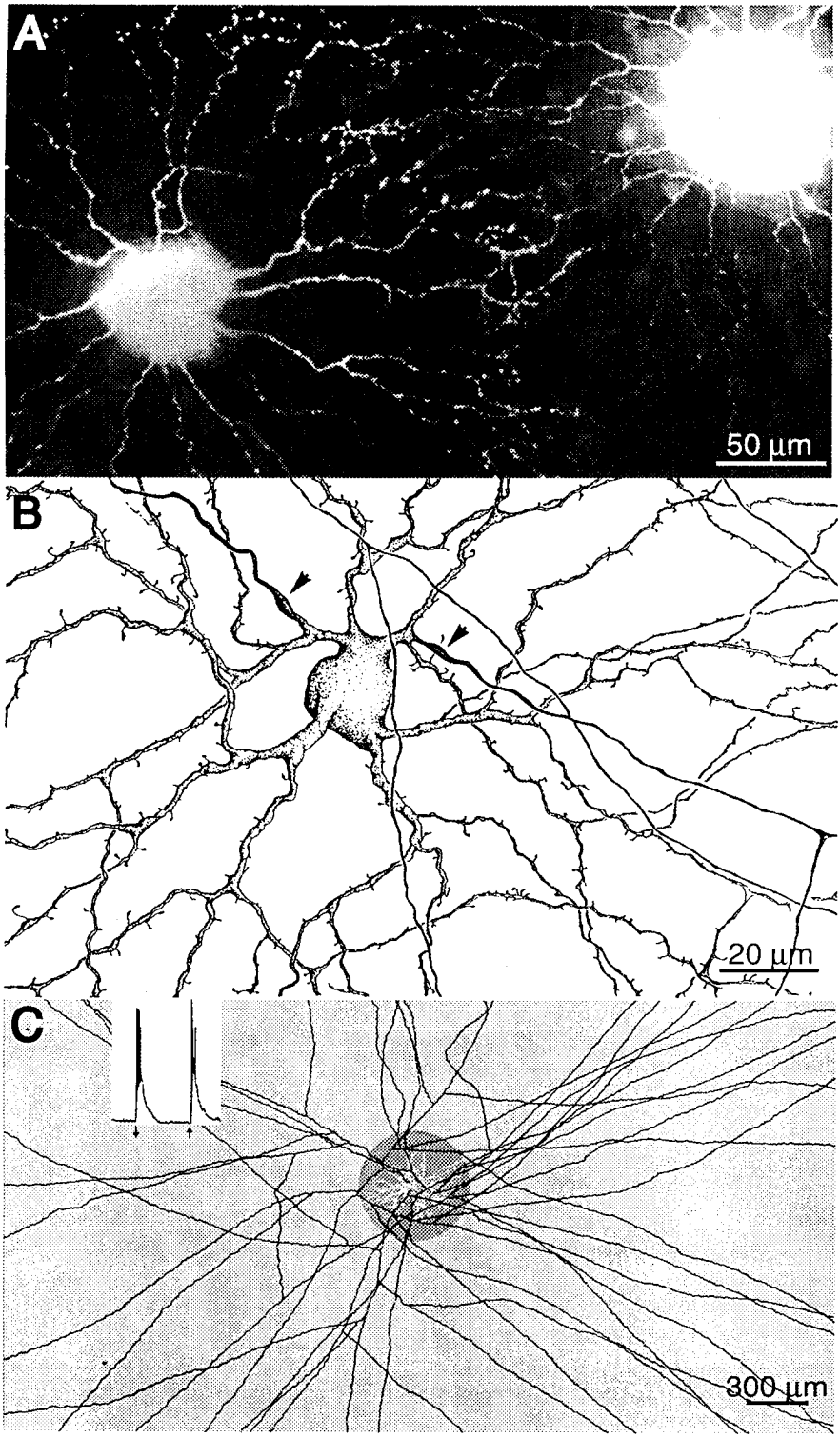
A
50 µm
B
20 µm
C
300 µm

Centrifugal Fibers. Specific brain regions in certain vertebrates, including fish, amphibia, reptiles, and birds, produce efferent axons that travel in the optic nerve to terminate in the inner retina. In birds, the isthmo-optic nucleus, a substantial structure with a definite retinotopic organization, projects about 10,000 fibers centrifugally to the inner retina to terminate on a special type of amacrine cell (Dowling and Cowan, 1966; Uchiyama and Ito, 1993). In fish, the olfactory bulb sends fibers containing a peptide luteinizing hormone–releasing hormone (LHRH) to contact interplexiform cells (Zucker and Dowling, 1987). Thus, the idea is not entirely far fetched that an odor, a memory, or a feeling could modify the construction of a visual image in the retina—that beauty could be literally in the eye of the beholder. However, little is known regarding the function of these centrifugal pathways (Uchiyama and Barlow, 1994).

Glial Cells. The retina contains a single, highly stereotyped glial cell, termed the *Müller cell.* Its cell body, recognized by its dark cytoplasm and polygonal shape, lies in the deeper tiers of the inner nuclear layer (INL) (see Fig. 6.3). Processes extend from this cell outward to reach the choroid layer and inward to ensheath the ganglion cells and terminate as "endfeet" at the vitreal surface (Fig. 6.3). Thus, each Müller cell spans the full thickness of the neural retina. One important consequence is that the cell accumulates potassium from the extracellular space (where it is released through neuronal activity) and then, by concentrating most of its potassium channels in its endfeet that abut the vitreous, the cell can siphon off excess potassium into the vitreous (Newman, 1986, 1987).

Another critical function of the Müller cell is to regenerate a *cis*-form of the visual pigment 11-*cis*-retinal, which the cone can convert to 11-*cis*-retinol for use in transduction (Mata et al., 2002). This reaction within the Müller cell, relative to the alternate pathway for regenerating retinol within the pigment epithelial cells, is 20-fold faster (to match the cone's high rate of bleaching). Rods cannot convert retinal to retinol, so they rely exclusively on the slower regenerating pathway within the pigment epithelial cells. Because rods are 20-fold more numerous than cones, this critically conserves the active form for use by cones.

CELL POPULATIONS

Spatial Density of Receptors. Cones and rods pack densely, occupying 90% of the two-dimensional receptor sheet with a residual extracellular space of about 10% (Fig. 6.10) (Packer et al., 1989). Animals active in both day and night, such as human, macaque, cat, and rabbit, assign about 5% of their receptors to cones and the rest to rods. If this seems counterintuitive, simply recall that the photon flux in daytime is many orders of

Fig. 6.9. Two types of amacrine cell in tangential view. **A:** Medium-field, "starburst" amacrine cells. Processes from adjacent cells associate to form a planar network with input from cone bipolar ribbon synapses and output to motion-sensitive ganglion cells, including the alpha and directionally selective ganglion cells. **B:** Wide-field amacrine cell whose proximal dendrites (spiny) emit multiple axons (arrowheads). **C:** Same cell at lower magnification. Cell fires transient burst of action potentials (inset) to ON and OFF of a stimulus to receptive field center (black disc) which corresponds to the dendritic field; action potentials travel centrifugally from the cell in all directions. [**A** from Tauchi and Masland, 1984; **B** and **C** from Stafford and Dacey, 1997.]

magnitude greater than that at night. Therefore, in daytime, the retina can operate effectively on a fraction of the photons striking the receptor sheet, whereas from dusk to dawn, every photon counts.

Cone density always peaks in central retina. Species whose lifestyle requires high spatial acuity, such as raptors scanning for prey from great heights or primates foraging for fine morsels at close range, pack cones so densely at the center (*fovea*) that rods are completely excluded (see Fig. 6.10). Each cone connects to a private (*midget*) bipolar cell followed by a midget ganglion cell, and this provides a neural image at the output as fine as the *grain* of the cone array. In human fovea, cone density reaches nearly 200,000/mm^2, providing 120 cones/degree, which is adequate to create a neural image of a grating as fine as 60 cycles/degree (Fig. 6.10; Curcio et

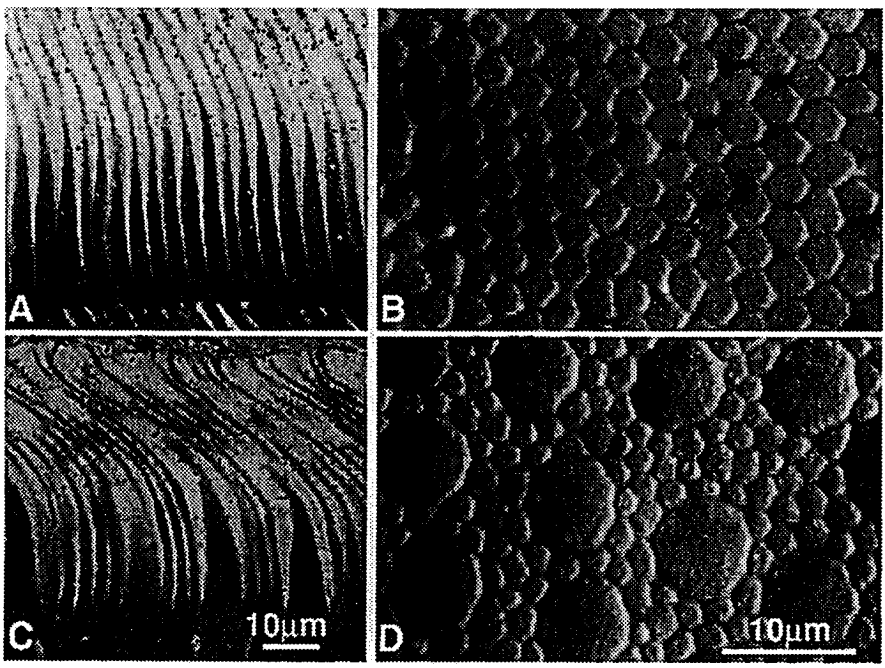

Fig. 6.10. Mosaic of photoreceptors (human). **A:** Fovea: radial section shows cone inner segments to be narrow and gently tapered, and the outer segments to be long and fine. **B:** Fovea: tangential section through base of inner segments shows hexagonal packing. Thus, fovea provides fine spatial sampling in daylight, but absence of rods renders it useless in twilight and starlight. **C:** Periphery: vertical section shows cone inner segments to be squatter but still tapered and surrounded by rod inner segments that are much finer and untapered. **D:** Periphery: tangential view shows about 10 rods per cone, which can boost the cone signal in twilight (see text). Although cones comprise only 10% of the mosaic, their apertures occupy 40% of available collecting area. This is advantageous in daylight when the cones need photons. Then the pupil narrows to accept only photons arriving parallel to the optical axis. These are efficiently captured by the cone's wave-guide mechanism. But the system also works at night, when the rods need photons. Now the pupil dilates to admit photons over a wide range of angles. These are poorly captured by the cone's wave-guide and thus escape to neighboring rods. [Light micrographs from Curcio et al., 1990.]

al., 1990; Williams, 1992; Smallman et al., 1996). In the eagle's fovea, cone density and spatial acuity are about double this, apparently reaching a biophysical limit. A higher cone density would require a still finer inner segment, with a wave-guide mechanism that could no longer prevent photons from escaping to a neighboring cone (Reymond, 1985).

Naturally once light intensity falls below cone threshold, the fovea, lacking rods, becomes a blind spot. It is easy to convince yourself of this. At dusk, just as your perception of color fades completely, note that you have also lost the ability to read fine print (as in *The New York Times*). Now hold your thumb at arm's length and, as your gaze steadies upon it, watch it disappear. At this distance, the thumb subtends about 1 degree on the retina, corresponding to the fovea's rod-free region. Thus, while your eyes are free to move, vision seems entirely normal and you do not suspect that 10^6 cones (and consequently about one quarter of your striate cortex) have been silenced (Baseler et al., 2002). Species that can accept somewhat coarser vision in daylight but need central acuity at night reduce cone density at the center to accommodate rods. Thus, cat cone density is almost 10-fold lower than human's in the central area (30,000/mm^2), and this allows for rods at 200,000/mm^2 (Williams et al., 1993b). Rod density commonly peaks at about 15–25 degrees from the center (Packer et al., 1989; Curcio et al., 1990; Young and Vaney, 1991; Williams et al., 1993b).

Toward the periphery receptor density declines, but receptor diameter generally increases. For example, in macaque retina (20–80 degrees) rod collecting increases about 2-fold, so that the total photon collecting area remains about constant; the same is true for cones (see Fig. 6.10D; Packer et al., 1989). This would make sense if the optical light gathering efficiency declines toward the periphery, because then a larger receptor could still collect enough light to fill its dynamic range. Such factors must be considered in comparing densities. For example, peak rod density is about 2-fold greater in cat than in human (400,000/mm^2 vs. 175,000/mm^2; e.g., Curcio et al., 1990; Williams, et al., 1993b), but the cat rod's collecting area is smaller by about the same factor. Thus, in terms of photon collecting area, these densities may be equivalent. One reason to make the cat rod finer is that the cat's eye collects more light (larger pupil, reflecting tapetum, etc.); therefore, a finer cross section allows the rod to serve as a single photon detector over a wider intensity range.

Spatial density of different cone types also varies with retinal location. For example, the very center of human retina, termed *foveola*, includes M and L, but not S, cones (Williams et al., 1981; Curcio et al., 1990). This makes functional sense because, when middle and long wavelengths are in sharp focus, short wavelengths are strongly blurred (Williams et al., 1993a). Therefore, to provide maximum spatial acuity, the foveola sacrifices trichromacy. In guinea pig and rabbit, S cones distribute sparsely in superior retina but densely in inferior retina, presumably because inferior retina views the sky (Röhlich et al., 1994). In mouse, there may be only a single cone type that co-expresses both a UV pigment and a middle wavelength (M) pigment (Lyubarsky et al., 1999; Applebury et al., 2000). Cones in inferior retina express mostly UV pigment, whereas those in superior retina express mostly M pigment (Szél et al., 1992; Applebury et al., 2000).

That photoreceptor density is so finely sculpted across the retina implies an efficient postreceptoral circuitry. Such local sculpting could evolve only if the small trades of

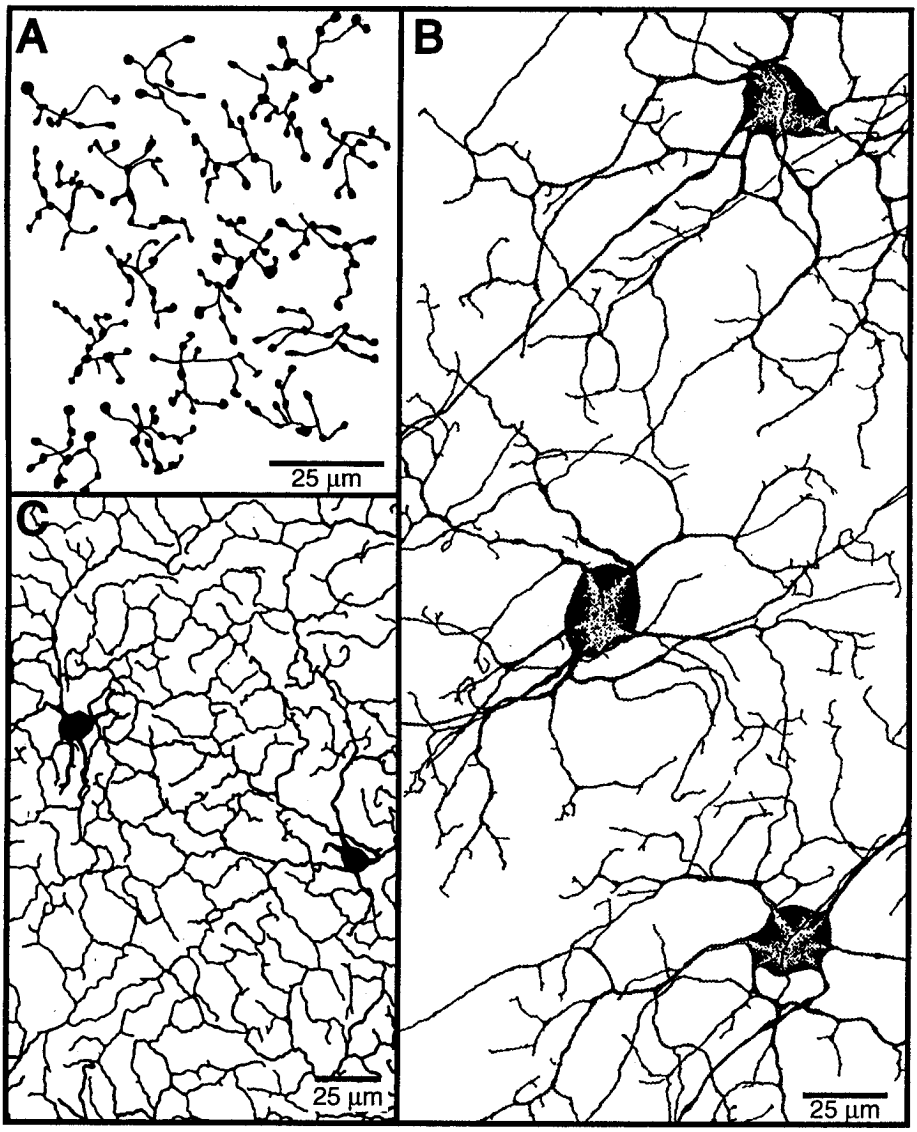

Fig. 6.11. **A:** Array of OFF midget bipolar terminals (macaque) in tangential view. Drawn from tissue immunostained for recoverin, about 10 mm beyond the fovea. The terminals "tile" the plane without overlap. **B:** Array of ON midget ganglion cells (human) in tangential view. Cells injected individually with neurobiotin, about 12 mm beyond fovea. The dendrites tile the plane without overlap and would collect input from many axons in the midget bipolar array shown in **A**. **C:** Array of directionally selective ganglion cells (only the OFF dendrites of the ON/OFF type are shown). One cell was injected with neurobiotin which then spread to adjacent cells. Note the characteristic "loopy" dendrites that tile the plane without overlap. Such tiling behavior holds for all ganglion cells studied so far, with one exception discussed in the text. [**A** from Wässle et al., 1991; **B** from Dacey, 1993; **C** from D. Vaney after Vaney, 1994.]

collecting area between rods and cones at each locus offered a selective advantage. For any such trade, the effect on signal-to-noise (S/N) ratio for photon capture would be proportional to the square root of the fractional change in area (Rose, 1973). For example, a 2-fold increase in cone collecting area would improve S/N for the cone system by at most 1.4-fold. But if subsequent neural stages that process these signals added noise by this factor or more, then any potential advantage of such a difference would be swamped. This alerts one to identify in the postreceptoral circuitry the key contribution to efficient (non-noisy) processing (see Functional Circuits, later).

Spatial Density of Postreceptoral Neurons. Postreceptoral cell types also distribute with characteristic spatial density (Wässle and Riemann, 1978). This has been determined by standard histological methods, by reconstruction from electron micrographs (e.g., Sterling et al., 1988; Cohen and Sterling, 1990b), and by immunostaining for a particular protein or epitope that fortuitously selects a particular type and stains the whole array. Thus, antibody to protein kinase C reveals the complete rod bipolar cell array (see Fig. 6.5; Young and Vaney, 1991); anti-Go_α shows the ON cone bipolar cells (Vardi, 1998), anti-recoverin shows OFF midget bipolar cells (Fig. 6.11A) (Milam et al., 1993; Wässle et al., 1994); anti-CCK shows S cone bipolars (Kouyama and Marshak, 1992); anti-calbindin shows the wide-field horizontal cells in cat and rabbit (Röhrenbeck et al., 1989); and anti-calretinin shows the AII amacrine cells (Wässle et al., 1995; for a review, see Hendry and Calkins, 1998). Also, because many cell types couple to their neighbors in the array, intracellular injection of a small tracer molecule, such as neurobiotin, has been used to establish the spatial densities (Figs. 6.11C and 6.12).

The spatial density of postreceptoral neurons follows the photoreceptors in peaking centrally and declining toward the periphery. As spatial density falls, a cell's dendritic tree expands to compensate, so "tiling," or a specific degree of overlap (see later), is maintained (see, e.g., Wässle et al., 1978b, 1981a,c). However, the number of neurons

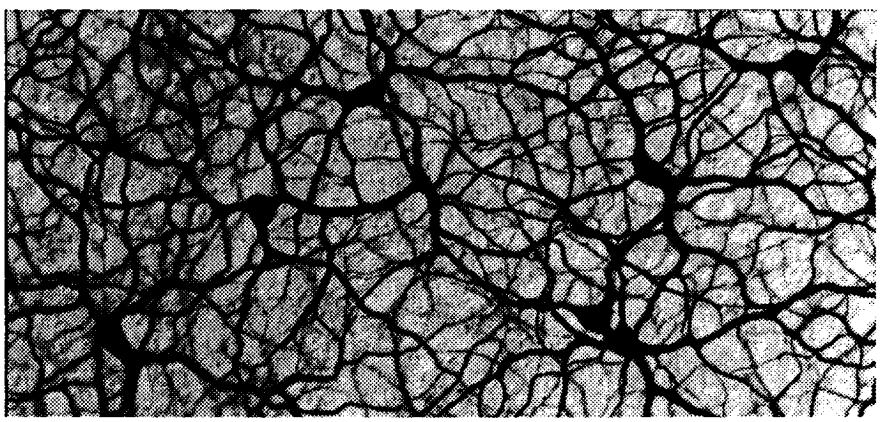

Fig. 6.12. Array of type A horizontal cells (rabbit) in tangential view. One cell was injected with neurobiotin, which then spread through gap junctions to reveal the whole array. Not the characteristic of this array: stout cables, strong coupling, and extensive overlap (cf. Fig. 6.12). [From S. Mills, after Mills and Massey, 1994.]

converging upon a particular cell type may increase or remain constant. For example, rods converging onto the rod bipolar cell increase from about 15 in macaque central retina to about 60 in the periphery, whereas the number of cones converging upon a given type of cone bipolar cell remains constant at 5–10 (Grünert et al., 1994). Photoreceptors converging upon a ganglion cell increase linearly. For example, about 35 cones converge upon a central beta cell, but 180 cones converge on a peripheral beta cell (Tsukamoto et al., 1990).

The Finest Ganglion Cell Array Sets Visual Acuity. Spatial resolution is set by the finest sampling array at the retinal output. To discriminate the fine lines of a grating from a homogeneous field requires one ganglion cell for each dark or bright line (Tsukamoto and Sterling, 1991; reviewed in Wässle and Boycott, 1991; Smallman et al., 1996). In the fovea, because a midget ganglion cell connects to only one cone, resolution corresponds to the cone sampling frequency. But outside the fovea, many cones converge on a midget ganglion cell (see Fig. 6.11B; Dacey, 1993), so resolution is set by the midget cell array. Similarly in cat, resolution is set by the beta cell array. Because pairs of ON and OFF of the same cell class (e.g., midget, beta) sample the same territory (see Fig. 6.15), resolution is set by the density of one of these arrays but not by their combined density (reviewed in Wässle and Boycott, 1991).

Tiling vs. Overlap of Neuronal Arbors. Along the *forward pathways from cones*, the neuronal arbors of a given type do not overlap. Instead they show mutual avoidance, also termed "territoriality" (Wässle et al., 1981a,b,c). Consequently, their fields tend to tile the plane of the retina, forming a quasi-regular meshwork (Panico and Sterling, 1995). This rule holds for dendrites of each cone bipolar type and for their axon terminals (see Fig. 6.11A; Cohen and Sterling, 1990a,b; Boycott and Wässle, 1991.

Ganglion cell dendritic fields also tile. This has been shown for the alpha cell and delta cell in cat (Dann et al., 1988; Dacey, 1989b), for the ON-OFF directionally selective ganglion cell in rabbit (see Fig. 6.11C; Vaney, 1994b), and for parasol and midget ganglion cells in primate (see Fig. 6.11B; Dacey and Brace, 1992; Dacey, 1993). The lattice structures formed by presynaptic cone bipolar axon arbors complement the postsynaptic ganglion cell dendritic arbors (cf. Fig. 6.11A vs. Fig. 6.11B). This connects the two arrays reliably while minimizing cost in materials and the volume occupied by the lattices (Panico and Sterling, 1995).

Overall, a cone terminal, being narrower than the bipolar dendritic field, contributes most of its synapses to one member of each bipolar array and a few synapses to some neighbors (Sterling, et al., 1988; Cohen and Sterling, 1990a). Similarly the cone bipolar axon arbor is narrower than the ganglion cell dendritic field so each bipolar contributes most of its synapses to one ganglion cell (cf. Fig. 6.6A vs. Fig. 6.6B; Fig. 6.11A vs. Fig. 6.11B). Consequently, a cone signal diverges very little on its course toward the retinal output, so each cone contributes most of its synaptic output to one member of a ganglion cell array (Sterling et al., 1988).

Along the *forward pathways from rods*, certain neural arbors *do* overlap. Thus, dendrites of neighboring rod bipolars overlap enough that every rod synapse, although approximating a point in the plane of the retina, contacts at least two bipolar cells (see Fig. 6.5; Sterling et al., 1988; Young and Vaney, 1991). Similarly, the AII cell's col-

lecting arbor in the inner plexiform layer overlaps more extensively, by 2- to 3-fold in central retina of cat, rabbit, and monkey and up to 10-fold in peripheral retina of rabbit (Vaney, 1985; Sterling et al., 1988; Vaney et al., 1991; Wässle et al., 1995). Thus, although the rod bipolar axon arbors tile without overlap (see Fig. 6.5; Sterling et al., 1988; Young and Vaney, 1991), the circuit leading from one rod diverges markedly (Sterling et al., 1988; Vardi and Smith, 1996).

Along *lateral pathways*, a given cell type does not show simple territorial behavior; instead, it overlaps with its neighbors, and sometimes they actually associate. Horizontal cell processes overlap enough that each retinal locus is "covered" by the arbors of 3–8 cells (Wässle et al., 1978a; Röhrenbeck et al., 1989). Furthermore, where horizontal cell processes of a given type cross each other, they form gap junctions and thus couple electrically. This holds for both the wide-field and narrow-field horizontal cells that connect with cones and for the axon arbors that connect to rods; thus, using both chemical and electrical synapses, these systems diverge extensively. Experimentally, this is convenient because a small tracer molecule injected into one neuron can reveal much of the network (see Fig. 6.12; Mills and Massey, 1994; Vaney, 1994a).

Wide-field amacrine cells behave similarly: their processes cross each other extensively and couple. Thus, although their somas distribute sparsely, their processes and synapses distribute densely, forming a rather fine meshwork (Masland, 1986; Dacey, 1989a; Vaney, 1990). Certain narrow-field amacrine cells are labeled by neurobiotin injected into an alpha or a parasol ganglion cell (Dacey and Brace, 1992; Vaney, 1994a; Xin and Bloomfield, 1997). Thus, coupling in lateral pathways is not limited to wide-field types, nor invariably to members of the same type.

The massive evidence of extensive cytoplasmic coupling between neurons is sobering in historical perspective. One hundred years ago, debate was fierce as to whether neurons were coupled ("reticularism") or entirely separate ("neuronism"). The two schools, led respectively by Camillo Golgi and Santiago Ramon y Cajal, heaped scorn upon each other and refused to consider seriously each other's observations. For about 50 years, it seemed that Cajal and the "neurone doctrine" had triumphed. But now it is clear that Cajal jumped to conclusions well beyond the resolution of the light microscope. Further, the drawings by reticularists, such as Dogiel (see Vaney, 2002), of apparently coupled ganglion cells may well have reflected spread of tracer (methylene blue) between coupled cells.

The starburst amacrine cell (both ON and OFF types) forms a different and distinctive pattern. The spatial densities are intermediate and their arbors are medium-field, so each retinal locus is covered by about 80 arbors. Yet, the individual processes do not cross each other but instead associate in bundles, thus forming a coarse, quasi-regular meshwork (see Fig. 6.9A).

Foveal Architecture Implies "Pursuit" Eye Movements. The foregoing aspects of retinal architecture reflect the broad central nervous system strategy for sensory surfaces: specialize one region to "sample" finely and assign a relatively large volume of brain to analyze the data. Concurrently, render the specialized surface mobile and evolve "attentional" mechanisms to allow the organism to select which region of the environment to analyze. In the primate retina, about half of the cones and ganglion cells are concentrated in the fovea, and a quarter of striate cortex is devoted to the fovea (re-

viewed in van Essen et al., 1992; Baseler et al., 2002). Apparently the fovea occupies only its fair share of cortex, i.e., in proportion to the ganglion cells that it contributes (Schein, 1988; Wässle et al., 1989). Although this has been disputed (Azzopardi and Cowey, 1993), it seems parsimonious to think that the brain allots computational space proportional to the information content of the input. Therefore, to devote more space than warranted purely by ganglion cell density would seem, *prima facie*, a poor investment.

The strategy of using the central retina for fine spatial sampling requires "smooth pursuit" eye movements to stabilize an object of interest upon the center. This minimizes motion in the image, reducing the need for central ganglion cells to code temporal information. But however, conversely, this strategy *maximizes* image motion seen by peripheral ganglion cells (Eckert and Buchsbaum, 1993a,b). Thus, within a given cell type response properties should vary with retinal location. A cat beta cell or primate midget cell that fires tonically to stabilized stimuli in central retina should fire more transiently to moving stimuli in peripheral retina. This has been found experimentally (Cleland et al., 1971; de Monasterio, 1978) and may in part explain why peripheral ganglion cells collect from more cones (Tsukamoto et al., 1990)—the better to measure transient signals.

Spatial Density of Müller Cells (Glia). The peripheral primate retina contains two Müller cells for each cone; however, the fovea contains one Müller cell for each cone (Burris et al., 2002). Processes of several Müller cells coat the lateral surfaces of each foveal cone synaptic terminal, but these sheets form small windows to permit gap junctions between the pedicles and avoid the basal surface of the pedicle (Fig. 6.13) (Tsukamoto et al., 1992; Bürris et al., 2002). Müller cell processes express at high density transporters for glutamate, GABA, etc. Consequently, their three-dimensional relationship to the synapse is important—either for *facilitating* "spillover" at the base of the cone terminal (Haverkamp and Wässle, 2000) or for *preventing* spillover between adjacent terminals (Burris et al., 2002).

SYNAPTIC CONNECTIONS

OUTER PLEXIFORM LAYER

Ribbon Synapse. The photoreceptor's chemical synapse employs a synaptic ribbon. This is a flat organelle whose long axis anchors near the presynaptic membrane (see Fig. 6.13). Synaptic vesicles tether to both faces of the ribbon via short filaments, so vesicles along the ribbon's basal edge touch the presynaptic membrane. Here they appear to "dock" ready for release. This occurs when the photoreceptor depolarizes, admitting calcium through channels in the presynaptic membrane all along the region where the ribbon anchors (reviewed in Matthews, 1996; Morgans, 2001; Wässle, 2003). The elongated active zone docks about 5- to 10-fold more vesicles than at a conventional synapse, and, because a vesicle need move only 30 nm on the ribbon to reach an emptied docking site, the ribbon has long suggested a mechanism for rapid "reloading" (Rao-Mirotznik et al., 1995).

This idea is now supported by capacitance measurements on isolated cells and terminals. A vesicle fusing to the presynaptic membrane increases the capacitance by

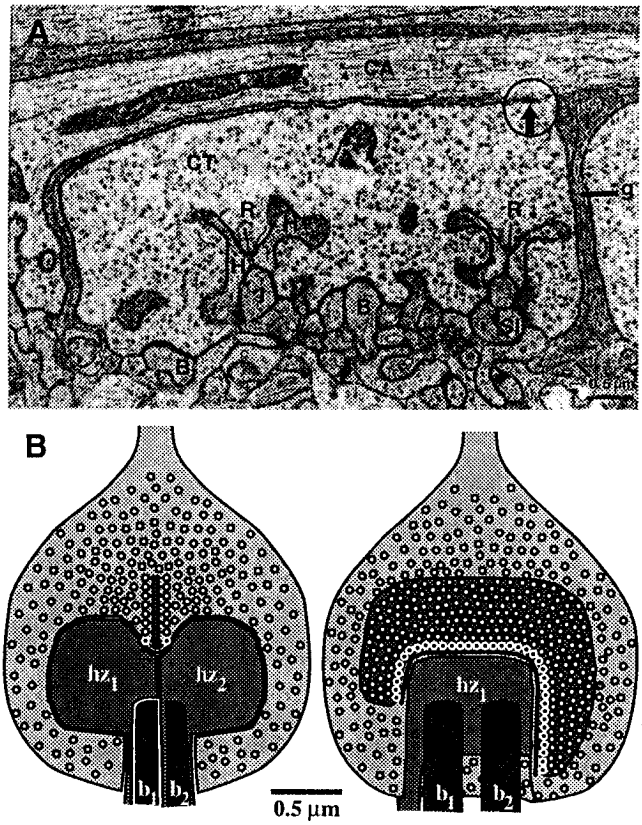

Fig. 6.13. **A:** Cone terminal in radial section (electron micrograph, macaque fovea). Two "triads" are present, each with a synaptic ribbon (r) pointing between two horizontal cell processes (H) toward an invaginating bipolar dendrite (IB). There are also "basal contacts" onto bipolar dendrites distant from the ribbon (B), and a gap junction (G) with the adjacent cone axon (CA). The complete terminal contains about 20 ribbon synapses. **B:** Rod terminal in orthogonal views (from three-dimensional reconstruction, cat central area). One ribbon points between two horizontal cell processes (hz) toward two rod bipolar dendrites (b). Note that bipolar dendrites are hundreds of nanometers distant from docked vesicles at base of ribbon. [**A** from Tsukamoto et al., 1992; **B** from Rao-Mirotznik et al., 1995.]

about 26 attoFarads (von Gersdorff and Matthews, 1994; von Gersdorff et al., 1996). When synchronous fusion of many vesicles is induced by a step depolarization, the increase in capacitance becomes measurable. Where the number of ribbon synapses is known, the peak fusion rate has been calculated at about 500 vesicles/ribbon/s (Parsons et al., 1994; von Gersdorff et al., 1996). Furthermore, the capacitance jump corresponds to the total number of vesicles tethered on all the ribbons in a terminal (von Gersdorff et al., 1996). These maximum evoked rates appear to represent the peak of the operating range, so normal rates may be more like 20–100 vesicles/ribbon/s (Rao et al., 1994b; Freed, 2000a,b). Indeed, a milder stimulus, raising intracellular calcium by 2 μM, fuses 400 vesicles/s in salamander rod, or about 50/s/ribbon (Townes-

Anderson et al., 1985; Rieke and Schwartz, 1996). A ribbon synapse outperforms a conventional synapse in both peak and sustained rates. A conventional synapse attains a peak rate of 150 vesicles/s (Borges et al., 1995) and a sustained rate of 20 vesicles/s (Borges et al., 1995; Stevens and Tsujimoto, 1995). The ribbon synapse appears to be present in all cases where transmitter release is modulated by graded potentials rather than spikes, probably because graded potentials permit much higher rates of information transfer (de Ruyter and Laughlin, 1996).

How the ribbon fascilitates rapid exocytosis is uncertain. The ribbon might serve as a "conveyor belt" along which vesicles move by a cytoplasmic motor. Indeed, such a motor, *kinesin*, is present on the ribbon (Muresan et al., 1999). But microtubules, the "tracks" for the kinesin motor, do not associate with the ribbon. Furthermore, the pool of vesicles equivalent to the number tethered to all the ribbons can be completely released when the patch electrode contains an ATP analog that is not hydrolyzed by kinesin (Heidelberger et al., 2002). Conceiveably, vesicles might move rapidly on the ribbon by passive diffusion—or simply be held in place and release their contents rapidly via "compound fusion," a mechanism used by certain neuroendocrine cells (Parsons and Sterling, 2003).

The rod terminal employs a single active zone with one ribbon and one invagination (see Fig. 6.13B). The invagination houses two types of postsynaptic process: horizontal cell spines and bipolar dendritic tips. The paired spines from overlapping horizontal cell axons penetrate deeply to place their glutamate receptors near the vesicle release site, within about 16 nm. The dendritic tips from two or more cells also penetrate but end quite far from the release sites, about 100–600 nm. In cross section, the invagination often seems to contain only three processes, so it was termed a "triad," but now we know that the invagination contains at least four processes (see Fig. 6.13B; Rao-Mirotznik et al., 1995). The crescent shape of the rod ribbon, its size (600 tethered vesicles), and the length of the active zone (130 docked vesicles) are all conserved across mammalian species.

The cone terminal employs multiple active zones, each with a ribbon and an invagination (see Fig. 6.13A). There are about 20 active zones per terminal in the fovea and 40 or more per terminal in the periphery (Ahnelt et al., 1990; Calkins and Sterling, 1996; Chun et al., 1996). Each invagination houses paired horizontal cell processes, one from a wide-field, the other from a narrow-field cell, and these penetrate deeply to end near the cone terminal's release sites (Fig. 6.13A; Kolb, 1970, 1974). One or two bipolar dendrites also invaginate at each active zone but less deeply, terminating 100–200 nm from the release sites (Fig. 6.13A; Kolb, 1970; Calkins and Sterling, 1996; Chun et al., 1996). The external, basal surface of the cone terminal forms symmetrical junctions termed *flat* or *basal* contacts with the tips of bipolar dendrites (Kolb, 1970; Calkins and Sterling, 1996; Haverkamp et al., 2000). All of the invaginating positions are occupied by ON bipolar dendrites, and many of the basal positions are occupied by OFF bipolar dendrites. The cone terminal membrane at the basal contacts bears neither a ribbon nor a conventional cluster of docked vesicles. Therefore, it was widely thought that ribbon synapses serve the ON dendrites by exocytosis and that basal synapses serve the OFF dendrites by some transmitter release mechanism yet to be identified (e.g., Kolb, 1994).

However, this simple rule does not hold. Many ON bipolar dendrites also receive basal contacts (Calkins and Sterling, 1996; Chun et al., 1996), and it becomes appar-

ent that the key functional difference between OFF and ON dendrites depends not on the junctional morphology but on which type of glutamate receptor they express. OFF bipolar cells express ionotropic glutamate receptors (iGluR), AMPA for one cell type and kainate for two other types (DeVries and Schwartz, 1999; Haverkamp et al., 2001a; Gruenert et al., 2002). ON bipolar cells express the metabotropic glutamate receptor, mGluR6 (Masu et al., 1995; Vardi et al., 2000a). Because iGluRs *open* a cation channel, whereas mGluR6 *closes* a cation channel, glutamate drives the membrane potentials of these cell classes in opposite directions. Despite the relatively huge distance from the vesicle release site to invaginating and flat bipolar dendrites (hundreds of nanometers), a single vesicle can still deliver pulses of transmitter in the 10 μM range by simple diffusion (Rao-Mirotznik et al., 1998). This concentration, which would be sustained for several milliseconds, corresponds to the effective concentrations for ON and OFF bipolar dendritic tips (de la Villa et al., 1995; Sasaki and Kaneko, 1996). Thus, a vesicle released at the ribbon synapse probably serves both invaginating and basal dendrites.

Nonribbon Synapses. Horizontal cell processes contain some small vesicles and in one case (human rod) clearly form conventional synapses onto the photoreceptor (Linberg and Fisher, 1988). However, this is the only known case, so it is uncertain whether GABA is released from horizontal cells via conventional vesicular mechanism or via a calcium-independent mechanism, such as a GABA transporter (Schwartz, 1987). The vesicular GABA transporter (vGAT) has been localized near the plasma membrane, suggesting a role in releasing GABA (Cueva et al., 2002; Jellali et al., 2002). In cold-blooded species the photoreceptor terminal is sensitive to GABA (e.g., Tachibana and Kaneko, 1984; reviewed in Piccolino, 1995), so one expects this as well in mammals. This has yet to be confirmed by physiology or immunocytochemistry, because antibodies to various subunits of $GABA_A$ and $GABA_C$ receptors do not stain the terminals. Cone bipolar dendrites do stain strongly for $GABA_A$ receptor just outside the invagination (Vardi and Sterling, 1994), and rod bipolar dendrites stain for $GABA_C$ receptor (Vardi and Sterling, 1994; Enz et al., 1996; Haverkamp et al., 2000). Physiologically, cone and rod bipolar dendrites express both a $GABA_A$ and a $GABA_C$ current, with a $GABA_A$-to-$GABA_C$ ratio of $\approx$4:1 (Shields et al., 2000). Therefore, horizontal cells may release transmitter diffusely along the interface between bipolar dendrites and photoreceptor terminals.

A few conventional synapses are present in the OPL. Mostly these are from GABAergic interplexiform processes onto bipolar dendrites (McGuire et al., 1984; Cohen and Sterling, 1990b). However, other transmitters may affect the OPL without benefit of conventional synapses. For example, the dopamine-containing processes ascending from the amacrine cell layer meander through the OPL without making conventional contacts. D_1 receptors are present in OPL (Veruki and Wässle, 1996; Nguyen et al., 1997; Koulen, 1999), and dopamine potently uncouples horizontal cell gap junctions (DeVries and Schwartz, 1989; Hampson et al., 1994; Xin and Bloomfield, 1999; He et al., 2000; reviewed in Weiler et al., 2000). In short, there is ample evidence here for "paracrine" effects of a transmitter (Witkovsky et al., 1993).

Gap Junctions. Electrical synapses (gap junctions) are present at three critical sites in the OPL. First, each cone terminal couples to its immediate neighbors via relatively

small junctions (see Fig. 6.13A). For example, each terminal in primate fovea is estimated to have 10–100 connexons (the multimeric channel that forms the junction) with its neighbors (Raviola and Gilula, 1973; Tsukamoto et al., 1990; DeVries et al., 2002). Second, each rod terminal forms a gap junction with each of two neighboring cone terminals (Kolb, 1977; Smith et al., 1986). Because there are about 20 rods for every cone, a cone must couple to about 40 rods (Sterling et al., 1988). These junctions feed rod signals into the cone terminal (Nelson, 1977; Schneeweis and Schnapf, 1995, 1999). Third, there are numerous, extensive gap junctions between horizontal cells. Wide-field cells couple and narrow-field cells couple, but the two types do not cross-couple (Mills and Massey, 1994; Vaney, 1994a).

INNER PLEXIFORM LAYER

The sole input to this layer derives from bipolar axon terminals. These form ribbon synapses, but the ribbons are generally smaller and more numerous than in a photoreceptor terminal. For example, compared with a rod ribbon's 600 vesicles with 130 docked, a rod bipolar terminal has relatively few vesicles—only 100 with 20 docked (Rao and Sterling, 1991). The rod bipolar terminal (cat) contains about 30 ribbons, whereas a cone bipolar terminal can contain more than 100 ribbons. The number of ribbons is distinctive for a given cell type at a given eccentricity and is highly regular, varying at most by 10% (McGuire et al., 1984; Cohen and Sterling, 1990b; Calkins et al., 1994; Tsukamoto et al., 2001).

The bipolar terminal does not invaginate, so one ribbon synapse cannot accommodate many postsynaptic processes. Instead, two postsynaptic processes align on either side of the linear active zone, forming a *dyad* (Fig. 6.14) (Dowling and Boycott, 1966). The postsynaptic elements at a dyad can be two ganglion cell dendrites, two amacrine processes, or one of each. Often, the amacrine process feeds back a conventional synapse onto the bipolar axon, in which case it is called a *reciprocal* synapse (e.g., Calkins and Sterling, 1996; Freed et al., 2003). Each bipolar type expresses a specific pattern. For example, the rod bipolar dyad always includes one process from an AII amacrine and another from a small subset of different amacrine types. The AII *never* gives a reciprocal synapse at the rod bipolar dyad, but the other amacrine types *always* do. Beta ganglion cell dendrites are *never* found at the rod bipolar dyad, but alpha cell dendrites are present at about 1 dyad of 30 (McGuire et al., 1984; Freed et al., 1987; Freed and Sterling, 1988).

Lateral connections in the IPL use conventional chemical synapses and gap junctions. Amacrine cells are the sole source of conventional synapses (Dowling and Boycott, 1966). Synaptic vesicles are invariably round, and presynaptic and postsynaptic densities show symmetrical thickening. Therefore, synapses cannot be classified as excitatory or inhibitory based on morphology. Commonly in cold-blooded (small-brained) animals, conventional synapses are arranged such that adjacent processes contact each other serially in long sequences (Dubin, 1976). These sequences might perform complex, local computations. However, the underlying circuits have not yet been worked out, and their actual function is unknown.

An electrical synapse is present at five classes of connection in the IPL. First, it interconnects certain types of cone bipolar cell, both homotypically (b_4–b_4) and heterotypically (b_3–b_4; Cohen and Sterling, 1990b). Second, it couples particular types of amacrine cell homotypically, such as the AII and wide-field types (Vaney, 1994b). Third,

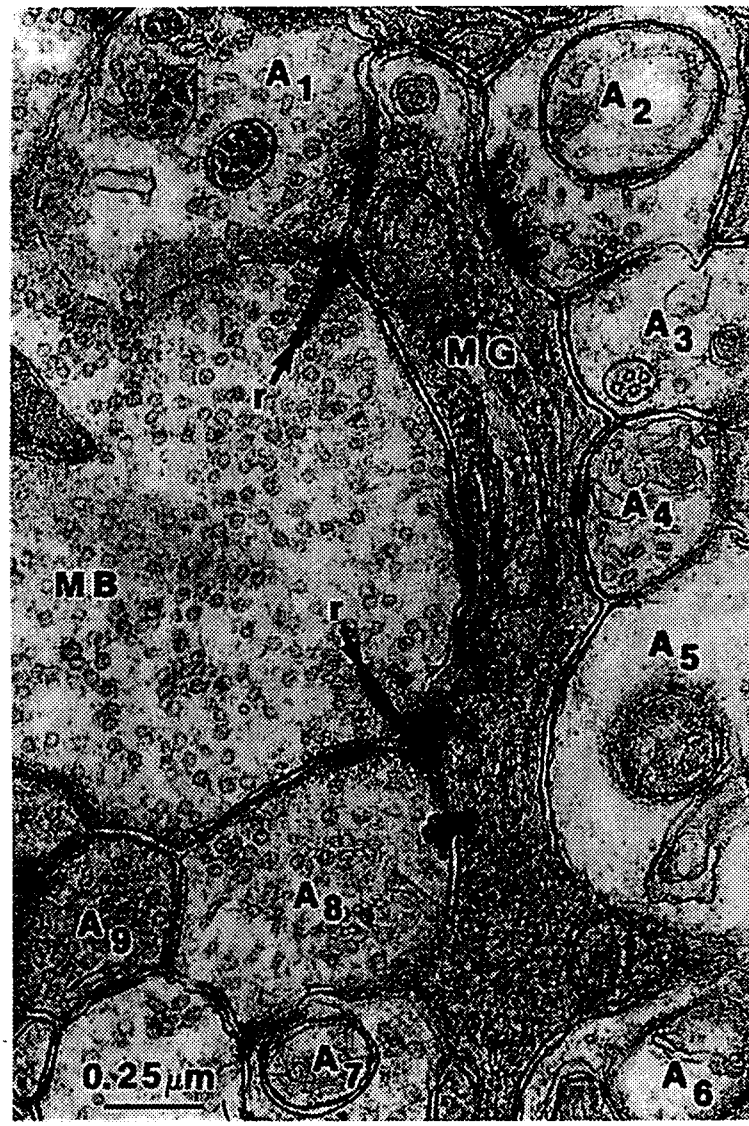

Fig. 6.14. Midget bipolar terminal (MB) in radial section (electron micrograph, macaque fovea). Two "dyads" are present, each with a presynaptic ribbon. The ribbon points between two postsynaptic processes, the dendrite of a midget ganglion cell (MG) and an amacrine process (A_1, A_8) that feeds back onto the bipolar terminal and forward onto the ganglion cell (A_8). Many other amacrine processes also contact the ganglion cell. [From Calkins and Sterling, 1996.]

it couples particular amacrine types to bipolar cells. For example, the largest electrical synapse in IPL couples an AII amacrine dendrite to an ON cone bipolar axon terminal (Kolb and Famiglietti, 1974; Sterling et al., 1988; Strettoi et al., 1990). This connection is apparently critical for vision under starlight, as is discussed later. Fourth, certain narrow-field amacrine cells couple to particular types of ganglion cell (alpha,

parasol; Dacey and Brace, 1992; Vaney, 1994b). Finally, certain types of ganglion cell couple homotypically without amacrine participation, e.g., the directionally sensitive ganglion cell (see Fig. 6.11C; Vaney, 1994a,b).

The ganglion cell differs from "output" cells in other brain regions. The cell is a relatively small, 10–25 μm soma, compared with 50–80 μm for the motoneuron and Purkinje cell. And ganglion cell dendrites typically extend for only 20–200 μm, compared with 1000 μm for the motoneuron. Correspondingly, the ganglion cell collects relatively few synapses: 60–100 for a central midget cell, 200 for a central beta cell, and 3000 for a peripheral beta and a central alpha cell (Freed and Sterling, 1988; Cohen and Sterling, 1992; Kier et al., 1995; Calkins et al., 1996). In contrast, a spinal alpha motoneuron collects about 10,000 synapses, and cerebellar Purkinje cell collects more than 100,000 synapses! Another difference: a ganglion cell collects synapses exclusively on dendrites and not the soma. By contrast, the motoneuron is encrusted with synapses over its entire surface (see Chap. 3), and the very design of the Purkinje cell seems to hinge on an antagonism between excitatory inputs to the dendritic tree and inhibitory inputs to the soma (see Chap. 7).

DEVELOPMENT

Understanding of how retinal circuits develop is rather fragmentary at present, so rather than attempt a synthesis, we note some current lines of investigation. A key effort is to identify mechanisms that generate the plethora of retinal cell types. This seems to involve specific transcription factors. For example, the Brn-3 family of POU domain transcription factors are expressed in subsets of retinal ganglion cells. These proteins first appear in ganglion cell precursors migrating from the zone of dividing neuroblasts to the future ganglion cell layer. Targeted disruption of the *Brn-3b* gene causes selective loss of 70% of ganglion cells but not other types (Gan et al., 1996); also, transgene expression of *Brn-3* members labels various types of amacrine and ganglion cells but not other types (Xiang et al., 1996). Still another POU-domain protein, RPF-1, is expressed in neuroblasts destined to become ganglion and amacrine cells (Zhou et al., 1996).

Another effort concerns the mechanisms that regulate cell number (Williams and Herrup, 1988). As is generally the case, excess cells are produced and then "pruned" by cell death ("apoptosis"). Thus, in cat by embryonic day 39, about 700,000 ganglion cells send axons into the optic nerve. They connect centrally and fire action potentials that drive geniculate neurons (Katz and Shatz, 1996). Nevertheless, by birth only 270,000 axons remain, and by 6 weeks postnatally, there are only about 180,000, which is the adult number (Williams et al., 1986). Why certain ganglion cells live while others die remains to be established, but the current best guess is that the process involves competition for a specific neurotrophin (reviewed in Katz and Shatz, 1996).

Prenatal firing of optic axons shapes geniculate development because blocking these action potentials prevents segregation of eye-specific geniculate layers (Penn et al., 1998). The activity may also help establish orderly two-dimensional maps of retina in central structures (Katz and Shatz, 1996; Katz and Crowley, 2002). This spontaneous ganglion cell firing is not random but rather sweeps across the retina in waves, so that adjacent cells fire together (Meister et al., 1991). The waves of firing are also associ-

ated with waves of intracellular calcium fluctuation in amacrine and ganglion cells that may be triggered by cholinergic amacrine cells (Zhou, 2001b). The waves may also be coordinated via electrical coupling and shared levels of extracellular potassium (Burgi and Grzywacz, 1994; Penn et al., 1994; Singer et al., 2001). Because "neurons that fire together, wire together," these waves of correlated activity may contribute to the orderly relationships at the far end of the optic nerve (Katz and Shatz, 1996). The need to generate these early waves of activity may explain why the earliest synaptic connections in the retina involve lateral rather than forward elements (Maslim and Stone, 1986).

In this early period, GABA and glycine excite ganglion cells and only later switch over to their more standard inhibitory actions (Fischer et al., 1998; Zhou, 2001a). For GABA and glycine to excite, the chloride equilibrium potential must be positive to the resting potential, implying that intracellular chloride concentration is higher during development than in the adult. Consistent with this prediction, the chloride transporter NKCC (which raises intracellular chloride) is high in early development and declines relative to KCC2 (which lowers intracellular chloride) about the time that GABA becomes inhibitory (Vu et al., 2000; Zhang et al., 2003).

At birth, the main ganglion cells in cat (alpha, beta, etc.) are easily recognized (Dann et al., 1988; Ramoa et al., 1988). But they are not yet connected to their intraretinal circuits because the photoreceptors are still proliferating, and the bipolar axons are just descending toward the IPL. As the eyes open (6–10 days postnatal), synaptogenesis enters high gear and is nearly complete by 4 weeks (Vogel, 1978; Maslim and Stone, 1986). Each cell type probably has its own programmed period and rate of synaptogenesis, and there is no simple way to characterize the sequence. Thus, it proceeds neither strictly centrifugally (ganglion cell → bipolar → receptor) nor vice versa (McArdle et al., 1977; cf. Nishimura and Rakic, 1987). Further, the genesis of retinal wiring, despite its coincidence with eye opening, appears to follow a genetic program and to be little affected by light or patterned stimulation. Thus, neither dark rearing nor occlusion by lid suture (which prevents patterned stimulation) much affects adult retinal morphology or physiology, even though such procedures profoundly alter the structure and function of the visual cortex (Daw and Wyatt, 1974; Hubel and Wiesel, 1977). However, ON and OFF ganglion cells express distinct firing properties during development, which may allow postsynaptic thalamic cells to distinguish between them and segregate their output into separate ON and OFF sublaminae (Stryker and Zahs, 1983; Wong and Oakley, 1996). Thus, developmental changes in retinal circuitry influence developmental changes in ganglion cell axon targeting.

Perinatal alpha and beta ganglion cells display immature dendritic arbors with excessive branches and spines, and their ON/OFF dendritic stratification is incomplete (Dann et al., 1988; Ramoa et al., 1988). Pruning of the ganglion dendritic arbors proceeds almost normally in the presence of TTX. Therefore, action potentials, which crucially shape the axon arbor, hardly affect the dendritic arbor (Wong et al., 1991). On the other hand, bipolar input (insensitive to TTX) apparently *does* shape the dendritic arbors. Thus, tonically hyperpolarizing ON bipolar cells during eye opening (by intraocular application of the mGluR6 agonist APB) arrests the normal progress of stratification (Bodnarenko et al., 1995). Furthermore, during synaptogenesis, a retinal ganglion cell's dendritic tree expands and contracts locally, bringing postsynaptic den-

dritic membrane into contact with presynaptic amacrine and bipolar cell release sites. Such dendritic remodeling depends on nicotinic acetylcholine receptors and local Ca^{2+} release from internal stores in the ganglion cell (Lohmann et al., 2002).

The synaptic connections in adult mammalian retina appear not to be "plastic." But in lower vertebrates (such as fish and amphibia), the retina continues to grow throughout life, adding nerve cells in concentric rings at the periphery to all three layers. The optic tectum, the main target of the fish and amphibian optic nerve, also continues to add neurons but in concentric crescents rather than in complete rings. This creates a topological mismatch between the retina and its map on the tectum. Consequently, the map requires continuous readjustment. This is accomplished by the continuous retraction of old retinotectal synapses, growth of the optic axons across the tectum, and the formation of new synapses (Easter and Stuermer, 1984; Reh and Constantine-Paton, 1984). If the neural retina is totally removed from the eye of a fish or amphibian, cells from the pigment epithelium de-differentiate, divide, and regenerate a whole new neural retina whose ganglion cell axons find their way to the brain and reconnect properly (Stone, 1950; Saito, 1999).

Another fascinating developmental plasticity is the shift in retinal wiring that in certain organisms accompanies changes in lifestyle. For example, the adult frog eats flies and has a type of ganglion cell tuned by specific circuits to "fly-like" stimuli (Barlow, 1953; Maturana et al., 1960). However, the tadpole eats algae and lacks this cell type. The fly-detecting ganglion cell and its neural circuitry develop as part of the many complex changes that accompany metamorphosis (Frank and Hollyfield, 1987). However, it seems fairly certain that its emergence is directed by a genetic program that operates whether or not the frog is ever confronted with a fly.

VISUAL TRANSDUCTION

Rods and cones share the same transduction mechanism (Fig. 6.15). The outer segment bears numerous cation channels permeable to Na^+ and Ca^{2+}. A channel flickers open upon binding four molecules of cGMP, and in the dark the intracellular concentration of cGMP is high. Therefore, at any instant about 10^6 channels are open. The result in darkness is a continuous inward sodium current at the outer segment, which is balanced by an outward potassium current at the inner segment. This circulating dark current depolarizes the receptor to about -40 mV. The cell's ionic balance is maintained by an active sodium/potassium exchanger operating continuously at the inner segment, which explains the large energy demand at this site and thus its need for densely packed mitochondria (see Fig. 6.4; reviewed in Yau, 1994; Pugh and Lamb, 1993, 2000).

The optical image focuses at the level of the *inner* segments (see Figs. 6.4 and 6.10). A photon contributing to this image penetrates the plasma membrane to enter the inner segment. Entering a rod, the photon may simply pass through, continuing on until it is finally trapped in a neighboring receptor. Which rod captures a given photon does not matter because at night the optical image is poor and subsequent pooling of rod signals is great. However, if a photon enters a *cone* inner segment roughly parallel to its long axis, it is trapped due to the densely packed and longitudinally oriented mitochondria that raise the refractive index. Thus, the cone inner segment's "wave-guide"

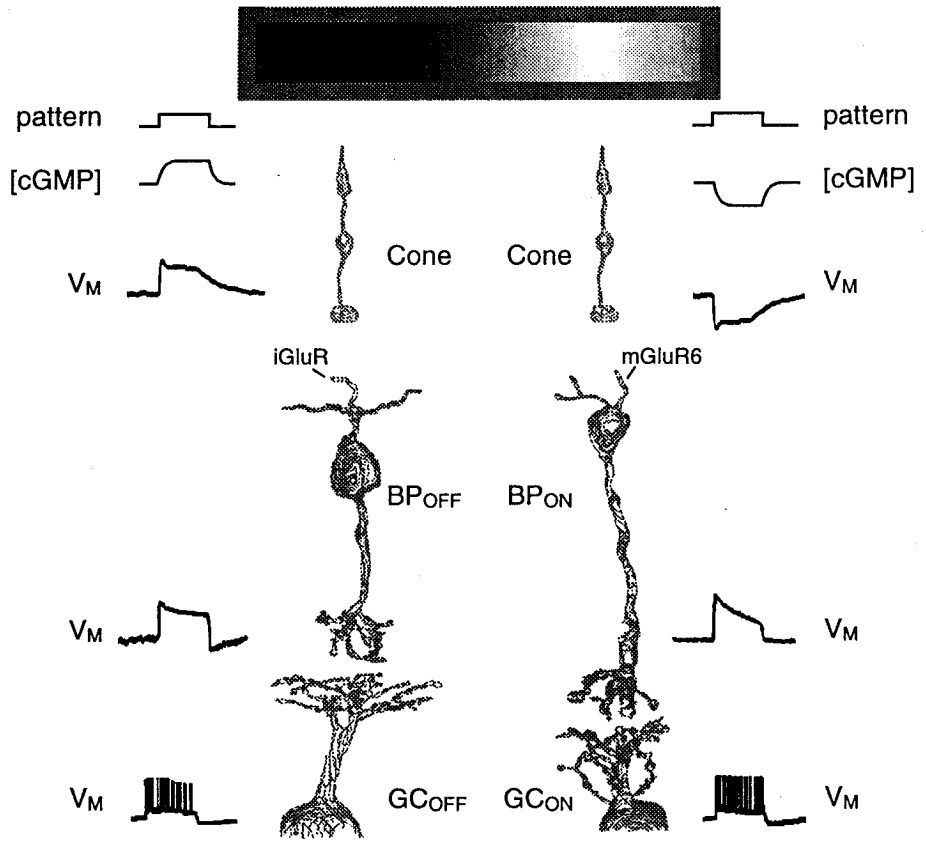

Fig. 6.15. Basics of transduction and forward signal transfer. One cycle of a dark/bright grating flashes briefly on a steady background. Light *decrement* for the left cone allows guanyl cyclase to raise [cGMP], thus opening cation channels in the outer segment and depolarizing the cone membrane potential (V_M). The cone terminal increases its discharge of glutamate onto ionotropic receptors (iGluR), depolarizing the OFF bipolar cell, thus releasing glutamate onto the OFF ganglion cell and causing it to spike. Light increment for the right cone isomerizes rhodopsin, triggering the G protein cascade that lowers [cGMP], thus closing cation channels in the outer segment and hyperpolarizing the cone membrane potential. The cone terminal ceases its tonic release of glutamate onto metabotropic (mGluR6) receptors, depolarizing the ON bipolar cell, thus releasing glutamate onto the ON ganglion cell and causing it to spike. This key step at the cone terminal, use of paired neurons to separately encode light decrement and increment, carries forward to the ganglion cells that feed the geniculostriate pathway, doubling the total dynamic range.

funnels photons toward the outer segment to preserve the correspondence between the optical image and the transduced image (Enoch, 1981).

A photon reaching the outer segment penetrates the stacked membrane discs (see Fig. 6.4) until it encounters a molecule of photopigment (rhodopsin) and transfers its energy. This isomerizes the vitamin A group attached to the opsin protein, activates the molecule, and causes it to activate several hundred molecules of the G-protein transducin. Transducin then activates hundreds of phosphodiesterase molecules that rapidly

hydrolyze cGMP, lowering its concentration. This closes the cation channels and reduces the Na^+ and Ca^{2+} influx ("dark current"), thus hyperpolarizing the outer segment. This signal spreads to the inner segment where voltage-gated channels further shape it temporally and boost its amplitude (reviewed in Pugh and Lamb, 1993; Yau, 1994) before sending it down the axon (Hsu et al., 1998).

The rod achieves the ultimate sensitivity: one photon isomerizes one rhodopsin molecule (Rh*), which lowers the cGMP concentration enough to suppress about 4% of the dark current. This gives a ≈0.7 pA signal with a signal/noise ratio of about 3.5 (Baylor et al., 1984). Although the rhodopsin molecule is quite stable, it does isomerize without a photon—by thermal agitation—producing ≈0.006 Rh*/rod/s. Because the next stage cannot distinguish a photic isomerization from a thermal one, this rate of "dark light" helps set the lower limit of visual sensitivity (reviewed in Barlow, 1982).

The rod sums linearly up to about 20 Rh* delivered as a flash, saturating completely to 100 Rh*/flash (Baylor et al., 1984). But to a background that steadily evokes 100 Rh* per integration time (corresponding to twilight), the rod can reduce its sensitivity and thus avoid saturation when the cone signal is declining toward its threshold. Complete saturation occurs at about 1000 Rh* per integration time (Tamura et al., 1989, 1991).

Rod adaptation arises from multiple mechanisms that affect individual steps of the phototransduction cascade, and many of these mechanisms depend on the intracellular level of Ca^{2+} (Pugh and Lamb, 2000; Burns and Lamb, 2003). An additional mechanism for adaptation, observed *in vivo*, involves the light-induced movement of the G-protein transducin from the rod outer segment to compartments in the inner segment and soma (Sokolov et al., 2002).

The cone is less sensitive by nearly 70-fold: 1 Rh* suppresses only about 0.06% of the dark current, but this response is buried by random fluctuations of the membrane current and so is undetectable. The cone signal first rises above the noise when about 100 Rh* arrive within its integration time; thus its threshold for signaling uses about the same fraction of the dark current as the rod (Schnapf et al., 1990). The cone signal turns on at the same rate as the rod, but turns off much faster, which is key to its shorter integration time and greater temporal resolution (Pugh and Lamb, 1993; Tachibanaki et al., 2001). As light intensity rises, several mechanisms turn down cone sensitivity to retain a linear response, and even in the brightest light the response does not saturate completely (Burkhardt, 1994). The mechanisms that arrest transduction and turn down its sensitivity involve feedback control by calcium at many levels of the cascade but are as yet incompletely understood (reviewed in Yau, 1994; Burns and Lamb, 2003).

DENDRITIC AND AXONAL PROPERTIES

PATTERNS OF FUNCTIONAL POLARIZATION

Classically, "dendritic" has implied passive current flow toward the soma and axon hillock. "Axonal" has implied active propagation away from the soma toward the presynaptic terminal. But in retina as elsewhere (see Chaps. 1 and 2), these simple definitions tend to dissolve. True, the forward "relay" neurons do display typical polarity. Indeed, the sequence: photoreceptor → bipolar cell → ganglion cell was Cajal's pri-

mary exemplar (together with the olfactory bulb's mitral cell; see Chap. 5) for his "law" of polarized conduction. However, photoreceptor and bipolar axons do not normally spike; rather they are passive, releasing transmitter upon graded depolarization (von Gersdorff and Matthews, 1994; Rieke and Schwartz, 1996). Also, these axon terminals *receive* modulatory inputs. Both points violate classical theory.

The lateral elements break *all* the classical rules (Piccolino, 1986). In fact, their designs seem almost *ad hoc*, each suited to accomplish a particular task. Thus, a horizontal cell collects input all along its processes and gives output at the same sites. Furthermore, because horizontal cells are strongly coupled, they present essentially a continuous sheet, passively integrating inputs and modulating outputs rather widely in space and time (Smith, 1995). A narrow or medium-field amacrine cell is also nonpolarized because its input and output tend to be near each other (Famiglietti, 1991; Calkins and Sterling, 1996). However, these amacrine processes are quite fine caliber, are not coupled, and may be passive. Consequently the output of such a cell may create a local feedback circuit for temporal sharpening (Freed et al., 2003).

The starburst amacrine cell, with dendrites like spokes of a wagon wheel (see Fig. 6.9), collects excitatory input uniformly along each branch but provides output only at the distal segments. Consequently, light stimulus sweeping across this cell proximo $\rightarrow$ distally excites the output more effectively than a stimulus moving disto $\rightarrow$ proximally (Euler et al., 2002). This effect, coupled with the starburst cell's asymmetrical connections to the directionally selective ganglion cell (Fried et al., 2002), may explain the mechanism for directional selectivity identified long ago (Barlow and Levick, 1965).

The wide-field amacrine cells present a bizarre twist to the theme of polarized conduction. As noted, these cells collect input conventionally via a dendritic tree that funnels PSPs toward the soma. Action potentials also arise conventionally, at an axon hillock, and propagate for millimeters across the retina (see Fig. 6.9). Unconventionally, though, each primary dendrite emits its own axon; thus, although the cell segregates its passive dendrites and spiking axons, the latter broadcast spikes radially in two dimensions.

The AII amacrine cell represents still another twist to the theme of functional polarity and active versus passive membrane. The cell collects its key input from rod bipolar synapses on its main arbor in the ON layer of the IPL and uses gap junctions with cone bipolar axon terminals as a local excitatory output. Because the AII collecting arbor is narrow-field, it should not require active membrane to propagate its signal, yet the cell produces large, fast depolarizations that are sensitive to TTX (Nelson, 1982; Boos, et al., 1993). Here, a voltage-sensitive membrane, rather than spreading signals beyond where passive conduction could take them, seems to provide a "thresholding" mechanism that amplifies nonlinearly to separate small signals from noise (Freed et al., 1987; Smith and Vardi, 1995).

Neighboring AII cells couple to one another with a conductance of about 700 pS, which promotes synchronous spiking in the network (Veruki and Hartveit, 2002). The importance of AII spiking for the ganglion cell response remains unclear because in dark-adapted retina (where the AII carries the rod signal), robust ganglion cell rsponses are recorded even when AII spikes are blocked with TTX (Taylor, 1999). The AII's response properties and the extent of AII-AII coupling depend strongly on the degree of light adaptation (Bloomfield et al., 1997; Xin and Bloomfield, 1999). Only a few of the 40 amacrine types have been studied, so further surprises are to be expected.

INDIVIDUAL RETINAL NEURONS ARE ELECTROTONICALLY COMPACT

The axons and main dendrites of feedforward neurons are relatively short and thick. Thus rod and cone axons, respectively, 0.5 and 1.6 μm diameter, range from 20 to 400 μm long (Hsu et al., 1998). Bipolar dendrites and axons are about the same thickness as photoreceptor axons but even shorter. Ganglion cell dendrites (beta and alpha) are also about 0.5–1.5 μm in diameter, and the arbors range from about 30 to 250 μm across. Consequently, all synapses onto these cells are calculated to be well within one space constant of the soma. Electrotonic considerations indicate that photovoltages transmitted to rod and cone terminals and EPSPs transmitted from distal dendrites to the ganglion cell soma are little attenuated (Koch et al., 1982; Freed et al., 1992; Kier et al., 1995; Hsu et al., 1998). Ganglion cells in the periphery (alpha, parasol) and certain cell types all across the retina are much larger than 250 μm, reaching up to 1 mm diameter (Berson et al., 1998; Peterson and Dacey, 1999). In these cells, active mechansisms, such as dendritic Na^+ channels, may allow transmission from distal dendrite to soma (Velte and Masland, 1999).

NEUROTRANSMITTERS AND POSTSYNAPTIC RECEPTORS

Essentially all of the transmitters identified elsewhere in the brain exist also in the retina. A transmitter can be assigned to a cell type upon immunocytochemical detection of (*1*) the endogenous transmitter, (*2*) its synthetic enzyme, and (*3*) transmitter receptors on postsynaptic cells. When no antibody is available, *in situ* hybridization for mRNA of the appropriate molecule also provides a clue, but the conclusion remains tentative because the mRNA may not be expressed. Commonly, a neuron that uses a particular transmitter also expresses a transporter molecule on its surface that binds the transmitter in the extracellular space and actively pumps its back into the cell. Müller cells are not known to release glutamate, but they do express receptors for amino acid transmitters and also transporters for both GABA and glutamate (reviewed in Newman and Reichenbach, 1996). Most recently, they are shown to release ATP, which activates A_1 adenosine receptors on ganglion cells and inhibits them, probably by modulating a GIRK (G-protein–regulated K^+ channel; Newman, 2003).

PHOTORECEPTORS TO HORIZONTAL AND BIPOLAR CELLS

Photoreceptors contain the excitatory amino acid glutamate and release it when depolarized. Two experimental *tours de force* seem conclusive. First, a turtle rod was sucked by its outer segment into a micropipette through which it could be electrically stimulated. The tip of a second pipette, bearing a patch of neuronal membrane ripped from a cultured hippocampal neuron, was moved close to the rod axon terminal. The membrane patch, which was "outside out" (see Chap. 2), contained the NMDA type of glutamate receptor. Electrically depolarized, the rod released a transmitter onto this "sniffer" patch, opening ion channels gated by the NMDA receptor (Copenhagen and Jahr, 1989). Second, the rod axon terminal was sucked into a pipette containing glutamate dehydrogenase plus NAD; then release of glutamate was measured directly by an increase in fluorescence due to the formation of $NADH_2$ (Ayoub et al., 1989).

Postsynaptic to photoreceptors, horizontal cells express iGluRs (AMPA and kainate) that open a cation channel with a reversal potential near zero (Haverkamp et al., 2000, 2001a,b). Thus, as the photoreceptor depolarizes to dark stimuli and releases glutamate

(see earlier and Fig. 6.15), the horizontal cell depolarizes. The OFF bipolar cell dendrites also express iGluRs and thus also depolarize to dark stimuli. Although horizontal and OFF bipolar cells express the same broad class of receptor (iGluRs), the particular combinations of receptor subunits differ (DeVries, 2000). This could explain how the effective concentration for a half-maximal response (EC_{50}) could be 0.5 mM for the horizontal cell and 10 μM for the bipolar cell (Sasaki and Kaneko, 1996). This sensitivity difference seems key to assembling multiple postsynaptic processes into a complex where they can all be activated by the same point source of glutamate (see Fig 6.13; Rao-Mirotznik et al., 1998).

The ON bipolar dendrites express a *metabotropic* glutamate receptor, mGluR6 (see Fig. 6.15A; Nomura et al., 1994). This receptor, highly localized to the tips of rod bipolar and ON cone bipolar dendrites, couples to a second messenger system requiring the G-protein, G_o (Vardi and Morigiwa, 1997; Dhingra et al., 2000, 2002). Glutamate binds this receptor to *close* an ion channel with reversal potential near zero and thus hyperpolarizes the cell. Light suppresses the photoreceptor's glutamate release to open this cation channel and depolarize the cell. This synapse has been termed "sign-reversing" and "inhibitory" because glutamate's action is to hyperpolarize, but the reversal potential is positive (i.e., excitatory). Therefore, it may be simplest to consider the ON bipolar cell as excited by bright stimuli and the OFF bipolar cell as excited by dark stimuli (both relative to the local mean intensity level).

By using two different receptors for the same transmitter, OFF and ON cone bipolar cells double the dynamic range for encoding intensity differences across a natural scene (see Fig. 6.18). Half of the bipolar cells carry signals greater than the local mean, and half carry signals less than the local mean. Their ganglion cells and corresponding cells in the lateral geniculate nucleus follow suit. Finally, at the level of simple cells in striate cortex, these signals recombine. The receptive field of a cortical "simple cell" comprises elongated ON and OFF subregions. Within an ON subregion firing is evoked by increased excitation from ON geniculate cells and decreased inhibition from OFF geniculate cells; conversely, within an OFF subregion firing is evoked by increased excitation from OFF geniculate cells and decreased inhibition from ON ganglion cells (Palmer and Davis, 1981; Ferster, 1988). Thus, each subregion, wired in "push-pull" fashion, uses the full dynamic range that was initially divided at the cone synapse. An important lesson here is that to understand the reason for a particular encoding procedure at one synapse, one may need to look ahead another four or five stages!

It was thought initially that the ON bipolar cell's mGluR6 couples to a G-protein that activates phosphodiesterase (PDE) to hydrolyze cGMP and close a cation channel, i.e., mimicking the mechanism for phototransduction (Nawy and Jahr, 1990; Shiells and Falk, 1990). But $Go_{\alpha 1}$, the protein coupled to mGluR6, although crucial to the ON light response, is not linked to PDE or cGMP hydrolysis, and thus the link between activation of $Go_{\alpha 1}$ and the closing of the cation channel remains a mystery (Vardi, 1998; Nawy, 1999; Dhingra et al., 2000, 2002).

HORIZONTAL TO PHOTORECEPTOR AND BIPOLAR CELLS

Horizontal cells use GABA. Although mammalian horizontal cells do not demonstrably accumulate exogenous GABA, they do contain it (Chun and Wässle, 1989). They

also express the GABA-synthetic enzyme glutamic acid decarboxylase (GAD) in one of two isoforms, GAD_{65} or GAD_{67} (Vardi and Sterling, 1994; Johnson and Vardi, 1998). Further, $GABA_A$ and $GABA_C$ receptors are expressed by cone bipolar and rod bipolar dendrites, implying a local source of GABA, presumably horizontal cells (Vardi et al., 1992; Vardi and Sterling, 1994; Enz et al., 1996; Shields et al., 2000). The cone axon terminal hyperpolarizes to ionophoresis of GABA, suggesting GABA feedback onto it (e.g., Tachibana and Kaneko, 1984; Wu, 1992; Pattnaik et al., 2000).

BIPOLAR TO GANGLION AND AMACRINE CELLS

Bipolar neurons use glutamate as a transmitter. Here the evidence rests mainly on the responsiveness of ganglion and amacrine cells to ionophoresed glutamate and its various agonists and antagonists. iGluRs are both expressed by ganglion cells and specific amacrine types (Cohen et al., 1994; reviewed in Wilson, 2003). Many different subunits of each receptor type are present (Vardi and Morigiwa, 1997; Qin and Pourcho, 1999a,b; Fletcher et al., 2000; Pourcho et al., 2001). However, in general amacrine cells express kainate receptors, whereas ganglion cells express AMPA and NMDA receptors (Grunert et al., 2002). Furthermore, various processes in the inner plexiform layer, including bipolar terminals, express metabotropic glutamate receptors (Hartveit et al., 1995; Brandstätter et al., 1996; Awatramani and Slaughter, 2001; Higgs et al., 2002).

Certain bipolar neurons contain glycine and appear to accumulate it from the extracellular medium (Cohen and Sterling, 1986; Pourcho and Goebel, 1987). Furthermore, some ganglion cells bear glycine receptors and respond to ionophoretic glycine with an increased Cl^- conductance that is blocked specifically by strychnine (Bolz et al., 1985; Koulen et al., 1996). However, it now appears that glycine enters the bipolar terminal via the gap junctions with the AII amacrine cell that accumulates it via a glycine transporter (Cohen and Sterling, 1986; Vaney et al., 1998). Thus, although bipolar cells contain glycine and apparently provide a glycine reservoir for the AII cell, they probably do not release it.

One striking complication is that certain bipolar cells contain endogenous GABA and express GAD (Wässle and Chun, 1988; Vardi and Auerbach, 1995). These cells represent two distinct types with axons in the OFF layer of the IPL (Kao et al., 2003). These cells express the vesicular transporters of both glutamate and GABA, and thus probably do release both transmitters (Kao et al., 2003). If so, a differential arrangement of postsynaptic receptors would permit this synapse to excite one member of its postsynaptic dyad (ganglion cell) while simultaneously inhibiting the other (AII amacrine cell).

AMACRINE CELLS

About half of all amacrine somas contain glycine and half contain GABA plus GAD (Vardi and Auerbach, 1995). However, GABA is expressed in many amacrine types that also express other transmitters. For example, the starburst amacrine cells that synthesize acetylcholine also synthesize GABA using both isoforms of GAD (Brecha et al., 1988; Kosaka et al., 1988; Vaney and Young, 1988; Vardi and Auerbach, 1995).

Other GABA amacrine cells contain dopamine, indoleamines, or neuropeptides such as somatostatin, vasoactive intestinal polypeptide, and substance P (Sagar, 1987; Vaney et al., 1989b; White et al., 1990; reviewed in Vaney, 1990, 2003; Casini and Brecha,

1992). Still other amacrine cells contain NADPH diaphorase, which synthesizes nitric oxide, so conceivably GABA in amacrine cells is never the sole transmitter (Sandell, 1985; Sagar, 1987). It remains unclear whether any cell co-releases GABA with its other transmitter/modulator, whether they are released at different spatial loci, or in response to different electrical or chemical signals (O'Malley et al., 1994).

Processes postsynaptic at amacrine synapses bear the standard receptor molecules. Thus, where glycine is presynaptic, there are postsynaptic glycine receptors (Freed and Sterling, 1988; Pourcho and Owczarzak, 1991; Sassoè-Pognetto et al., 1994); where GABA is presynaptic, there are postsynaptic $GABA_A$ or $GABA_C$ receptors (Vardi and Sterling, 1994; Enz et al., 1996). Bipolar terminals express both $GABA_A$ and $GABA_C$ receptors, whereas ganglion cells express mainly $GABA_A$ (Shields et al., 2000). $GABA_A$ currents are more transient than $GABA_C$ currents, and thus the relative expression of these two receptors will temporally shape light-evoked inhibition (Shields et al., 2000).

Unlike GABA, dopamine can act in a "paracrine" fashion, reaching postsynaptic targets tens of microns beyond its site of release. Thus, the D_1 receptors distribute much more widely than the conventional dopaminergic synapses (Witkovsky et al., 1993; Veruki and Wässle, 1996). Neuropeptide receptors tend to have many subtypes. For example, for somatostatin there are five types, one of which, SSRT2a, has been localized in retina to the rod bipolar terminal (Reisine and Bell, 1995; Vasilaki et al., 1996). Acetylcholine released by the starburst amacrine cell also must have different receptors because the direction selective cell is affected by nicotinic blockers (ionotropic), whereas alpha and beta cells are also affected by muscarinic agonists (metabotropic) (Schmidt et al., 1987).

Matters already seem complicated by multiple presynaptic transmitters and multiple subtypes of postsynaptic receptor. But they are profoundly more so because many postsynaptic receptors, including those for glutamate, GABA, dopamine, indoleamines, and peptides, couple to various G-proteins, and these trigger a variety of "second messenger" systems. For example, G_{olf} is expressed by wide-field horizontal cells and ganglion cells in the IPL; G_o is expressed by ON bipolar cells and by certain amacrine processes in IPL (Vardi et al., 1993). Because a given G-protein can couple to more than one type of downstream effector, the possible signaling pathways must be very large. Thus, one senses an underlying neurochemical network at least as complex as the network of anatomical connections.

FUNCTIONAL CIRCUITS

HOW EFFICIENT IS THE RETINA?

Having described the main types of retinal neuron and their connections, transmitters, etc., we are nearly ready to consider how the anatomical wiring serves function. But first we should ask how well does the retina perform? The first steps of phototransduction are inefficient: only about one-third of the photons striking the retina are absorbed by a rhodopsin molecule, and only half of these cause isomerization (reviewed in Sterling et al., 1987). Yet once activated, an Rh* projects this information through subsequent stages with remarkable reliability. Thus, a single Rh* activates several hundred transducin (G-protein) molecules and thence a comparable number of PDE cat-

alytic subunits (Leskov et al., 2000), leading reliably to two or three spikes in several ON ganglion cells and to suppression of two or three spikes in several OFF ganglion cells (Barlow et al., 1971; Mastronarde, 1983; Vardi and Smith, 1996).

Once a single photon signal reaches a ganglion cell, to be useful it must sum efficiently with other such signals. If noise were added along the way, e.g., due to random release of synaptic vesicles, or if the signal were to saturate some stage along the transmission pathway, information would be lost and the image would be degraded. Yet we discriminate stimuli near threshold with very little information loss along neural circuits. The evidence stems from "ideal observer" computer models that perform any specified discrimination simply based on the number of photons counted. The models take account of losses due to optics, photoreceptor sampling, and transduction. But thereafter, they operate ideally, i.e., with no further information loss due to neural mechanisms (Geisler, 1989). It turns out that for a suitable stimulus we approach the sensitivity of an ideal observer to within a factor of 2–3 in both dim and bright light (Crowell and Banks, 1988; Savage and Banks, 1992). Therefore, the sum of all stages—from transduction to the ultimate site of discrimination—must not lose any more information than this. Thus retinal circuits must be extremely efficient—as implied by the fine sculpting of the receptor mosaic (described earlier). This alerts us to circuit mechanisms that prevent noise and saturation.

CIRCUITS FOR GANGLION CELL RECEPTIVE FIELD

Center. The center circuit turns out to be fairly simple: the cones co-spatial with the ganglion cell dendritic field modulate glutamate release onto dendrites of cone bipolar cells whose axons contact the ganglion cell dendritic tree. Brightening these cones depolarizes the ON bipolar cells and delivers glutamate to ON ganglion cell dendrites; dimming these cones depolarizes the OFF bipolar cells and delivers glutamate to OFF ganglion cell dendrites (see Fig. 6.15A). Thus, the "center" circuit is purely excitatory.

The number of cones that connect directly to a ganglion cell dendritic arbor depends on species, retinal location, and ganglion cell type. For example, in cat, about 35 cones overlie a central beta cell dendritic field and employ about 15 bipolar cells to contact it with nearly 200 synapses (Fig. 6.16) (Cohen and Sterling, 1992). About 625 cones overlie a central alpha cell and use about 150 bipolar cells with nearly 450 synapses (Fig. 6.16; Freed and Sterling, 1988). In these respects, a peripheral beta cell resembles a central alpha cell (Kolb and Nelson, 1993; Kier et al., 1995).

In primates, the receptive field centers are much smaller. For example, in the fovea a single cone contacts a pair of "midget" bipolar cells (ON and OFF) that in turn contact, respectively, ON and OFF "midget" ganglion cells. This 1:1 bipolar-to-ganglion cell connection is accomplished with only about 50 synapses (Calkins et al., 1994). In the periphery, e.g., 20 degrees, about 10 cones overlie the midget ganglion cell. Here, although each cone still contacts its own private midget bipolar cell, several of these converge onto a midget ganglion cell (Dacey, 1996; Goodchild et al., 1996b). The wider-field ganglion cells in primate fovea, "parasol" and "garland" cells, collect on the order of 30–50 cones (Calkins and Sterling, 2003).

What explains the alpha cell's transient response to a steady center stimulus versus the beta cell's sustained response (see Fig. 6.7)? Multiple mechanisms cooperate: (*1*) only one type of bipolar cell contacts the alpha cell, and it has a large transient re-

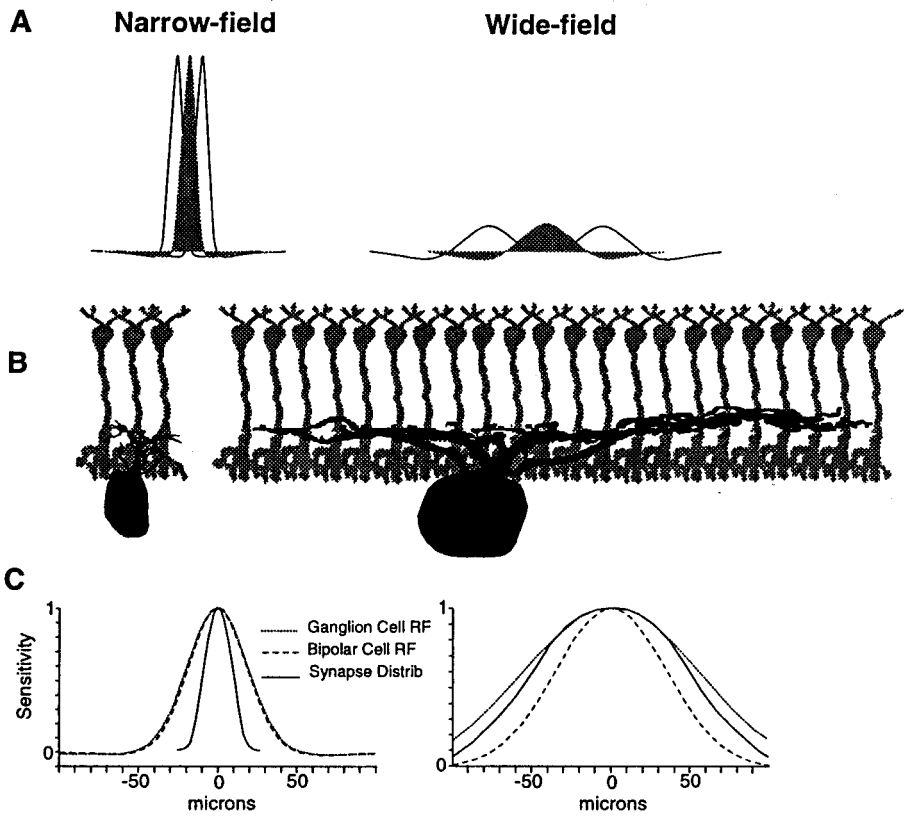

Fig. 6.16. Circuits for the ganglion cell receptive field center. **A:** Sensitivity profiles of central beta and alpha cell receptive fields. Beta cell is 8-fold more sensitive than an alpha cell to a small spot (just covering the beta center). Beta centers are narrow and closely spaced; alpha centers are broader and coarsely spaced. **B:** Beta cell collects about 80 synapses from the b_1 bipolar array, whereas the alpha cell collects 450 b_1 synapses. **C:** Beta gaussian sensitivity profile is shaped mainly by the bipolar receptive field center, which is broad due to optical blur and cone coupling (see Fig. 6.17); the synapse distribution across the narrow beta dendritic tree hardly matters. Alpha gaussian sensitivity profile is shaped partly by the bipolar centers, but more importantly by the dome-like distribution of synapses across the dendritic tree. The beta cell's greater peak sensitivity is due to its greater density of synapses/retinal area. [After Freed and Sterling, 1988; Freed et al., 1992.]

sponse, whereas three types of bipolar cell contact the beta cell and carry sustained as well as transient responses (see Fig. 6.6B; Nelson and Kolb, 1983; Freed and Sterling, 1988; Cohen and Sterling, 1992; Freed, 2000a,b). (*2*) Starburst amacrine processes, coplanar with the alpha dendritic arbor, associate with it, whereas starburst processes have access to only a small fraction of the beta dendritic arbor (Vardi et al., 1989; Luo et al., 1996). (*3*) Bipolar input to the starburst cell, mediated by kainate receptors, transiently releases acetylcholine onto ganglion cell dendrites (Famiglietti, 1991; Linn et al., 1991). (*4*) Nicotinic receptors so activated depolarize but rapidly desensitize

(Kaneda et al., 1995). (*5*) Glycinergic amacrine synapses from narrow-field amacrine cells provide many synapses to the alpha cell and may antagonize the center excitation (Freed and Sterling, 1988). (*6*) Voltage-gated sodium channels for the alpha cell action potential inactivate rapidly (Kaneda and Kaneko, 1991). (*7*) Alpha cells have very low impedence, which may contribute to a faster time constant (Cohen, 2001; O'Brien et al., 2002). In short, this key physiological difference between the alpha and beta cell types arises partly from differences at the *inter*cellular level (wiring) and partly from differences at the *intra*cellular level (different receptors and channels).

Surround. The inhibitory surround arises first at the cone terminal (Fig. 6.17) (e.g., Baylor et al., 1971; Smith and Sterling, 1990). Whereas a bright spot hyperpolarizes a central cone, a bright annulus hyperpolarizes surrounding cones. This suppresses their tonic excitation of horizontal cells, reducing GABA released onto the central cone and causing it to *de*polarize, in antagonism to its light response (Fig. 6.17D; Leeper and Charlton, 1985). Illuminating a small patch of cones, corresponding to the ganglion cell center, hardly affects horizontal cells because the patch constitutes at most a few

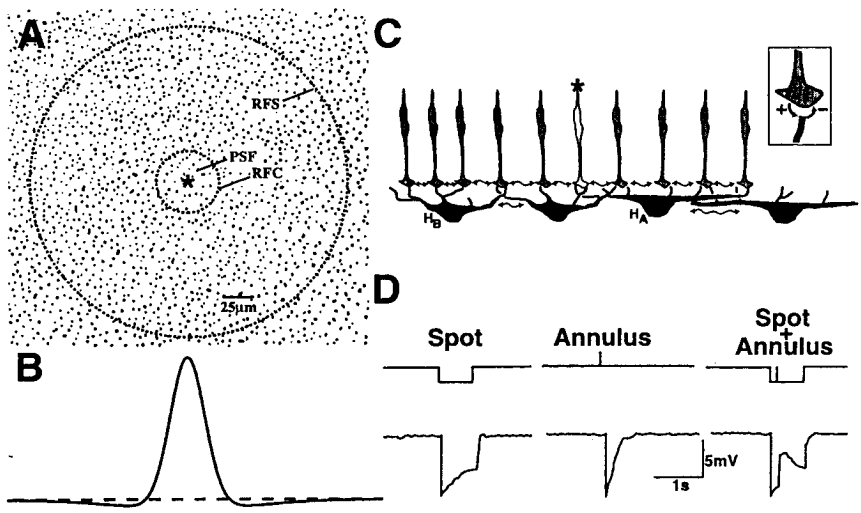

Fig. 6.17. **A:** Cone array in cat central area (24,000/mm^2). A point of light striking the cornea spreads, due to optical blur, to stimulate about 10 cones (PSF = point spread function). The signal spreads farther, due to coupling at cone terminals, to create a receptive field center (RFC) for one cone (*) that encompasses about 50 cones. Inhibitory feedback via horizontal cells causes a receptive field surround (RFS) encompassing about 1200 cones. **B:** Sensitivity profile (difference-of-Gaussians) calculated for the cone receptive field. **C:** Neural circuit thought to shape the cone sensitivity profile: center shaped by optics plus coupling; surround shaped by inhibitory feedback (inset): its narrow, deep region set by narrow, weakly coupled H_B cell; its broad, shallow region set by broad, strongly coupled H_A cell. **D:** Intracellular recordings from turtle cone demonstrate its center-surround receptive field: a spot hyperpolarizes the center cone (*); an annulus causes a brief hyperpolarization by scattering light onto the center; the annulus plus the spot demonstrates the surround's depolarizing effect. [A–C from Smith, 1995; D from Gerschenfeld et al., 1980.]

percent of the horizontal cell input. But covering a wide field of cones (50–80 times as many cones as the center) is effective. Experiments suggest that the electrical effect of modulating a hemi-gap junction at the tip of the horizontal cell spine might contribute to modulating the cone terminal (Kamermans et al., 2001).

The bipolar cell, by summing center-surround receptive fields of 5–10 converging cones, begins at the OPL to establish its own center-surround receptive field (Werblin and Dowling, 1969; Kaneko, 1970; Dacey et al., 2000). Another contribution to the bipolar cell's surround comes from horizontal cell release of GABA onto $GABA_A$ receptors on the bipolar dendrite (Vardi et al., 1992; Vardi and Sterling, 1994; Haverkamp and Wässle, 2000). Cone glutamate release drives ON and OFF bipolar cells in opposite directions depending on their glutamate receptor (mGluR for ON, iGluR for OFF).

Horizontal cell GABA release also drives ON and OFF bipolar cells in opposite directions, but does so using only one class of receptor: GABA-gated chloride channels. So, how might this work? The two bipolar classes express different chloride transporters on their dendrites—NKCC,(a chloride accumulator) for ON cells, and KCC2 (a chloride extruder) for OFF cells Vardi et al., 2000b). Therefore, one idea is that NKCC sets the ON cell's chloride reversal potential positive to rest and that KCC2 sets the OFF cell's chloride reversal negative to rest (Vardi et al., 2000b). However, the ON bipolar axon terminal also expresses GABA-gated chloride reversal potentials that appear to be hyperpolarizing (E_{Cl} negative to rest). This would imply an intracellular gradient of chloride, which has not been found (Satoh et al., 2001; Billups and Attwell, 2002). The puzzle remains.

The bipolar response pattern carries forward via excitatory synapses onto the ganglion cell. Consequently, when a beta cell sums 100 excitatory cone signals in its center, it also sums the antagonism of their surrounds; when an alpha cell sums 625 cone signals for its center, it likewise sums their antagonism. Because the alpha surround represents many more cone surrounds than the beta surround, it is noticeably stronger (see Fig. 6.16; Freed and Sterling, 1988; Smith and Sterling, 1990). The efficacy of this lateral inhibitory circuit was demonstrated by injecting current into a horizontal cell and observing its suppression of light-evoked firing in ganglion cells (Mangel, 1991).

Lateral circuits of the IPL also contribute to the ganglion cell surround. Bipolar axons beyond the ganglion cell dendritic field excite amacrine arbors and spread signals toward the ganglion cell where they release glycine or GABA onto presynaptic bipolar terminals and ganglion cell dendrites (Pourcho and Owczarzak, 1989; Grünert and Wässle, 1990; Crooks and Kolb, 1992; Vardi and Sterling, 1994; Calkins and Sterling, 1996; Cook and McReynolds, 1998; Taylor, 1999; Flores-Herr et al., 2001; Roska and Werblin, 2001). Correspondingly, inhibitory conductances are recorded in the ganglion cell to broad stimuli but not to narrow ones (Freed and Nelson, 1994; Flores-Herr et al., 2001).

HOW RETINAL CIRCUITS SERVE VISION

NATURAL SCENES CONTAIN FINE DETAIL AT LOW CONTRAST

To appreciate how retinal circuitry serves visual performance, consider a scene from nature: a sheep among cottonwoods as viewed by a predator (wildcat) at 10 meters

(Fig. 6.18A). At this distance the retinal image contains detail that is fine with respect to the grain of the ganglion cell mosaic. For example, the dark tip of the sheep's nose projected onto the cat's retina fills a beta cell's receptive field center. But the detail in this scene differs from that in an eye chart or a newspaper where the contrast is high (white/black = 100/10). In nature, the contrast tends to be low, more like 100/90 and even 100/99, and this is apparent in the photometer reading across the scene (Fig. 6.18B; Srinivasan et al., 1982).

To create the optical *image* of a low-contrast *scene* requires lots of light. You can verify this simply by viewing fine detail at a distance where it begins to blur. Decrease the intensity, either by dimming the light or by viewing through a dark glass, and the detail is utterly lost. Increase the intensity, and further detail emerges until the light is very bright. This can hardly be news, for who is unaware that visual acuity deteriorates after sunset? But why? Consider the explanation by Albert Rose, a pioneer in video engineering.

Rose (1973) likens the retina to a black canvas on which photons paint a scene in the pointillist style. To render one picture element (pixel) black and the others white (high contrast) requires at least $N - 1$ photons, where N is the number of pixels in the array. However, to render this pixel *gray*, say an intensity 99% of the surrounding white pixels, requires the gray pixel to receive 99 photons while the others receive 100. Thus, the number of photons needed to render this scene is $100N - 1$; more generally, the lower the contrast in a scene, the more light is needed to represent it in an image.

There is an additional fact of physics to consider: photons arrive at a given point randomly in time. Their temporal fluctuation causes uncertainty regarding the true intensity at this point and is thus termed *photon noise*. As for all random processes that follow Poisson distribution, this noise (i.e., standard deviation) is proportional to the square root of the mean. Consequently, to paint a pixel pale gray (1% dimmer than its neighbors) using random photons requires not 100 photons per pixel, as with the determinate dots of a pointillist, but the *square* of 100, i.e., 10,000 photons! To represent for an instant (≈50 ms) in gray the finest detail that human optics can project onto the retinal canvas would require a single cone to register about 10,000 photons—and that is about what is available in strong daylight. In short, to register fine detail at low contrast, every possible photon must be transduced to minimize photon noise. This

Fig. 6.18. How narrow-field and wide-field arrays "filter" the transduced image of a natural scene. **A:** Photograph of a bighorn sheep among the cottonwoods. Spatial detail is represented as peaks and troughs of intensity around some mean level. **B:** Photometer scan across the middle of the image (between the arrows). Much discernible structure, e.g., fine branches, differs from the mean by only a few percent. Were this scene viewed by a mountain lion at 10 meters, one pixel would correspond roughly to one cone, and the intensity axis would correspond roughly to the signal amplitude across the cone array. Dimensions and spacings of the narrow-field and wide-field receptive fields are also indicated. **C:** Signal amplitude after filtering by narrow-field cell array. Subtraction by the surrounds of the shared signal component has reset the mean to zero; pooling by the centers has reduced the noisy fluctuations. **D:** Signal amplitude after filtering by the wide-field cell array. Again, a zero mean, but the broad pooling and sparse sampling has removed all but the coarsest spatial detail, thereby clearing the wide-field cell's dynamic range to efficiently encode motion. [Photograph by A. Pearlman; computations for B–D by R. Rao-Mirotznik and M. Eckert.]

A

B

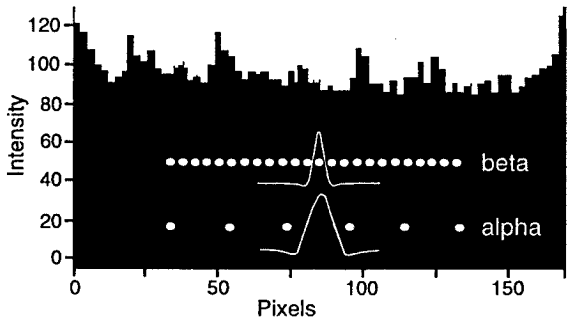
120
100
80
60
40
20
0
Intensity
beta
alpha
0
50
100
150
Pixels

C

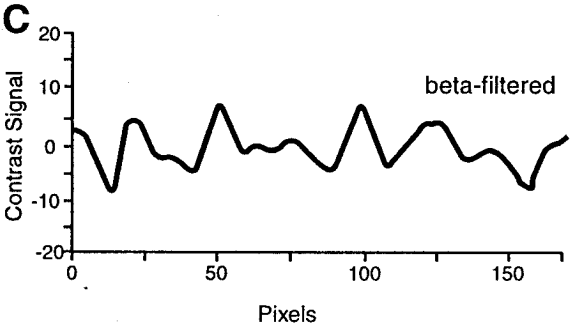
20
10
0
-10
-20
Contrast Signal
beta-filtered
0
50
100
150
Pixels

D

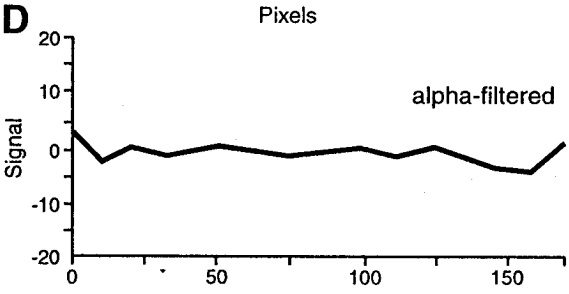
Pixels
20
10
0
-10
-20
Signal
alpha-filtered
0
50
100
150

explains why baseball players tracking a white flyball (subtending only a few cones) against a bright sky do not wear sunglasses (Sterling et al., 1992).

TO *TRANSMIT* A LOW-CONTRAST NEURAL IMAGE REQUIRES MANY SIGNALING EVENTS

One problem is that photon fluctuation in the optical image carries forward into the neural image at the level of the cones. Here, there are additional sources of noise because each step in transduction depends on random processes whose noise levels follow the same "square-root law" as photons. For example, cation channels in the cone outer segment flicker open and shut as they bind and release molecules of cGMP. The closing of a given channel at any instant does not represent a fall in the concentration of cGMP (any more than a single bump of a gas molecule on the wall of a container represents pressure) and therefore does not represent a transduction event. Only a fall in the *average* number of open channels signifies transduction; so again, the S/N ratio is $N/\sqrt{N}$. To represent at the first neural stage a 1% difference in the optical image requires 10,000 photosuppressible channels—and that is about 10% of what is available at any instant in one cone (Yau, 1994).

The next problem is that a synapse can transmit only a limited number of intensity levels. This is determined by the number of synaptic vesicles that it can modulate over its modest integration time. For example, a cone terminal has been calculated to release 100 vesicles/s at each of 20 ribbon synapses (Rao et al., 1994a), but over its integration time of about 50 ms, this is only 100 vesicles. Assuming that vesicle release is temporally random, the terminal could transmit at most 10 levels ($\sqrt{100}$). This may be somewhat fewer levels than a cone outer segment could encode given that a threshold stimulus uses 5% of its photosuppressible conductance. So how can the cone terminal match the information content at its output to the number of vesicles available for transmission? The question applies equally to the ganglion cell—which fires hundreds of spikes/s (Kuffler, 1953), but over its 100-ms integration time, only 10–20 spikes are fired. So broadly, the question is how to transfer a low-contrast signal using noisy elements of limited information capacity.

EFFICIENT CODING STRATEGIES

It is well known in the fields of information theory and image processing that a channel's capacity to transmit information increases logarithmically with S/N ratio and linearly with temporal bandwidth (Shannon and Weaver, 1949; Attick and Redlich, 1992; van Hateren, 1992; reviewed in Laughlin, 1994). So given a neural channel's limited capacity, circuits should use this capacity efficiently by maximizing the S/N ratio, removing redundancy, and subdividing the signal to segment the spatial and temporal bandwidths.

Center Mechanisms Improve the S/N Ratio. First, wherever possible, a circuit should reduce accumulated noise *before* transmitting the signal forward. This prevents noise from occupying precious channel capacity needed for the signal; it also prevents noise from being amplified, which would make its removal at a later stage more difficult. To reduce photon noise and transduction noise, adjacent cone terminals pool their signals by electrical coupling. This little reduces their amplitudes because signals in adjacent

cones are similar ("correlated"). However, it strongly attenuates noise because random fluctuations in adjacent cones are *un*correlated. Consequently, the ratio of signal to noise improves (Lamb and Simon, 1976). Pooling loses the very finest detail in the optical image (cf. Fig. 6.18B vs. Fig. 6.18C). However, some of what seems to be "fine detail" in this static image is simply photon fluctuation captured over the brief integration time of the photographic exposure. Coupling human foveal cones blurs the neural image less than than the eye blurs the optical image, yet coupling improves the S/N ratio for middle spatial frequencies by about 77% (DeVries et al., 2002).

Further pooling of cone signals occurs by convergence of cones onto bipolar cells and bipolar cells onto the ganglion cell (see Fig. 6.16). Thus, the final weighting of cone signals across the ganglion cell center is the combination of many factors: optical blur, cone-coupling, cone-to-bipolar-to-ganglion cell convergence, and the domed distribution of bipolar synapses across the ganglion cell dendritic field (see Fig. 6.16C; Freed et al., 1992; Kier et al., 1995). The net effect is a Gaussian weighting (Rodieck, 1965; Enroth-Cugell and Robson, 1966; Linsenmeier et al., 1982). This seems to be no accident but rather occurs to express another computational strategy. Such a dome-like weighting for summing partially correlated signals optimally improves the beta ganglion cell S/N ratio compared with a single cone by about 5-fold (Tsukamoto et al., 1990). As a consequence of all the preceding mechanisms to improve the S/N ratio in the ganglion cell, it can detect an optimal center spot when the contrast is less than 1% (Derrington and Lennie, 1982; Linsenmeier et al., 1982; Dhingra et al., 2003). This is just what is needed to transmit the low-contrast features in a natural scene (see Fig. 6.18).

"Surround" Mechanism Reduces Redundancy. The second image-processing strategy is to strip each cone's signal of information that is also carried by the neighbors. What they share, essentially, is the *mean* intensity across the a small region of the scene (see Fig. 6.18B). This signal component, being redundant, can be removed without loss of the essential news that a given cone (or patch of cones) is dimmer or brighter than the mean. This strategy is executed by horizontal cells: they pool signals from thousands of cone and effectively measure the local mean; then they subtract it from the cone terminal via the circuit mechansims already noted. By transmitting forward along the excitatory pathway, only the *difference between the local signal and the mean*, the proportion of the dynamic range devoted to differences is increased, and this improves the fineness with which small differences can be transferred.

Note that the ganglion cell surround seems not concerned, as commonly suggested, with "edge detection" or "image sharpening." Rather, it reflects a widely used image-processing strategy, termed *predictive coding* (Srinivasan et al., 1982). A signal averaged over some region "predicts" a value for the center; then only the difference between the predicted value and the actual value is propagated. The best theoretical prediction "weights" the values near the center most strongly because they best predict the center value. The theory also suggests that in dim light the surround should become broader and shallower to get the best prediction, and indeed this occurs in ganglion cells (Derrington and Lennie, 1982; Srinivasan et al., 1982; van Hateren, 1993).

There is computational value in giving the surround a precise shape and adjusting it for different intensities: it gives the optimal "prediction." This may explain why there are two types of horizontal cell with different degrees of coupling and the ability to

vary it. A large-scale compartmental model shows that when wide-field horizontal cells alone feed back onto the cone, the surround is too broad and shallow, and when narrow-field horizontal cells alone feed back, the surround is too narrow and deep. But when both feed back, the cone surround has the proper shape (Smith, 1995). Stronger coupling broadens and flattens the modeled cone surround. This suggests one reason to reduce dopamine in darkness—to increase horizontal cell coupling and thereby optimize predictive coding of an image as it becomes progressively noisier.

Parallel Circuits Expand Dynamic Range and Divide Spatiotemporal Bandwidth. The third image-processing strategy is to use multiple, parallel circuits, each specialized for a different aspect of the image. This permits a given circuit to devote its full channel capacity to a small component of the original signal and transmit that component efficiently. The ON and OFF cone bipolar cells provide a good example: predictive coding at the cone terminals effectively subtracts the background, thus allowing small signals to fluctuate about a mean of zero (see Fig. 6.18C). Further, circuits that excite ON bipolar cells carry signals above the mean and circuits that excite OFF bipolar cells carry signals below the mean, allowing each bipolar group to encode only half of the total deviation—with a consequent doubling of the dynamic range. This also permits the corresponding ganglion cells to use high spike rates to signal decrements as well as increments, which improves their transfer. Predictably, blocking the ON bipolar circuits with an mGluR6 agonist reduces behavioral sensitivity to light increments but not decrements (Schiller et al., 1986).

Beta and alpha cells represent another key example of parallel processing strategy to achieve efficient coding. The beta cell's narrow center and fine sampling array render it sensitive to fine spatial detail at low contrast but *in*sensitive to coarser structure; thus, the beta cell's contrast sensitivity declines at low spatial frequencies (Derrington and Lennie, 1982). The alpha cell fills this gap. Although its broad center and sparse sampling array render it insensitive to fine stationary detail, these same properties improve its sensitivity to lower spatial frequencies. It is as though the two arrays view the world through screens of different mesh (see Fig. 6.18C).

And there is another advantage: the alpha cell can do for fine temporal correlations in the visual scene what the beta cell does for fine spatial correlations. A low-contrast spot moving rapidly across the cone mosaic adds to each cone only modest numbers of extra photons. It would be impossible, by examining the output of any single cone, to distinguish this signal from photon fluctuation. However, the S/N ratio could be improved by summing the temporally correlated signals from a sequence of cones. In this case the most valuable information in the signal is that which is most sharply demarcated in time—that is, the transient. Furthermore, the larger the region that can be devoted to temporal averaging, the greater is the sensitivity to high velocity. Thus, both major features of the alpha cell—its large receptive field center and its transient response—suit it to extend the range of motion detection beyond what the beta cell can do.

Because a channel's information capacity depends linearly on temporal bandwidth and only on the log of the S/N ratio, retinal circuits could transmit more information by segmenting the temporal bandwidth than by incrementally improving S/N ratio. This might explain why ON and OFF classes of cone bipolar cell both comprise *four* different types. Because each bipolar type collects from the same set of cones, they are

bombarded by synaptic vesicles at the same rate and should have similar S/N ratios. However, by expressing different ion channels, different glutamate receptors, etc., they could carry different temporal bandwidths from the cone (Cohen and Sterling, 1990a,b). Some observations from fish support this (Saito et al., 1985), and studies of OFF bipolar cells in ground squirrel confirm it: one morphological type of bipolar cell senses cone glutamate release with fast-adapting AMPA receptors and responds transiently, whereas two other types sense the same glutamate with slow-adapting kainate receptors and respond more slowly and sustainedly (DeVries and Schwartz, 1999; DeVries, 2000). Different types of bipolar cell also vary their output, releasing glutamate quanta of different sizes and at different rates. For example, the transient ON bipolar cell in cat releases about two quanta/synapse/s to steady illumination, rising 10-fold to a flash, whereas the sustained ON bipolar cells release up to 50 quanta/synapse/s, and these quanta are much smaller than those from the transient cell (Freed, 2000a,b). Bipolar responses may be further shaped by different GABA-mediated conductances at the axon terminal (Euler and Masland, 2000; Shields et al., 2000; Freed et al., 2003). Finally, bipolar responses are shaped by intrinsic mechanisms, such as voltage-dependent potassium currents (Hu and Pan, 2002).

Ribbon Synapses Transfer Information at High Rates. When noise has been reduced by spatial pooling, when redundant information has been stripped by predictive coding, and when different temporal bandwidths have been assigned to different bipolar types, there remains another problem: how to transfer signals to the ganglion cell? Assuming vesicle release to be temporally random (reviewed in Korn and Faber, 1991; Frerking and Wilson, 1996), a ganglion cell would require many vesicles to signal a small change within the receptive field center. An alpha cell responds to a spot on the receptive field center at contrasts as low as 1% (Dhingra et al., 2003). If coding were accomplished simply by Poisson release, a 1% contrast would require at least 10,000 vesicles over the ganglion cell's integration time (100 ms). For an alpha ganglion cell bearing about 1000 bipolar (ribbon) synapses, this would require 100 vesicles/synapse/s. Smaller beta cells in cat central retina and midget ganglion cells in primate fovea, which collect 10- to 40-fold fewer synapses, are far noisier and do not respond to such low contrasts (Lee et al., 1990; Croner and Kaplan, 1995).

Additional Strategies and Circuits Needed to Optimize Signal Transfer. The retina needs additional strategies (and circuits) to optimize information transfer. For example, one expects an efficient computational strategy and corresponding circuits for color (Buchsbaum and Gottschalk, 1983; reviewed in Calkins and Sterling, 1999). Also, there may be mechanisms to reduce randomness in the timing of transmitter release (Freed et al., 2003) and mechanisms to generate strong temporal correlations in firing by adjacent ganglion cells (Meister and Berry, 1999)—both of which could improve coding efficiency. To prevent response saturation, which as noted would reduce efficiency (i.e., lose information), there needs to be mechanisms to adjust local sensitivity, i.e., mechanisms for adaptation/gain control. For example, an ON ganglion cell's sensitivity to a steady, bright stimulus to its center resets downward within about 100 ms (Cleland and Freeman, 1988). This adaptation occurs in small "subunits" across the ganglion cell center, so it cannot be due to horizontal cells, whose fields are broader than the center. Possi-

bly, the subunit represents a bipolar cell that adapts or a narrow-field amacrine cell that responds focally and feeds back negatively onto the bipolar axon terminal (see Fig. 6.14; Dong and Werblin, 1998; Roska et al., 1998; Shiells and Falk, 1999).

Beyond adapting to a first-order property, such as intensity, ganglion cells adapt to second-order properties, such as contrast (Shapley and Victor, 1978; Victor, 1987). When contrast increases, a ganglion cell adapts by (*1*) rapidly reducing response sensitivity, (*2*) shortening integration time, and (*3*) increasing firing rate. The decreased sensitivity and shortened integration time persist while high contrast remains, whereas the increased firing rate declines slowly (over tens of seconds; Smirnakis et al., 1997; Chander and Chichilnisky, 2001; Baccus and Meister, 2002). Adaptations of sensitivity and integration time depend in part on intrinsic properties of bipolar and ganglion cells (Kim and Rieke, 2001; Rieke, 2001). Contrast adaptation also occurs over different spatial scales: over <1 mm (scale of the classic center-surround) and over several millimeters (well beyond classical receptive field; Enroth-Cugell and Jakiela, 1980; Brown and Masland, 2001). The adapting signal is transferred over several millimeters by long-range, spiking amacrine cells of the sort shown in Fig. 6.9 (Cook et al., 1998; Demb et al., 1999).

These different expressions of contrast adaptation may serve slightly different functions (Demb, 2002). Shorter integration time reduces sensitivity to low temporal frequencies, which contain partially redundant components of the visual scene that can be eliminated when the signal is strong. Lower sensitivity avoids response saturation. Rapidly increasing spike rate usefully signals the new (high contrast) environment, but prolonging the high spike rate is expensive metabolically (Attwell and Laughlin, 2001). Thus, the subsequent slow reduction in spike rate would conserve energy.

Another strategy to improve signal transfer is "nonlinear spatial summation," the signature property of alpha (Y) cells (Enroth-Cugell and Robson, 1966; Hochstein and Shapley, 1976a,b; Victor et al., 1977). An alpha cell can be excited by a small spot of appropriate contrast (i.e., bright for an ON cell) placed anywhere in the receptive field center, and because spatial summation is nonlinear, the response is not "vetoed" by a similar spot of opposite contrast elsewhere in the receptive field. This renders the cell sensitive to small objects and fine patterns (i.e., high spatial frequencies) and also to "second-order" motion defined by spatiotemporal changes in contrast on a fine scale (Baker, 1999; Demb et al., 2001b). Nonlinear summation occurs because transmitter release from bipolar cells onto an alpha cell is rectified; i.e., release can increase above a basal level more than it can decrease below that level (Demb et al., 2001a; Fig. 6.19). Nonlinear responses can be evoked from the far periphery of the receptive field where they are driven by spiking amacrine cells (McIlwain, 1964, 1966; Derrington et al., 1979; Demb et al., 1999).

CIRCUITS FOR DAYLIGHT, TWILIGHT, AND STARLIGHT

Over the course of the day, intensity shifts by *ten billion-fold*, but a ganglion cell's spike rate can vary only by 100-fold (Sakmann and Creutzfeldt, 1969). To cover the huge intensity range, two fundamentally different circuits are required: a *cone bipolar circuit* for graded photoreceptor signals (see Fig. 6.15) and a *rod bipolar circuit* for binary signals (Fig. 6.20). By using gap junctions as neural switches, the two circuits can share key components (Fig. 6.21).

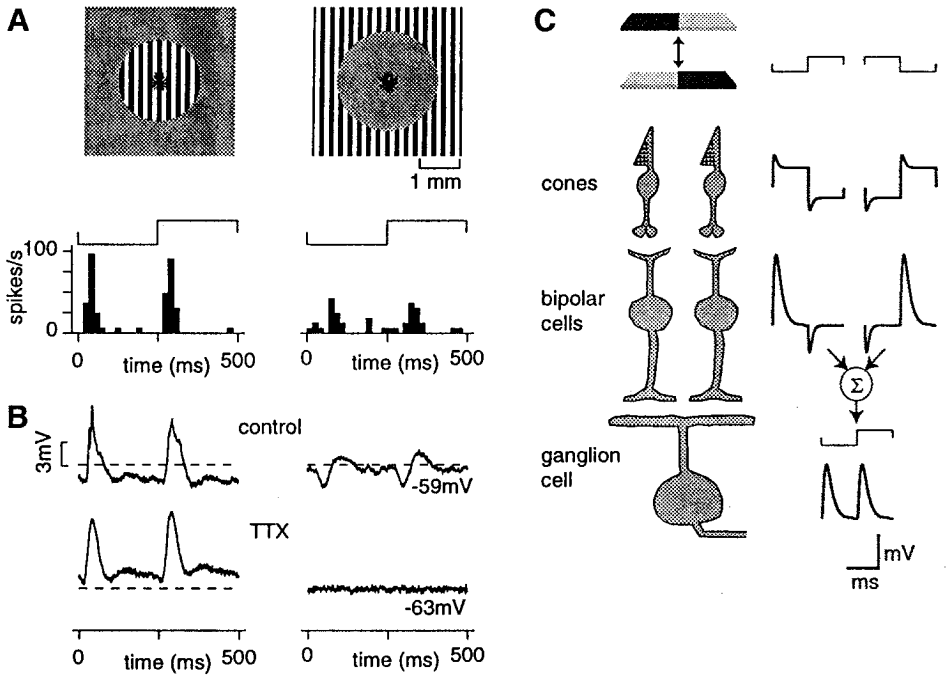

Fig. 6.19. Nonlinear subunits in the Y cell receptive field. **A:** A fine grating (≈100 micron bars) reversed contrast over the receptive field center and near surround (left) or over the far surround (right). At each reversal, a Y-type (alpha) ganglion cell fired a burst of spikes. The burst to the peripheral grating was slightly delayed relative to the burst to the central grating. [Data from Demb et al., 2001a.] **B:** Control traces show the membrane potential (spikes clipped; same cell as in **A**). At each reversal, the central grating caused a tonic hyperpolarization plus transient depolarizations; whereas the peripheral grating caused a transient hyperpolarization followed by a depolarization. When the spikes were blocked with bath-applied tetrodotoxin, the response to the central grating was little affected, but the response to the peripheral grating was abolished. This implies that the peripheral response is driven by an amacrine cell that fires TTX-sensitive spikes. (Dashed line indicates resting potential to a gray field of mean luminance.) **C:** Circuit diagram to explain the response to a central contrast-reversing grating. A cone responds linearly (equal but opposite responses to a dark and light bar); whereas a bipolar responds nonlinearly (large depolarization to a dark bar and small hyperpolarization to a light bar). A ganglion cell that sums the output of two bipolar cells, responding out-of-phase, generates a frequency-doubled response. This model ganglion cell response approximates the voltage response in **B**. Some of the nonlinearity in the bipolar cell may arise in the cone response. [Hennig et al., 2002.]

Daylight, of course, activates the cone bipolar circuit, whose key features for efficiently transferring graded signals will be recalled: coupling of cone terminals (reduce noise), negative feedback (reduce redundancy), and multiple ribbon synapses at both synaptic stages (high vesicle rates encode finely graded signals). At twilight, when ambient light intensity falls below cone threshold (100 photons cone^{-1} integration time^{-1}), this circuit fails. However, rods are now desaturating. Because there are 20 rods per cone and because a rod integrates for about 6-fold longer, signals are available from 12,000 photons transduced by rods. The 40 rod terminals immediately surrounding each

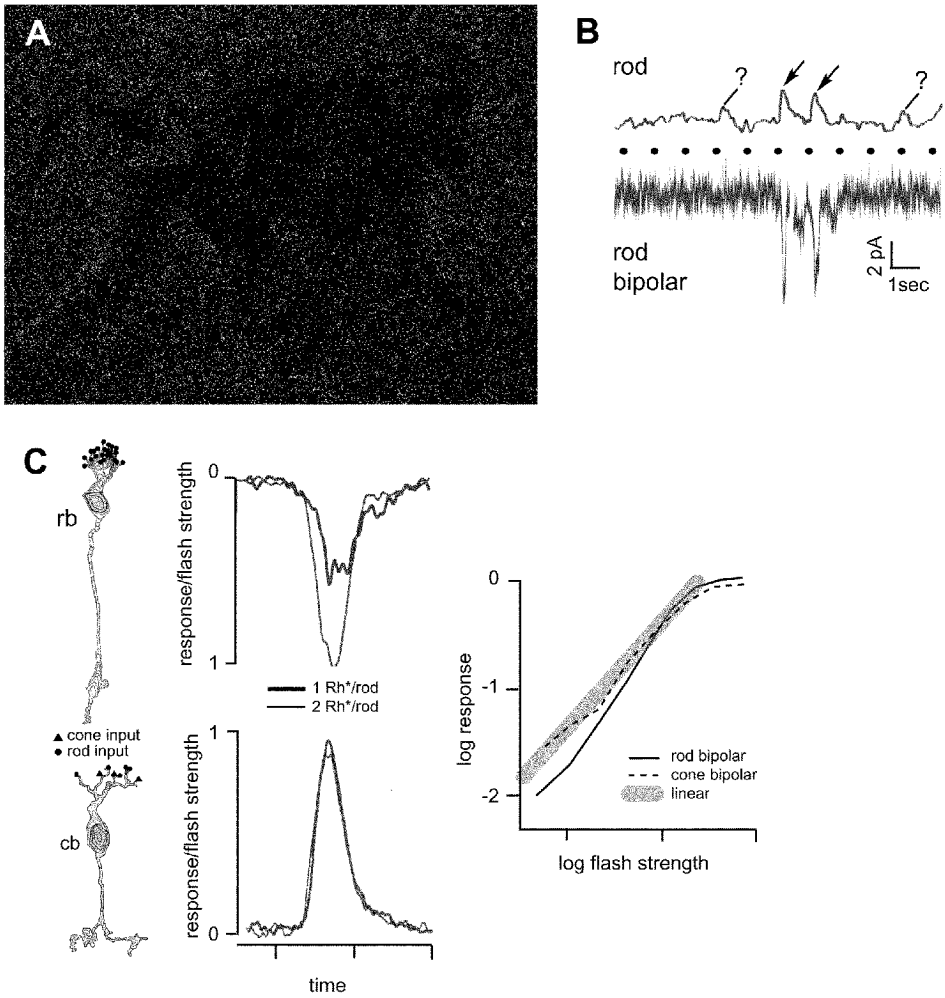

Fig. 6.20. **A:** Faint image of a baboon in starlight painted by photons in "pointillist" fashion. Probability of each pixel receiving a photon was governed by poisson distribution whose mean corresponded roughly to the intensities used by Field and Rieke (2002). **B:** Single-photon event in a rod (mouse) rises clearly above the continuous noise (arrows) only when it is considerably larger than average. Same event in the rod bipolar is faster with much improved signal-to-noise. Dotted trace represents flash timing. **C:** Left: rod bipolar cell collects chemical synapses from 20 rods and cone bipolar cell from only a few rods. However, each rod probably pools signals from neighboring rods via gap junctions. Middle: Response amplitudes normalized for flash intensity. Cone bipolar response doubles for twice the intensity, but rod bipolar response more than doubles. Right: Input/output curve for cone bipolar is essentially linear, but for rod bipolar it is clearly nonlinear. [Image, courtesy of A. Hsu and R. Smith; neurons, reprinted from Tsukamoto et al., 2001; responses replotted from Field and Rieke, 2002.]

cone terminal couple to it via gap junctions and thus inject this graded signal to be carried forward by the cone bipolar circuit (Kolb, 1977; Nelson, 1977; Smith et al., 1986; Sterling et al., 1988; DeVries and Baylor, 1995; Schneeweis and Schnapf, 1995).

When ambient intensity falls to one photon/rod/integration time, photons are spread too thinly to provide a graded signal. Thus, the cone bipolar circuit is not needed and,

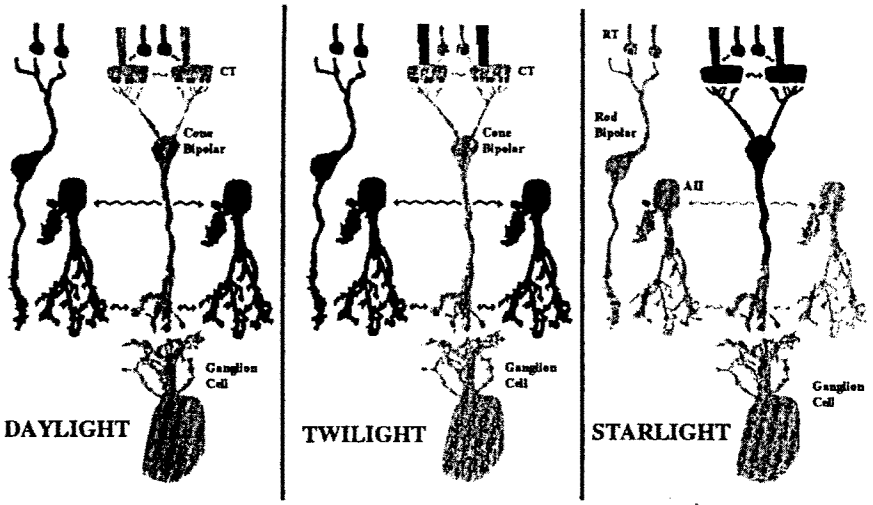

Fig. 6.21. To convey the full range of environmental intensities efficiently (i.e., minimizing neural noise and retinal thickness) requires three different circuits that partially overlap, plus three sets of gap junctions ((~~)) to switch between them. In *daylight*, cone signals are graded and thus require many ribbon synapses for transfer (both at OPL and IPL). In *twilight*, rod signals are graded and thus also require many ribbon synapses. Rods obtain access to these by turning on their gap junctions to cone terminals, in effect "parasitizing" the multiple ribbon synapses available at both stages of the cone bipolar circuit. In *starlight*, rod signals are binary and thus require only one ribbon synapse (see Fig. 6.13). The single-photon response cannot transfer via coupling to the cone terminal because the many rods lacking a photon add too much noise. Therefore, the rod-cone junction turns off, and the binary signal transfers via the rod's single ribbon synapse to the rod bipolar cell. The latter's response will be coarsely graded over some part of the intensity range (due to rod convergence) and thus will require multiple ribbon synapses—which are present in the rod bipolar terminal. The AII cell's response will be more finely graded (due to rod bipolar convergence) and thus will require yet more ribbon synapses. The AII cell obtains access to these by turning on its gap junctions with cone bipolar terminals. Coupling the AII cells, indirectly via the cone bipolar terminals and also directly via AII–AII junctions, spreads current widely enough to enlarge the ganglion cell's summation area well beyond its dendritic tree. This improves the signal/noise ratio in very dim light but would degrade acuity in brighter light. Therefore, both sets of junction are regulated and presumably uncouple in twilight and daylight. See text.

worse, the coupling of many receptors that lack photons to one rod that does capture a photon would inject continuous "dark noise" from the transduction cascade. Noise in this rod would increase by the square root of the number of noisy rods coupled to it (i.e., ≈6-fold), and this would obliterate its single Rh* response. To protect the Rh* response from noise and to preserve its amplitude, the rod-cone gap junctions should uncouple at very low intensities and switch over to the rod bipolar circuit (Smith et al., 1986). Although rod-cone uncoupling has not been demonstrated directly, two rod pathways have been demonstrated psychophysically: a fast one for middle intensities (twilight) and a slower one for lowest intensities (starlight). Because their intensity ranges overlap for certain rates of a flickering stimulus, they can be made to cancel (Stockman et al., 1995). Presumably these pathways correspond, respectively, to the rod-

driven cone bipolar circuit and the rod bipolar circuit (see Fig. 6.21; reviewed in Sharpe and Stockman, 1999; Bloomfield and Dacheux, 2001).

The starlight circuit's first task is to transfer a binary signal: 0 or 1 Rh*. "0" is represented by tonic vesicle release from the rod's single ribbon synapse, and "1" is represented by a pause in release. However, assuming release is temporally random, some extra-long intervals between quanta will occur that the bipolar cell might "mistake" for a pause. The release rate should be high enough to prevent this source of spurious single-photon signals. A model of the circuit suggests that 50–100 vesicles/s might be sufficient (Rao et al., 1994b; van Rossum and Smith, 1998). This roughly fits measured rates for ribbon synapses (as noted earlier) and suggests why the rod bipolar circuit requires only one ribbon synapse at the first stage.

However, at the next stage, 20 to 120 rods converge on a rod bipolar cell, and this exposes another problem for processing starlight signals. Only one of these rods is likely to carry an Rh* response, but the others will carry noise, which, if transferred to the rod bipolar cell, would increase its noise (again, as the square root of the convergence)—and swamp the single Rh* response in the bipolar cell. To prevent this, the rod synapse acts nonlinearly, amplifying large signals more than small ones (see Fig. 6.20). This removes the small, noisy events by thresholding (van Rossum and Smith, 1998; Field and Rieke, 2002). But the Rh* events in a rod vary in amplitude, many hardly rising above the noise. Thresholding removes the noise but also these small photon signals, a process that has been vividly termed "throwing out the smaller babies with the bath" (Wilson, 2002). You might think that discarding photon events in dim light would be a bad strategy. But because small events are much more likely to be noise than photons, it actually proves to be an excellent computational bet, improving S/N by more than 350-fold (Field and Rieke, 2002)! At higher intensities, where every rod captures at least one photon, linear amplification is a better bet, and indeed a direct pathway from rods to OFF bipolar cells acts linearly (Soucy et al., 1998; Hack et al., 1999; Tsukamoto et al., 2001; Field and Rieke, 2002).

At all except the lowest intensities, the rod bipolar cell's large convergence gives it, not a binary signal, but a coarsely graded one. Consistent with this, instead of using one ribbon (as at the rod output), the rod bipolar axon uses 30 ribbon synapses at its output (Sterling et al., 1988). The AII cell collecting from about 30 rod bipolar cells needs to transfer a more finely graded signal, and for this it couples electrically to cone bipolar terminals that contribute 150–2000 synapses to a ganglion cell. Thus, the overall pattern of the rod bipolar circuit is a stepwise expansion in number of ribbon synapses to match the stepwise increase in signal pooling. The rod bipolar circuit's "parasitic" use of the cone bipolar terminals as final input to ganglion cells saves space, which, in a tissue constrained to be thin ($\leq$250 μm), is at a premium.

Tuning the Circuits. Rod circuits, like the cone circuit, are also tuned for efficiency at different intensities by modulated coupling (reviewed in Sterling, 1995; Demb and Pugh, 2002). In twilight, to preserve spatial acuity, ganglion cell receptive field centers should be narrow. But if cone bipolar axons were coupled to AII cells, cone signals would spread laterally in the AII network and degrade spatial acuity (Sterling, 1983). Therefore, the cone bipolar–AII junctions might remain uncoupled until starlight, when the noisy optical image can be transmitted most efficiently by expanding the gan-

glion cell center (Barlow et al., 1957). Indeed, AII–cone bipolar junctions *do* uncouple when cGMP rises within the bipolar cell in response to nitric oxide production (Mills and Massey, 1995), and this mechanism may serve the transition to starlight intensities. Also in starlight, as noted, rods should uncouple from cones, but whether they do is not established (Schneeweis and Schnapf, 1999).

Finally, in starlight, the AII–AII junctions should couple, but to a variable degree. This coupling reduces noise by signal averaging, and also interacts with the AII cell's voltage-sensitive mechanism (Nelson, 1982; Boos et al., 1993; Veruki and Hartveit, 2002). This mechanism, by "thresholding," may remove noise that would otherwise swamp the Rh* signals when 30 rod bipolar cells converge on an AII cell (Freed et al., 1987; Smith and Vardi, 1995). However, it could also spread spurious spikes through the AII network. A computational model suggests that by matching coupling to the noise level (which shifts with light intensity), the circuit can maximize thresholding and minimize spurious spiking (Smith and Vardi, 1995). Dopaminergic synapses on the AII soma (Pourcho, 1982; Voight and Wässle, 1987) uncouple AII–AII junctions (Hampson et al., 1992), and because retinal dopamine declines in darkness, AII coupling should rise. Of course, once neuromodulators of coupling are identified, such as NO and dopamine, the question arises: What signals and effectors modulate the modulators? These are concerns for the future.

CONCLUDING REMARKS

We have noted that once photons are transduced, most of their information reaches the brain. Retinal circuits achieve this astonishing efficiency in part by finely dividing responsibility. Thus, we have distinguished circuits that (*1*) divide the dynamic range around the local mean intensity (ON and OFF), (*2*) divide the spatiotemporal bandwidth (beta vs. alpha, P vs. M), (*3*) divide the color spectrum (blue-yellow, red-green), and (*4*) divide vast diurnal shifts in intensity (cone bipolar vs. rod bipolar). Also key to efficient forward transfer are the ribbon synapses that can fuse vesicles and reload at very high rates, and also contributing are various linear mechanisms that reduce noise at each stage of summation by spatial averaging and optimal weighting.

Several *nonl*inear mechanisms were noted: "thresholding" for the single Rh* signal at the rod output (Field and Rieke, 2002); thresholding of the multi-Rh* signal by the AII cell (Smith and Vardi, 1995); rectification by the cone bipolar cells, which produces "nonlinear subunits"; and mechanisms for fast and slower "contrast gain control" (reviewed in Demb, 2002). Intuitively, nonlinear mechanisms should involve amacrine cells—with their many different types, their rich possibilities for chemical signaling, and their spiking behavior. So far we know little about amacrine synaptic circuits *between* cells or about their second-messenger circuits *within* cells. These are puzzles for the future. However, rapid technical advances in unraveling the retina's synaptic organization, new methods for *in vitro* recording, and molecular biology lead one to think that the future is near.

REFERENCES for Retina
In: The Synaptic Organization of the Brain (Shepherd GM ed)
New York: Oxford University Press.

Ahnelt, P., Keri, C., and Kolb, H. 1990. Identification of pedicles of putative blue-sensitive cones in the human retina. J. Comp. Neurol. 293:39-53.

Amthor, F.R., Takahashi, E.S., and Oyster, C.W. 1989a. Morphologies of rabbit retinal ganglion cells with complex receptive fields. J. Comp. Neurol. 280:97-121.

Amthor, F.R., Takahashi, E.S., and Oyster, C.W. 1989b. Morphologies of rabbit retinal ganglion cells with concentric receptive fields. J. Comp. Neurol. 280:72-96.

Applebury, M.L., Antoch, M.P., Baxter, L.C., Chun, L.L., Falk, J.D., Farhangfar, F., Kage, K., Krzystolik, M.G., Lyass, L.A., and Robbins, J.T. 2000. The murine cone photoreceptor: a single cone type expresses both S and M opsins with retinal spatial patterning. Neuron 27:513-523.

Atick, J.J. and Redlich, A.N. 1992. What does the retina know about natural scenes? Neural Comp. 4:196-210.

Attwell, D. and Laughlin, S. 2001. An energy budget for signaling in the grey matter of the brain. Journal of Cerebral Blood Flow and Metabolism 21:1133-1145.

Awatramani, G.B. and Slaughter, M.M. 2001. Intensity-dependent, rapid activation of presynaptic metabotropic glutamate receptors at a central synapse. J. Neurosci. 21:741-749.

Ayoub, G.S., Korenbrot, J.I., and Copenhagen, D.R. 1989. The release of endogenous glutamate from isolated cone photoreceptors of the lizard. Neurosci. Res. (Suppl.) 10:547-556.

Azzopardi, P. and Cowey, A. 1993. Preferential representation of the fovea in the primary visual cortex. Nature 361:719-721.

Baccus, S.A. and Meister, M. 2002. Fast and slow contrast adaptation in retinal circuitry. Neuron 36:909-919.

Baker, L.P., Nielson, M.D., Impey, S., Hacker, B.M., Poser, S.W., Chan, M.Y.M., and Storm, D.R. 1999. Regulation and immunohistochemical localization of BetaGamma-stimulated adenylyl cyclases in mouse hippocampus. J. Neurosci. 19:180-192.

Barlow, H.B. 1953. Summation and inhibition in the frog's retina. J. Physiol. 119:69-88.

Barlow, H.B. 1982. General principles: The senses considered as physical instruments. Chapter 1 in Cambridge texts in the physiological sciences 3: The senses. Edited by H.B. Barlow and J.D. Mollon. Cambridge University Press, Cambridge, England.

Barlow, H.B., Fitzhugh, R., and Kuffler, S.W. 1957. Change of organization in the receptive fields of the cat's retina during dark adaptation. J. Physiol. 137:338-354.

Barlow, H.B. and Levick, W.R. 1965. The mechanism of directionally selective units in rabbit's retina. J. Physiol. 178:477-504.

Barlow, H.B., Levick, W.R., and Yoon, M. 1971. Responses to single quanta of light in retinal ganglion cells of the cat. Vision Res. S3:87-101.

Baseler, H.A., Brewer, A.A., Sharpe, L.T., Moreland, A.B., Jagle, H., and Wandell, B.A. 2002. Reorganization of human cortical maps caused by inherited photoreceptor abnormalities. Nat. Neurosci. 5:364-370.

Baylor, D.A., Fuortes, M.G.F., and O'Bryan, P.M. 1971. Receptive fields of cones in the retina of the turtle. J. Physiol. 214:265-294.

Baylor, D.A., Nunn, B.J., and Schnapf, J.L. 1984. The photocurrent, noise and spectral sensitivity of rods of the monkey *Macaca fascicularis*. J. Physiol. 357:575-607.

Berson, D.M., Dunn, F.A., and Takao, M. 2002. Phototransduction by retinal ganglion cells that set the circadian clock. Science 295:1070-1073.

Berson, D.M., Isayama, T., and Pu, M. 1999. The eta ganglion cell type of cat retina. J. Comp. Neurol. 408:204-219.

Berson, D.M., Pu, M., and Famiglietti, E.V. 1998. The zeta cell: a new ganglion cell type in cat retina. J. Comp. Neurol. 399:269-288.

Billups, D. and Attwell, D. 2002. Control of intracellular chloride concentratoin and GABA response polarity in rat retinal ON bipolar cells. J. Physiol. 545:183-198.

Bloomfield, S.A. 1992. Relationship between receptive and dendritic field size of amacrine cells in the rabbit retina. J. Neurophysiol. 68:711-725.

Bloomfield, S.A. and Dacheux, R.F. 2001. Rod vision: pathways and processing in the mammalian retina. Prog. Ret. & Eye Res. 20:351-384.

Bloomfield, S.A., Xin, D., and Osborne, T. 1997. Light-induced modulation of coupling between AII amacrine cells in the rabbit retina. Vis. Neurosci. 14:565-576.

Bodnarenko, S.R., Jeyarasasingam, G., and Chalupa, L. 1995. Development and regulation of dendritic stratification in retinal ganglion cells by glutamate-mediated afferent activity. J. Neurosci. 15:7037-7045.

Bolz, J., Thier, P., Voight, T., and Wässle, H. 1985. Action and localization of glycine and taurine in the cat retina. J. Physiol. 362:395-413.

Boos, R., Schneider, H., and Wässle, H. 1993. Voltage- and transmitter-gated currents of AII-amacrine cells in a slice preparation of the rat retina. J. Neurosci. 13:2874-2888.

Borges, S., Gleason, E., Turelli, M., and Wilson, M. 1995. The kinetics of quantal transmitter release from retinal amacrine cells. Proc. Natl. Acad. Sci. USA 92:6896-6900.

Bowmaker, J.K., Govardovskii, V.I., Shukolyukov, S.A., Zueva, L.V., Hunt, D.M., Sideleva, V.G., and Smirnova, O.G. 1994. Visual pigments and the photic environment: the cottoid fish of lake Baikal. Vision Res. 34:591-605.

Boycott, B.B. and Dowling, J.E. 1969. Organization of the primate retina: Light microscopy. Philos. Trans. R. Soc. Lond. (Biol) 255:109-184.

Boycott, B.B. and Wässle, H. 1974. The morphological types of ganglion cells of the domestic cat's retina. J. Physiol. 240:397-419.

Boycott, B.B. and Wässle, H. 1991. Morphological classification of bipolar cells of the primate retina. Eur. J. Neurosci. 3:1069-1088.

Brainard, D.H., Roorda, A., Yamauchi, Y., Calderone, J.B., Metha, A., Neitz, M., Neitz, J., Williams, D.R., and Jacobs, G.H. 2000. Functional consequences of the relative numbers of L and M cones. J. Opt. Soc. Am. A 17:607-614.

Brandstätter, J.H., Koulen, P., Kuhn, R., van der Putten, H., and Wässle, H. 1996. Compartmental localization of a metabotropic glutamate receptor

(mGluR7): two different active sites at a retinal synapse. J. Neurosci. 16:4749-4756.
Brecha, N., Johnson, D., Peichl, L., and Wässle, H. 1988. Cholinergic amacrine cells of the rabbit retina contain glutamate decarboxylase and gamma-aminobutyrate immunoreactivity. Proc. Natl. Acad. Sci. USA 85:6187-6191.
Brown, S.P. and Masland, R.H. 2001. Spatial scale and cellular substrate of contrast adaptation by retinal ganglion cells. Nat. Neurosci. 4:44-51.
Buchsbaum, G. and Gottschalk, A. 1983. Trichromacy, opponent colours coding and optimum colour information transmission in the retina. Proc. R. Soc. Lond. B 220:89-113.
Burgi, P.-Y. and Grzywacz, N.M. 1994. Model for the pharmacological basis of spontaneous synchronous activity in developing retinas. J. Neurosci. 14:7426-7439.
Burkhardt, D.A. 1994. Light adaptation and photopigment bleaching in cone photoreceptors in situ in the retina of the turtle. J. Neurosci. 14:1091-1105.
Burns, M.E. and Lamb, T.D. 2003. Visual transduction by rod and cone photoreceptors. Visual Neurosciences. Edited by L. Chalupa and J.S. Werner. MIT Press, Cambridge MA.
Burris, C., Klug, K., Ngo, I.-T., Sterling, P., and Schein, S. 2002. How Müller glial cells in macaque fovea coat and isolate the synaptic terminals of cone photoreceptors. J. Comp. Neurol. 453:100-111.
Cajal, S.R. 1972. The structure of the retina. Edited by S.A. Thorpe and M. Glickstein. Charles C. Thomas, Springfield IL.
Calkins, D. and Sterling, P. 2003. Synaptic connections of OFF parasol ganglion cells in primate fovea. (Submitted) .
Calkins, D.J., Schein, S., Tsukamoto, Y., and Sterling, P. 1994. M and L cones in *Macaque* fovea connect to midget ganglion cells via different numbers of excitatory synapses. Nature 371:70-72.
Calkins, D.J. and Sterling, P. 1996. Absence of spectrally specific lateral inputs to midget ganglion cells in primate retina. Nature 381:613-615.
Calkins, D.J. and Sterling, P. 1999. Evidence that circuits for spatial and color vision segregate at the first retinal synapse. Neuron 24:313-321.
Calkins, D.J., Tsukamoto, Y., and Sterling, P. 1996. Foveal cones form basal as well as invaginating contacts with diffuse ON bipolar cells. Vision Res. 36:3373-3381.
Casini, G. and Brecha, N.C. 1992. Colocalization of vasoactive intestinal polypeptide and GABA immunoreactivities in a population of wide-field amacrine cells in the rabbit retina. Vis. Neurosci. 8:373-378.
Chander, D. and Chichilnisky, E.J. 2001. Adaptation to temporal contrast in primate and salamander retina. J. Neurosci. 21:9904-9916.
Chun, M.-H., Grünert, U., Martin, P.R., and Wässle, H. 1996. The synaptic complex of cones in the fovea and in the periphery of the macaque monkey retina. Vision Res. 36:3383-3395.
Chun, M.-H. and Wassle, H. 1989. GABA-like immunoreactivity in the cat retina: electron microscopy. J. Comp. Neurol. 279:55-67.
Cleland, B.G., Dubin, M.W., and Levick, W.R. 1971. Sustained and transient neurones in the cat's retina and lateral geniculate nucleus. J. Physiol. 217:473-496.
Cleland, B.G. and Freeman, A.W. 1988. Visual adaptation is highly localized in the cat's retina. J. Physiol. 404:591-611.
Cleland, B.G. and Levick, W.R. 1974. Brisk and sluggish concentrically organized ganglion cells in the cat's retina. J. Physiol. (Lond.) 240:421-456.
Cohen, E. and Sterling, P. 1986. Accumulation of [^{3}H] glycine by cone bipolar neurons in the cat retina. J. Comp. Neurol. 250:1-7.
Cohen, E. and Sterling, P. 1990a. Convergence and divergence of cones onto bipolar cells in the central area of cat retina. Philos. Trans. R. Soc. Lond. (Biol) 330:323-328.
Cohen, E. and Sterling, P. 1990b. Demonstration of cell types among cone bipolar neurons of cat retina. Philos. Trans. R. Soc. Lond. B 330:305-321.
Cohen, E. and Sterling, P. 1992. Parallel circuits from cones to the on-beta ganglion cell. Eur. J. Neurosci. 4:506-520.
Cohen, E.D. 2001. Synaptic mechanisms shaping the light-response in retinal ganglion cells. Prog. Brain Res. 131:215-228.
Cohen, E.D., Zhou, Z.J., and Fain, G.L. 1994. Ligand-gated currents of alpha and beta ganglion cells in the cat retinal slice. J. Neurophysiol. 72(3):1260-1269.
Cook, P.B., Lukasiewicz, P.D., and McReynolds, J.S. 1998. Action potentials are required for the lateral transmission of glycinergic transient inhibition in the amphibian retina. J. Neurosci. 18:2301-2308.
Cook, P.B. and McReynolds, J.S. 1998. Modulation of sustained and transient lateral inhibitory mechanisms in the mudpuppy retina during light adaptation. J. Neurophysiol. 79:197-204.
Cook, P.B. and Werblin, F.S. 1994. Spike initiation and propagation in wide field transient amacrine cells of the salamander retina. J. Neurosci. 14:3852-3861.
Copenhagen, D.R. and Jahr, C.E. 1989. Release of endogenous excitatory amino acids from turtle photoreceptors. Nature 341:536-539.
Croner, L.J. and Kaplan, E. 1995. Receptive fields of P and M ganglion cells across the primate retina. Vision Res. 35:7-24.
Crooks, J. and Kolb, H. 1992. Localization of GABA, glycine, glutamate and tyrosine hydroxylase in the human retina. J. Comp. Neurol. 315:287-302.
Crowell, J.A. and Banks, M.S. 1988. Physical limits of grating visibility: fovea and periphery. Invest. Ophthalmol. Vis. Sci. 29:139. [Abstract]
Cueva, J.G., Haverkamp, S., Reimer, R.J., Edwards, R., Wässle, H., and Brecha, N.C. 2002. Vesicular gamma-aminobutyric acid transporter expression in amacrine and horizontal cells. J. Comp. Neurol. 445:227-237.
Curcio, C.A., Allen, K.A., Sloan, K.R., Lerea, C.L., Hurley, J.B., Klock, I.B., and Milam, A.H. 1991. Distribution and morphology of human cone photoreceptors stained with anti-blue opsin. J. Comp. Neurol. 312:610-624.
Curcio, C.A., Sloan, K.R., Kalina, R.E., and Hendrickson, A.E. 1990. Human photoreceptor topography. J. Comp. Neurol. 292:497-523.
Dacey, D., Packer, O.S., Diller, L., Branard, D., Peterson, B., and Lee, B. 2000. Center surround receptive field structure of cone bipolar cells in primate retina. Vision Res. 40:1801-1811.
Dacey, D.M. 1989a. Axon-bearing amacrine cells of the Macaque monkey retina. J. Comp. Neurol. 284:275-293.
Dacey, D.M. 1989b. Monoamine-accumulating ganglion cell type of the cat's retina. J. Comp. Neurol. 288:59-80.

Dacey, D.M. 1990. The dopaminergic amacrine cell. J. Comp. Neurol. 301:461-489.
Dacey, D.M. 1993. The mosaic of midget ganglion cells in the human retina. J. Neurosci. 13:5334-5355.
Dacey, D.M. 1996. Circuitry for color coding in the primate retina. Proc. Natl. Acad. Sci. USA 93:582-588.
Dacey, D.M. and Brace, S. 1992. A coupled network for parasol but not midget ganglion cells in the primate retina. Vis. Neurosci. 9:279-290.
Dacey, D.M. and Lee, B.B. 1994. The 'blue-on' opponent pathway in primate retina originates from a distinct bistratified ganglion cell type. Nature 367:731-735.
Dacey, D.M., Lee, B.B., Stafford, D.K., Pokorny, J., and Smith, V.C. 1996. Horizontal cells of the primate retina: cone specificity without spectral opponency. Science 271:656-659.
Dacheux, R.F. and Raviola, E. 1986. The rod pathway in the rabbit retina: a depolarizing bipolar and amacrine cell. J. Neurosci. 6(2):331-345.
Dacheux, R.F. and Raviola, E. 1995. Light responses from one type of ON-OFF amacrine cells in the rabbit retina. J. Neurophysiol. 74:2460-2467.
Dann, J.F., Buhl, E.H., and Peichl, L. 1988. Postnatal dendritic maturation of alpha and beta ganglion cells in cat retina. J. Neurosci. 8:1485-1499.
Daw, N.W. and Wyatt, H.J. 1974. Raising rabbits in a moving visual environment: An attempt to modify directional sensitivity in the retina. J. Physiol. 240:309-330.
de la Villa, P., Kurahashi, T., and Kaneko, A. 1995. L-glutamate-induced responses and cGMP-activated channels in three subtypes of retinal bipolar cells dissociated from the cat. J. Neurosci. 15:3571-3582.
de Monasterio, F.M. 1978. Properties of concentrically organized X and Y ganglion cells of macaque retina. J. Neurophysiol. 41:1394-1417.
de Monasterio, F.M., Schein, S.J., and McCrane, E.P. 1981. Staining of blue-sensitive cones of the macaque retina by a fluorescent dye. Science 213:1278-1281.
de Ruyter van Steveninck, R. and Laughlin, S.B. 1996. The rate of information transfer at graded-potential synapses. Nature 379:642-645.
Demb, J.B. 2002. Multiple mechanisms for contrast adaptation in the retina. Neuron 36:781-783.
Demb, J.B., Haarsma, L., Freed, M.A., and Sterling, P. 1999. Functional circuitry of the retinal ganglion cell's nonlinear receptive field. J. Neurosci. 19:9756-9767.
Demb, J.B. and Pugh, E.N. 2002. Connexin 36 forms synapses essential for night vision. Neuron 36:551-553.
Demb, J.B., Zaghloul, K., Haarsma, L., and Sterling, P. 2001a. Bipolar cells contribute to nonlinear spatial summation in the brisk transient (Y) ganglion cell in mammalian retina. J. Neurosci. 21:7447-7454.
Demb, J.B., Zaghloul, K., and Sterling, P. 2001b. Cellular basis for the response to second-order motion cues in Y retinal ganglion cells. Neuron 32:711-721.
Derrington, A.M. and Lennie, P. 1982. The influence of temporal frequency and adaptation level on receptive field organization of retinal ganglion cells in cat. J. Physiol. 333:343-366.
Derrington, A.M., Lennie, P., and Wright, M.J. 1979. The mechanism of peripherally evoked responses in retinal ganglion cells. J. Physiol. 289:299-310.
DeVries, S.H. 2000. Bipolar cells use kainate and AMPA receptors to filter visual information into separate channels. Neuron 28:847-856.
DeVries, S.H. and Baylor, D.A. 1995. An alternative pathway for signal flow from rod photoreceptors to ganglion cells in mammalian retina. Proc. Natl. Acad. Sci. USA 92:10658-10662.
DeVries, S.H., Qi, X., Smith, R.G., Makous, W., and Sterling, P. 2002. Electrical coupling between mammalian cones. Curr. Biol. 12:1900-1907.
DeVries, S.H. and Schwartz, E.A. 1989. Modulation of an electrical synapse between solitary pairs of catfish horizontal cells by dopamine and second messengers. J. Physiol. 414:351-375.
DeVries, S.H. and Schwartz, E.A. 1999. Kainate receptors mediate synaptic transmission between cones and 'Off' bipolar cells in a mammalian retina. Nature 397:157-160.
Dhingra, A., Jiang, M., Wang, T.-L., Lyubarsky, A., Savchenko, A., Bar-Yehuda, T., Sterling, P., Birnbaumer, L., and Vardi, N. 2002. Light response of retinal ON bipolar cells requires a specific splice variant of Gao. J. Neurosci. 22:4878-4884.
Dhingra, A., Lyubarsky, A., Jiang, M., Pugh Jr., E.N., Birnbaumer, L., Sterling, P., and Vardi, N. 2000. The light response of ON bipolar neurons requires G_{ao}. J. Neurosci. 20:9053-9058.
Dhingra, N.K., Kao, Y.-H., Sterling, P., and Smith, R.G. 2003. Contrast threshold of a brisk-transient ganglion cell. J. Neurophysiol. 89:2360-2369
Dong, C.-J. and Werblin, F.S. 1998. Temporal contrast enhancement via GABAC feedback at bipolar terminals in the tiger salamander retina. J. Neurophysiol. 79:2171-2180.
Dowling, J.E. 1986. Dopamine: A retinal neuromodulator? Trends Neurosci. 9:236-240.
Dowling, J.E. and Boycott, B.B. 1966. Organization of the primate retina: electron microscopy. Proc. R. Soc. Lond. B 166:80-111.
Dowling, J.E. and Cowan, W.M. 1966. An electron microscope study of normal and degenerating centrifugal fiber terminals in the pigeon retina. Z. Zellforsch. 71:14-28.
Dubin, H. 1976. The inner plexiform layer of the vertebrate retina: a quantitative and comparative electron microscopic analysis. J. Comp. Neurol. 140:479-506.
Easter, S.S. and Stuermer, C. 1984. An evaluation of the hypothesis of shifting terminals in goldfish optic tectum. J. Neurosci. 4:1052-1063.
Eckert, M.P. and Buchsbaum, G. 1993a. Effect of tracking strategies on the velocity structure of two-dimensional image sequences. J. Opt. Soc. Am. 10:1582-1585.
Eckert, M.P. and Buchsbaum, G. 1993b. Efficient coding of natural time varying images in the early visual system. Philos. Trans. R. Soc. Lond. B 339:385-395.
Enoch, J.M. 1981. Retinal receptor orientation and photoreceptor optics. Vertebrate photoreceptor optics. Edited by J.M. Enoch and F.L.Jr. Tobey. Springer-Verlag, Berlin.

Enroth-Cugell, C. and Jakiela, H.G. 1980. Suppression of cat retinal ganglion cell responses by moving patterns. J. Physiol. 302:49-72.
Enroth-Cugell, C. and Robson, J.G. 1966. The contrast sensitivity of retinal ganglion cells of the cat. J. Physiol. 187:517-552.
Enz, R., Brandstätter, J.H., Wässle, H., and Bormann, J. 1996. Immunocytochemical localization of $GABA_C$ receptor rho subunits in the mammalian retina. J. Neurosci. 16:4479-4490.
Euler, T., Detwiler, P.B., and Denk, W. 2002. Directionally selective calcium signals in dendrites of starburst amacrine cells. Nature 418:845-852.
Euler, T. and Masland, R.H. 2000. Light-evoked responses of bipolar cells in a mammalian retina. J. Neurophysiol. 83:1817-1829.
Euler, T., Schneider, H., and Wässle, H. 1996. Glutamate responses of bipolar cells in a slice preparation of the rat retina. J. Neurosci. 16:2934-2944.
Famiglietti Jr., E.V. and Kolb, H. 1976. Structural basis for ON- and OFF-center responses in retinal ganglion cells. Science 194:193-195.
Famiglietti, E.V. 1991. Synaptic organization of starburst amacrine cells in rabbit retina: analysis of serial thin sections by electron microscopy and graphic reconstruction. J. Comp. Neurol. 309:40-70.
Famiglietti, E.V. 1992a. Dendritic co-stratification of ON and ON-OFF directionally selective ganglion cells with starburst amacrine cells in rabbit retina. J. Comp. Neurol. 324:322-335.
Famiglietti, E.V. 1992b. Polyaxonal amacrine cells of rabbit retina: size and distribution of PA1 cells. J. Comp. Neurol. 316:406-421.
Ferster, D. 1988. Spatially opponent excitation and inhibition in simple cells of the cat visual cortex. J. Neurosci. 8:1172-1180.
Field, G.D. and Rieke, F. 2002. Nonlinear signal transfer from mouse rods to bipolar cells and implications for visual sensitivity. Neuron 34:773-785.
Fischer, K.F., Lukasiewicz, P.D., and Wong, R.O.L. 1998. Age-dependent and cell class-specific modulation of retinal ganglion cell bursting activity by GABA. J. Neurosci. 18:3767-3778.
Fletcher, E.L., Hack, I., Brandstätter, J.H., and Wässle, H. 2000. Synaptic localization of NMDA receptor subunits in the rat retina. J. Comp. Neurol. 420:98-112.
Flores-Herr, N., Protti, D.A., and Wässle, H. 2001. Synaptic currents generating the inhibitory surroound of ganglion cells in the mammalian retina. J. Neurosci. 21:4852-4863.
Frank, B.D. and Hollyfield, J.G. 1987. Retinal ganglion cell morphology in the frog, *Rana pipiens*. J. Comp. Neurol. 266:413-434.
Freed, M.A. 1992. GABAergic circuits in the mammalian retina. Progress in Brain Research. Edited by R.R. Mize, R.E. Marc, and A.M. Sillito. Elsevier Science Publishers.
Freed, M.A. 2000a. Parallel cone bipolar pathways to ganglion cell use different rates and amplitudes of quantal excitation. J. Neurosci. 20:3956-3963.
Freed, M.A. 2000b. Rate of quantal excitation to a retinal ganglion cell evoked by sensory input. J. Neurophysiol. 83:2956-2966.
Freed, M.A. and Nelson, R. 1994. Conductances evoked by light in the ON-beta ganglion cell of the cat retina. Vis. Neurosci. 11:261-269.
Freed, M.A., Pflug, R., Kolb, H., and Nelson, R. 1996. ON-OFF amacrine cells in cat retina. J. Comp. Neurol. 364:556-566.
Freed, M.A., Smith, R.G., and Sterling, P. 1987. Rod bipolar array in the cat retina: pattern of input from rods and GABA-accumulating amacrine cells. J. Comp. Neurol. 266:445-455.
Freed, M.A., Smith, R.G., and Sterling, P. 1992. Computational model of the on-alpha ganglion cell receptive field based on bipolar circuitry. Proc. Natl. Acad. Sci. USA 89:236-240.
Freed, M.A., Smith, R.G., and Sterling, P. 2003. Timing of quantal release from the retinal bipolar terminal is regulated by a feedback circuit. (Submitted) .
Freed, M.A. and Sterling, P. 1988. The ON-alpha ganglion cell of the cat retina and its presynaptic cell types. J. Neurosci. 8:2303-2320.
Frerking, M. and Wilson, M. 1996. Effects of variance in mini amplitude on stimulus-evoked release: a comparison of two models. Biophys. J. 70:2078-2091.
Fried, S.I., Münch, T.A., and Werblin, F.S. 2002. Mechanisms and circuitry underlying directional selectivity in the retina. Nature (this issue).
Gan, L., Xiang, M., Zhou, L., Wagner, D.S., Klein, W.H., and Nathans, J. 1996. POU domain factor Brn-3b is required for the development of a large set of retinal ganglion cells. Proc. Natl. Acad. Sci. USA 93:3920-3925.
Geisler, W.S. 1989. Sequential ideal-observer analysis of visual discriminations. Psychol. Rev. 96:267-314.
Gerschenfeld, H.M., Piccolino, M., and Neyton, J. 1980. Feed-back modulation of cone synapses by L-horizontal cells of turtle retina. J. Exp. Biol. 89:177-192.
Goodchild, A.K., Chan, T.L., and Grünert, U. 1996a. Horizontal cell connections with short-wavelength-sensitive cones in macaque monkey retina. Vis. Neurosci. 13:833-845.
Goodchild, A.K., Ghosh, K.K., and Martin, P.R. 1996b. Comparison of photoreceptor spatial density and ganglion cell morphology in the retina of human, macaque monkey, cat, and the marmoset *Callithrix jacchus*. J. Comp. Neurol. 366:55-75.
Grünert, U., Haverkamp, S., Fletcher, E.L., and Wässle, H. 2002. Synaptic distribution of ionotropic glutamate receptors in the inner plexiform layer of the primate retina. J. Comp. Neurol. 447:138-151.
Grünert, U., Martin, P.R., and Wässle, H. 1994. Immunocytochemical analysis of bipolar cells in the macaque monkey retina. J. Comp. Neurol. 348:607-627.
Grünert, U. and Wässle, H. 1990. GABA-like immunoreactivity in the macaque monkey retina: A light and electron microscopic study. J. Comp. Neurol. 297:509-524.
Hack, I., Peichl, L., and Brandstätter, J.H. 1999. An alternative pathway for rod signals in the rodent retina: Rod photoreceptors, cone bipolar cells, and the localization of glutamate receptors. Proc. Natl. Acad. Sci. USA 96:14130-14135.
Hampson, E.C., Vaney, D.I., and Weiler, R. 1992. Dopaminergic modulation of gap junction permeability between amacrine cells in mammalian retina. J. Neurosci. 12(12):4911-4922.
Hampson, E.C.G.M., Weiler, R., and Vaney, D.I. 1994. pH-gated dopaminergic modulation of horizontal cell gap junctions in mammalian retina. Proc. R. Soc. Lond. B 255:67-72.

Hartveit, E., Brandstätter, J.H., Enz, R., and Wässle, H. 1995. Expression of the mRNA of seven metabotropic glutamate receptors (mGluR1 to 7) in the rat retina. An *in situ* hybridization study on tissue sections and isolated cells. Eur. J. Neurosci. 7:1472-1483.

Hattar, S., Liao, H.-W., Takao, M., Berson, D.M., and Yau, K.-W. 2002. Melanopsin-containing retinal ganglion cells: architecture, projections, and intrinisc photosensitivity. Science 295:1065-1070.

Haverkamp, S., Grünert, U., and Wässle, H. 2000. The cone pedicle, a complex synapse in the retina. Neuron 27:85-95.

Haverkamp, S., Grünert, U., and Wässle, H. 2001a. Localization of kainate receptors at the cone pedicles of the primate retina. J. Comp. Neurol. 436:471-486.

Haverkamp, S., Grünert, U., and Wässle, H. 2001b. The synaptic architecture of AMPA receptors at the cone pedicle of the primate retina. J. Neurosci. 21:2488-2500.

Haverkamp, S. and Wässle, H. 2000. Immunocytochemical analysis of the mouse retina. J. Comp. Neurol. 424:1-23.

He, S., Weiler, R., and Vaney, D.I. 2000. Endogenous dopaminergic regulation of horizontal cell coupling in the mammalian retina. J. Comp. Neurol. 418:33-40.

Heidelberger, R., Sterling, P., and Matthews, G. 2002. Roles of ATP in depletion and replenishment of the releasable pool of synaptic vesicles. J. Neurophysiol. 88:98-106.

Hendry, S.H.C. and Calkins, D.J. 1998. Neuronal chemistry and functional organization in the primate visual system. Trends Neurosci. 21:344-349.

Hennig, M.H., Funke, K., and Worgotter, F. 2002. The influence of different retinal subcircuits on the nonlinearity of ganglion cell behavior. J. Neurosci. 22:8726-8738.

Higgs, M.H., Romano, C., and Lukasiewicz, P.D. 2002. Presynaptic effects of group III metabotropic glutamate receptors on excitatory synaptic transmission in the retina. Neuroscience 115:163-172.

Hochstein, S. and Shapley, R.M. 1976a. Linear and nonlinear spatial subunits in Y cat retinal ganglion cells. J. Physiol. (Lond.) 262:265-284.

Hochstein, S. and Shapley, R.M. 1976b. Quantitative analysis of retinal ganglion cell classifications. J. Physiol. 262:237-264.

Hsu, A., Tsukamoto, Y., Smith, R.G., and Sterling, P. 1998. Functional architecture of primate rod and cone axons. Vision Res. 38:2539-2549.

Hsu, A.C.C. 1998. Optimal transfer of form and color information through the primate retina.

Hu, H.J. and Pan, Z.H. 2002. Differential expression of K^+ currents in mammalian retinal bipolar cells. Vis. Neurosci. 19:163-173.

Hubel, D.H. and Wiesel, T.N. 1977. Functional architecture of macaque monkey visual cortex. Proc. R. Soc. Lond. B 198:1-59.

Isayama, T., Berson, D.M., and Pu, M. 2000. Theta ganglion cell type of cat retina. J. Comp. Neurol. 417:32-48.

Jacobs, G.H. 1993. The distribution and nature of colour vision among the mammals. Biol. Rev. 68:413-471.

Jacoby, R., Stafford, D., Kouyama, N., and Marshak, D. 1996. Synaptic inputs to ON parasol ganglion cells in the primate retina. J. Neurosci. 16:8041-8056.

Jellali, A., Stussi-Garaud, C., Gasmier, B., Rendon, A., Sahel, J.A., Dreyfus, H., and Picaud, S. 2002. Cellular localization of the vesicular inhibitory amino acid transporter in the mouse and human retina. J. Comp. Neurol. 449:76-87.

Jensen, R.J. 1995. Receptive-field properties of displaced starburst amacrine cells change following axotomy-induced degeneration of ganglion cells. Vis. Neurosci. 12:177-184.

Johnson, M.A. and Vardi, N. 1998. Regional differences in GABA and GAD immunoreactivity in rabbit horizontal cells. Vis. Neurosci. 15:743-753.

Kamermans, M., Fahrenfort, I., Schultz, K., Janssen-Bienhold, U., Sjoerdsma, T., and Weiler, R. 2001. Hemichannel-mediated inhibition in the outer retina. Science 292:1178-1180.

Kaneda, M., Hashimoto, M., and Kaneko, A. 1995. Neuronal nicotinic acetylcholine receptors of ganglion cells in the cat retina. Jpn. J. Physiol. 45:491-508.

Kaneda, M. and Kaneko, A. 1991. Voltage-gated sodium currents in isolated retinal ganglion cells of the cat: Relation between the inactivation kinetics and the cell type. Neurosci. Res. 11:261-275.

Kaneko, A. 1970. Physiological and morphological identification of horizontal, bipolar and amacrine cells in goldfish retina. J. Physiol. 207:623-633.

Kao, Y.-H., Lassová, L., Sterling, P., and Vardi, N. 2003. Evidence that two types of retinal bipolar cell use both glutamate and GABA. (Submitted) .

Kaplan, E. and Shapley, R.M. 1982. X and Y cells in the lateral geniculate nucleus of Macaque monkeys. J. Physiol. 330:125-143.

Katz, L.C. and Crowley, J.C. 2002. Development of cortical circuits: lessons from ocular dominance columns. Nat. Rev. Neurosci. 3:34-42.

Katz, L.C. and Shatz, C.J. 1996. Synaptic activity and the construction of cortical circuits. Science 274:1133-1138.

Kier, C.K., Buchsbaum, G., and Sterling, P. 1995. How retinal microcircuits scale for ganglion cells of different size. J. Neurosci. 15:7673-7683.

Kim, K.J. and Rieke, F. 2001. Temporal contrast adaptation in the input and output signals of salamander retinal ganglion cells. J. Neurosci. 21:287-299.

Koch, C., Poggio, T., and Torre, V. 1982. Retinal ganglion cells: a functional interpretation of dendritic morphology. Philos. Trans. R. Soc. Lond. B 298:227-264.

Kolb, H. 1970. Organization of the outer plexiform layer of the primate retina: electron microscopy of Golgi-impregnated cells. Philos. Trans. R. Soc. Lond. B 258:261-283.

Kolb, H. 1974. The connections between horizontal cells and photoreceptors in the retina of the cat: Electron microscopy of golgi preparations. J. Comp. Neurol. 155(1):1-14.

Kolb, H. 1977. The organization of the outer plexiform layer in the retina of the cat: Electron microscopic observations. J. Neurocytol. 6:131-153.

Kolb, H. 1994. The architecture of functional neural circuits in the vertebrate retina. Invest. Ophthalmol. Vis. Sci. 35:2385-2404.

Kolb, H. and Dekorver, L. 1991. Midget ganglion cells of the parafovea of the human retina: A study by electron microscopy and serial section reconstructions. J. Comp. Neurol. 303:617-636.

Kolb, H. and Famiglietti, E.V. 1974. Rod and cone pathways in the inner plexiform layer of cat retina. Science 186:47-49.

Kolb, H. and Nelson, R. 1993. OFF-alpha and OFF-beta ganglion cells in cat retina: II. Neural circuitry as revealed by electron microscopy of HRP stains. J. Comp. Neurol. 329:85-110.
Kolb, H., Nelson, R., and Mariani, A. 1981. Amacrine cells, bipolar cells and ganglion cells of the cat retina: a Golgi study. Vision Res. 21:1081-1114.
Kolb, H. and West, R.W. 1977. Synaptic connections of the interplexiform cell in the retina of the cat. J. Neurocytol. 6:155-170.
Korn, H. and Faber, D. 1991. Quantal analysis and synaptic efficacy in the CNS. Trends Neurosci. 14:439-445.
Kosaka, T., Tauchi, M., and Dahl, J.L. 1988. Cholinergic neurons containing GABA-like and/or glutamic acid decarboxylase-like immunoreactivities in various brain regions of the rat. Exp. Brain Res. 70:605-617.
Koulen, P. 1999. Postnatal development of GABAA receptor beta 1, beta 2/3, and gamma2 immunoreactivity in the rat retina. J. Neurosci. Res. 57:185-194.
Koulen, P., Sassoè-Pognetto, M., Grünert, U., and Wässle, H. 1996. Selective clustering of $GABA_A$ and glycine receptors in the mammalian retina. J. Neurosci. 16:2127-2140.
Kouyama, N. and Marshak, D.W. 1992. Bipolar cells specific for blue cones in the Macaque retina. J. Neurosci. 12:1233-1252.
Kuffler, S.W. 1953. Discharge patterns and functional organization of mammalian retina. J. Neurophysiol. 16:37-68.
Lamb, T.D. and Simon, E.J. 1976. The relation between intercellular coupling and electrical noise in turtle photoreceptors. J. Physiol. 263:257-286.
Lankheet, M.J.M., Rowe, M.H., van Wezel, R.J.A., and van de Grind, W.A. 1996. Horizontal cell sensitivity in the cat retina during prolonged dark adaption. Vis. Neurosci. 13:885-896.
Laughlin, S.B. 1994. Matching coding, circuits, cells, and molecules to signals: General principles of retinal design in the fly's eye. Prog. Ret. & Eye Res. 13:165-196.
Lee, B.B., Pokorny, J., Smith, V.C., Martin, P.R., and Valberg, A. 1990. Luminance and chromatic modulation sensitivity of macaque ganglion cells and human observers. J. Opt. Soc. Am. A 7:2223-2236.
Leeper, H.F. and Charlton, J.S. 1985. Response properties of horizontal cells and photoreceptor cells in the retina of the tree squirrel, *Sciurus carolinensis*. J. Neurophysiol. 54:1157-1166.
Leskov, I.B., Klenchin, V.A., Handy, J.W., Whitlock, G.G., Govardovskii, V.I., Bownds, M.D., Lamb, T.D., Pugh Jr., E.N., and Arshavsky, V.Y. 2000. The gain of rod phototransduction: reconciliation of biochemical and electrophysiological measurements. Neuron 27:525-537.
Li, W., Zhang, J., and Massey, S.C. 2002. Coupling pattern of S1 and S2 amacrine cells in the rabbit retina. Vis. Neurosci. 19:119-131.
Linberg, K.A. and Fisher, S.K. 1988. Ultrastructural evidence that horizontal cell axon terminals are presynaptic in the human retina. J. Comp. Neurol. 268:281-297.
Linn, D.M., Blazynski, C., Redburn, D.A., and Massey, S.C. 1991. Acetylcholine release fron the rabbit retina mediated by kainate receptors. J. Neurosci. 11:111-122.
Linsenmeier, R.A., Frishman, L.J., Jakiela, H.G., and Enroth-Cugell, C. 1982. Receptive field properties of X and Y cells in the cat retina derived from contrast sensitivity measurements. Vision Res. 22:1173-1183.
Lohmann, C., Myhr, K.L., and Wong, R.O.L. 2002. Transmitter-evoked local calcium release stabilizes developing dendrites. Nature 418:177-181.
Luo, M., Pu, M., and Sterling, P. 1996. Volumes of beta and alpha cell dendritic arbors peak in different strata. Soc. Neurosci. [Abstract]
Lyubarsky, A.L., Falsini, B., Pennesi, M.E., Valentini, P., and Pugh Jr., E.N. 1999. UV- and midwave-sensitive cone-driven retinal responses of the mouse: a possible phenotype for coexpression of cone photopigments. J. Neurosci. 19:442-455.
MacNeil, M.A. and Masland, R.H. 1998. Extreme diversity among amacrine cells: implications for function. Neuron 20:971-982.
Mangel, S.C. 1991. Analysis of the horizontal cell contribution to the receptive field surround of ganglion cells in the rabbit retina. J. Physiol. 442:211-234.
Mariani, A.P. 1984. Bipolar cells in monkey retina selective for the cones likely to be blue-sensitive. Nature 308:184-186.
Martin, P.R., Lee, B.B., White, A.J.R., Solomon, S.G., and Rüttiger, L. 2001. Chromatic sensitivity of ganglion cells in the peripheral primate retina. Nature 410:933-936.
Masland, R.H. 1986. The functional architecture of the retina. Sci. Amer. 254:102-111.
Masland, R.H. 2001. The fundamental plan of the retina. Nat. Neurosci. 4:877-886.
Masland, R.H., Mills, J.W., and Cassidy, C. 1984. The functions of acetylcholine in the rabbit retina. Proc. R. Soc. Lond. B 223:121-139.
Maslim, J. and Stone, J. 1986. Synaptogenesis in the retina of the cat. Brain Res. 373:35-48.
Massey, S.C. and Redburn, D.A. 1985. Light evoked release of acetylcholine in response to a single flash: cholinergic amacrine cells receive ON and OFF input. Brain Res. 328:374-377.
Mastronarde, D.N. 1983. Correlated firing of cat retinal ganglion cells. II. Responses of X- and Y- cells to single quantal events. J. Neurophysiol. 49:325-349.
Masu, M., Iwakabe, H., Tagawa, Y., Miyoshi, T., Yamashita, M., Fukuda, Y., Sasaki, H., Hiroi, K., Nakamura, Y., and Shigemoto, R. 1995. Specific deficit on the ON response in visual transmission by targeted disruption of the mGluR6 gene. Cell 80:757-765.
Mata, N.L., Radu, R.A., Clemmons, R.C., and Travis, G.H. 2002. Isomerization and oxidation of vitamin A in cone-dominant retina: a novel pathway for visual-pigment regneration in daylight. Neuron 36:69-80.
Matthews, G. 1996. Neurotransmitter release. Annu. Rev. Neurosci. 19:219-233.
Maturana, H.R., Lettvin, J.Y., McCulloch, W.S., and Pitts, W.H. 1960. Anatomy and physiology of vision in the frog (*Rana pipiens*). J. Gen. Physiol. 43:129-175.
McArdle, C.B., Dowling, J.E., and Masland, R.H. 1977. Development of outer segments and synapses in the rabbit retina. J. Comp. Neurol. 175:253-274.
McGuire, B.A., Stevens, J.K., and Sterling, P. 1984. Microcircuitry of bipolar cells in cat retina. J. Neurosci. 4:2920-2938.

McIlwain, J.T. 1964. Receptive fields of optic tract axons and lateral geniculate cells: Peripheral extent and barbiturate sensitivity. J. Neurophysiol. 27:1154-1173.
McIlwain, J.T. 1966. Some evidence concerning the physiological basis of the periphery effect in the cat's brain. Exp. Brain Res. 1:265-271.
Meister, M. and Berry II, M.J. 1999. The neural code of the retina. Neuron 22:435-450.
Meister, M., Wong, R.O.L., Baylor, D.A., and Shatz, C.J. 1991. Synchronous bursts of action potentials in ganglion cells of the eveloping mammalian retina. Science 252:939-943.
Milam, A.H., Dacey, D.M., and Dizhoor, A.M. 1993. Recoverin immmunoreactivity in mammalian cone bipolar cells. Vis. Neurosci. 10:1-12.
Mills, S.L. and Massey, S.C. 1994. Distribution and coverage of A- and B-type horizontal cells stained with Neurobiotin in the rabbit retina. Vis. Neurosci. 11:549-560.
Mills, S.L. and Massey, S.C. 1995. Differential properties of two gap junctional pathways made by AII amacrine cells. Nature 377:734-737.
Mills, S.L. and Massey, S.C. 1999. AII amacrine cells limit scotopic acuity in central macaque retina: a confocal analysis of calretinin labeling. J. Comp. Neurol. 411:19-34.
Morgans, C.W. 2001. Localization of the $alpha_{1F}$ calcium channel subunit in the rat retina. Invest. Ophthalmol. Vis. Sci. 42:2414-2418.
Murakami, M., Miyachi, E.-I., and Takahashi, K.-I. 1995. Modulation of gap junctions between horizontal cells by second messengers. Chapter 6 in Progress in retinal and eye research Elsevier Science Ltd., London.
Muresan, V., Lyass, A., and Schnapp, B.J. 1999. The kinesin motor KIF3A is a component of the presynaptic ribbon in vertebrate photoreceptors. J. Neurosci. 19:1027-1037.
Müller, B. and Peichl, L. 1993. Horizontal cells in the cone-dominated tree shrew retina: morphology, photoreceptor contacts, and topographical distribution. J. Neurosci. 13:3628-3646.
Nakamura, Y., McGuire, B.A., and Sterling, P. 1980. Interplexiform cell in cat retina: Identification by uptake of gamma-[^{3}H]aminobutyric acid and serial reconstruction. Proc. Natl. Acad. Sci. USA 77(1):658-661.
Nawy, S. 1999. The metabotropic receptor mGluR6 may signal through G_o, but not phosphodiesterase, in retinal bipolar cells. J. Neurosci. 19:2938-2944.
Nawy, S. and Jahr, C.E. 1990. Suppression by glutamate of cGMP-activated conductance in retinal bipolar cells. Nature 346:269-271.
Neitz, J., Carroll, J., Yamauchi, Y., Neitz, M., and Williams, D.R. 2002. Color perception is mediated by a plastic neural mechanism that is adjustable in adults. Neuron 35:783-792.
Neitz, M., Neitz, J., and Jacobs, G.H. 1991. Spectral tuning of pigments underlying red-green color vision. Science 252:971-974.
Nelson, P., Famiglietti, E.V., and Kolb, H. 1978. Intracellular staining reveals different levels of stratification for On- and Off-center ganglion cells of the cat retina. J. Neurophysiol. 41:472-483.
Nelson, R. 1977. Cat cones have rod input: a comparison of the response properties of cones and horizontal cell bodies in the retina of the cat. J. Comp. Neurol. 172:109-136.
Nelson, R. 1982. AII amacrine cells quicken time course of rod signals in the cat retina. J. Neurophysiol. 47:928-947.
Nelson, R. and Kolb, H. 1983. Synaptic patterns and response properties of bipolar and ganglion cells in the cat retina. Vision Res. 23:1183-1195.
Nelson, R. and Kolb, H. 1985. A17: A broad-field amacrine cell in the rod system of the cat retina. J. Neurophysiol. 54:592-614.
Newman, E. and Reichenbach, A. 1996. The Müller cell: a functional element of the retina. Trends Neurosci. 19:307-312.
Newman, E.A. 1986. High potassium conductance in astrocyte endfeet. Science 233:453-454.
Newman, E.A. 1987. Distribution of potassium conductance in mammalian Müller(glial) cells: A comparative study. J. Neurosci. 7:2423-2432.
Newman, E.A. 2003. Glial cell inhibition of neurons by release of ATP. (Submitted) .
Nguyen, P.V., Marin, L., and Atwood, H.L. 1997. Synaptic physiology and mitochondrial function in crayfish tonic and phasic motor neurons. J. Neurophysiol. 78:281-294.
Nishimura, Y. and Rakic, P. 1987. Synaptogenesis in primate retina proceeds rom the ganglion cells towards the photoreceptors. Neurosci. Res. Suppl. 6:253-268.
O'Brien, B.J., Isayama, T., Richardson, R., and Berson, D.M. 2002. Intrinsic physiological properties of cat retinal ganglion cells. J. Physiol. 538:787-802.
O'Malley, D.M., Sandell, J.H., and Masland, R.H. 1994. Co-release of acetylcholine and GABA by the starburst amacrine cells. J. Neurosci. 12:1394-1408.
Ohtsuka, T. 1985. Relation of spectral types to oil droplets in cones of turtle retina. Science 229:874-877.
Oyster, C.W., Takahashi, E.S., Cilluffo, M., and Brecha, N.C. 1985. Morphology and distribution of tyrosine hydroxylase-like immunoreactive neurons in the cat retina. Proc. Natl. Acad. Sci. USA 82:6335-6339.
Packer, O., Hendrickson, A., and Curcio, C. 1989. Photoreceptor topography of the retina in the adult pigtail Macaque (*Macaca nemestrina*). J. Comp. Neurol. 288:165-183.
Palmer, L.A. and Davis, T.L. 1981. Receptive field structure in cat striate cortex. J. Neurophysiol. 46:260-276.
Panico, J. and Sterling, P. 1995. Retinal neurons and vessels are not fractal but space filling. J. Comp. Neurol. 361:479-490.
Parsons, T. and Sterling, P. 2003. Synaptic ribbon: conveyor belt or safety belt? (Submitted) .
Parsons, T.D., Lenzi, D., Almers, W., and Roberts, W.M. 1994. Calcium-triggered exocytosis and endocytosis in an isolated presynaptic cell: Capacitance measurements in saccular hair cells. Neuron 13(4):875-883.
Pattnaik, B., Jellali, A., Sahel, J., Dreyfus, H., and Picaud, S. 2000. $GABA_C$ receptors are localized with microtubule-associated protein 1B in mammalian cone photoreceptors. J. Neurosci. 20:6789-6796.
Peichl, L. and González-Soriano, J. 1994. Morphological types of horizontal cell in rodent retinae: A comparison of rat, mouse, gerbil, and guinea pig. Vis. Neurosci. 11:501-517.

Penn, A.A., Wong, R.O.L., and Shatz, C.J. 1994. Neuronal coupling in the developing mammalian retina. J. Neurosci. 14:3805-3815.
Perry, V.H., Oehler, R., and Cowey, A. 1984. Retinal ganglion cells that project to the dorsal lateral geniculate nucleus in the macaque monkey. Neurosci. 12:1101-1123.
Peters, B.N. and Masland, R.H. 1996. Responses to light of starburst amacrine cells. J. Neurophysiol. 75:469-480.
Peterson, B.B. and Dacey, D.M. 1999. Morphology of wide-field, monostratified ganglion cells of the human retina. Vis. Neurosci. 16:107-120.
Piccolino, M. 1986. Cajal and the retina: a 100-year retrospective. Trends Neurosci. 9:521-525.
Piccolino, M. 1995. Cross-talk between cones and horizontal cells through the feedback circuit. Chapter 9 in Neurobiology and clinical aspects of the outer retina. Edited by M.B.A. Djamgoz, S. Archer, and S. Vallerga. Chapman & Hall, London.
Piccolino, M., Neyton, J., and Gerschenfeld, H.M. 1984. Decrease of gap-junction permeability induced by dopamine and cyclic adenosine 3',5'-monophosphate in horizontal cells of turtle retina. J. Neurosci. 4:2477-2488.
Polyak, S.L. 1941. The retina. University of Chicago Press.
Potts, A.M., Hodges, D., Shelman, C.B., Fritz, K.J., Levy, N.S., and Mangnall, Y. 1972. Morphology of the primate optic nerve. I. Method and total fiber count. Invest. Ophthalmol. Vis. Sci. 11:980-988.
Pourcho, R. 1982. Dopaminergic amacrine cells in the cat retina. Brain Res. 252:101-109.
Pourcho, R.G. and Goebel, D.J. 1987. Visualization of endogenous glycine in cat retina: An immunocytochemical study with Fab fragments. J. Neurosci. 7:1189-1197.
Pourcho, R.G. and Owczarzak, M.T. 1989. Distribution of GABA immunoreactivity in the cat retina: A light- and electron-microscopic study. Vis. Neurosci. 2:425-435.
Pourcho, R.G. and Owczarzak, M.T. 1991. Glycine receptor immunoreactivity is localized at amacrine synapses in cat retina. Vis. Neurosci. 7:611-618.
Pourcho, R.G., Qin, P., and Goebel, D.J. 2001. Cellular and subcellular distribution of NMDA receptor subunit NR2B in the retina. J. Comp. Neurol. 433:75-85.
Pu, M. and Amthor, F.R. 1990. Dendritic morphologies of retinal ganglion cells projecting to the nucleus of the optic tract in the rabbit. J. Comp. Neurol. 302:657-674.
Pugh Jr., E.N. 2000. Rhodopsin flash photolysis in man. J. Physiol. 248:393-412.
Pugh Jr., E.N. and Lamb, T.D. 1993. Amplification and kinetics of the activation steps in phototransduction. Biochim. Biophys. Acta 1141:111-149.
Qin, P. and Pourcho, R.G. 1999a. AMPA-selective glutamate receptor subunits GluR2 and GluR4 in the cat retina: an immunocytochemical study. Vis. Neurosci. 16:1105-1114.
Qin, P. and Pourcho, R.G. 1999b. Localization of AMPA-selective glutamate receptor subunits in the cat retina: a light- and electron-microscopic study. Vis. Neurosci. 16:169-177.
Ramoa, A., Campbell, G., and Shatz, C.J. 1988. Dendritic growth and remodeling of cat retinal ganglion cells during fetal and postnatal development. J. Neurosci. 8:4239-4261.
Rao-Mirotznik, R., Buchsbaum, G., and Sterling, P. 1998. Transmitter concentration at a three-dimensional synapse. J. Neurophysiol. 80:3163-3172.
Rao-Mirotznik, R., Harkins, A., Buchsbaum, G., and Sterling, P. 1995. Mammalian rod terminal: Architecture of a binary synapse. Neuron 14:561-569.
Rao, R., Buchsbaum, G., and Sterling, P. 1994. Minimum rate of transmitter release at a cone active zone. Invest. Ophthalmol. Vis. Sci. 35:2125. [Abstract]
Rao, R., Buchsbaum, G., and Sterling, P. 1994. Rate of quantal transmitter release at the mammalian rod synapse. Biophys. J. 67:57-63.
Rao, R. and Sterling, P. 1991. Synaptic apparatus associated with transmission of a single photon event. Soc. Neurosci. [Abstract]
Raviola, E. and Gilula, N.B. 1973. Gap junctions between photoreceptor cells in the vertebrate retina. Proc. Natl. Acad. Sci. USA 70:1677-1681.
Reh, T. and Constantine-Paton, M. 1984. Retinal ganglion cell terminals change their porjection sites during larval development of *Rana pipiens*. J. Neurosci. 4:442-457.
Reid, R.C. and Shapley, R.M. 2002. Space and time maps of cone photoreceptor signals in macaque lateral geniculate nucleus. J. Neurosci. 22:6158-6175.
Reisine, T. and Bell, G.I. 1995. Molecular properties of somatostatin receptors. Neurosci. 67:777-790.
Reymond, L. 1985. Spatial visual acuity of the eagle *Aquila audax*: A behavioural, optical and anatomical investigation. Vision Res. 25:1477-1491.
Rieke, F. 2001. Temporal contrast adaptation in salamander bipolar cells. J. Neurosci. 21:9445-9454.
Rieke, F. and Schwartz, E.A. 1996. Asynchromous transmitter release: control of exocytosis and endocytosis at the salamander rod synapse. J. Physiol. 493:1-8.
Rodieck, R.W. 1965. Quantitative analysis of cat retinal ganglion cell response to visual stimuli. Vision Res. 5:583-601.
Rodieck, R.W. 1989. Starburst amacrine cells of the primate retina. J. Comp. Neurol. 285:18-37.
Rodieck, R.W. and Brening, R.K. 1983. Retinal ganglion cells: Properties, types, genera, pathways and trans-species comparisons. Brain Behav. Evol. 23:121-164.
Rodieck, R.W., Brening, R.K., and Watanabe, M. 1993. The origin of parallel visual pathways. Chapter 8 in Contrast sensitivity. Edited by R. Shapley and D.M.K. Lam. MIT Press, Cambridge MA.
Rodieck, R.W. and Watanabe, M. 1993. Survey of the morphology of macaque retinal ganglion cells that project to the pretectum, superior colliculus, and parvicellular laminae of the lateral geniculate nucleus. J. Comp. Neurol. 338:289-303.
Roorda, A. and Williams, D.R. 1999. The arrangement of the three cone classes in the living human eye. Nature 397:520-522.

Rose, A. 1973. Vision: Human and electronic. Edited by W.L. Wolfe. Plenum Press, New York NY.
Roska, B., Nemeth, E., and Werblin, F.S. 1998. Response to change is facilitated by a three-neuron disinhibitory pathway in the tiger salamander retina. J. Neurosci. 18:3451-3459.
Roska, B. and Werblin, F. 2001. Vertical interactions across ten parallel, stacked representations in the mammalian retina. Nature 410:583-587.
Röhlich, P., Van Veen, T., and Szél, A. 1994. Two different visual pigments in one retinal cone cell. Neuron 13:1159-1166.
Röhrenbeck, J., Wässle, H., and Boycott, B.B. 1989. Horizontal cells in the monkey retina: Immuocytochemical staining with antibodies against calcium binding proteins. Eur. J. Neurosci. 1:407-420.
Sagar, S.M. 1987. Somatostatin-like immunoreactive material in the rabbit retina: immunohistochemical staining using monoclonal antibodies. J. Comp. Neurol. 266:291-299.
Saito, H.-A. 1983. Morphology of physiologically identified X-, Y-, and W-type retinal ganglion cells of the cat. J. Comp. Neurol. 221:279-288.
Saito, T. 1999. Development and regeneration of the retina. The Retinal Basis of Vision. Edited by J. Toyoda, M. Murakami, A. Kaneko, and T. Saito. elsevier, Tokyo.
Saito, T., Kujiraoka, T., Yonaha, T., and Chino, Y. 1985. Reexamination of photoreceptor-bipolar connectivity patterns in carp retina: HRP-EM and Golgi-EM studies. J. Comp. Neurol. 236:141-160.
Sakmann, B. and Creutzfeldt, O.D. 1969. Scotopic and mesopic light adaptation in the cat's retina. Pflügers Arch. 313:168-185.
Sandell, J.H. 1985. NADPH diaphorase cells in the mammalian inner retina. J. Comp. Neurol. 238:466-472.
Sandell, J.H. and Masland, R.H. 1986. A system of indoleamine-accumulating neurons in the rabbit retina. J. Neurosci. 6:3331-3347.
Sandmann, D., Boycott, B.B., and Peichl, L. 1996. The horizontal cells of artiodactyl retinae: a comparison with Cajal's descriptions. Vis. Neurosci. 13:735-746.
Sasaki, T. and Kaneko, A. 1996. L-glutamate-induced responses in OFF-type bipolar cells of the cat retina. Vision Res. 36:787-795.
Sassoè-Pognetto, M., Wässle, H., and Grünert, U. 1994. Glycinergic synapses in the rod pathway of the rat retina: Cone bipolar cells express the alpha-1 subunit of the glycine receptor. J. Neurosci. 14:5131-5146.
Satoh, H., Kaneda, M., and Kaneko, A. 2001. Intracellular chloride concentration is higher in rod bipolar cells than in cone bipolar cells of the mouse retina. Neurosci. Lett. 310:161-164.
Savage, G.L. and Banks, M.S. 1992. Scotopic visual efficiency: Constraints by optics, receptor properties, and rod pooling. Vision Res. 32:645-656.
Schein, S. 1988. Anatomy of Macaque fovea and spatial densities of neurons in foveal representation. J. Comp. Neurol. 269:479-505.
Schiller, P.H., Sandell, J.H., and Maunsell, J.H.R. 1986. Functions of the ON and OFF channels of the visual system. Nature 322:824-825.
Schmidt, M., Humphrey, M.F., and Wässle, H. 1987. Action and localization of acetylcholine in the cat retina. J. Neurophysiol. 58:997-1015.
Schnapf, J.L., Nunn, B.J., Meister, M., and Baylor, D.A. 1990. Visual transduction in cones of the monkey *Macaca fascicularis*. J. Physiol. 427:681-713.
Schneeweis, D.M. and Schnapf, J.L. 1995. Photovoltage of rods and cones in the macaque retina. Science 268:1053-1056.
Schneeweis, D.M. and Schnapf, J.L. 1999. The photovoltage of Macaque cone photoreceptors: adaptation, noise, and kinetics. J. Neurosci. 19:1203-1216.
Schwartz, E. 1987. Depolarization without calcium can release gamma-aminobutyric acid from a retinal neuron. Science 238:350-355.
Shannon, C.E. and Weaver, W. 1949. The mathematical theory of communication. University of Illinois Press, Urbana.
Shapley, R. and Perry, V.H. 1986. Cat and monkey retinal ganglion cells and their visual functional roles. Trends Neurosci. 9:229-235.
Shapley, R.M. and Victor, J.D. 1978. The effect of contrast on the transfer properties of cat retinal ganglion cells. J. Physiol. 285:275-298.
Sharpe, L.T. and Stockman, A. 1999. Rod pathway: the importance of seeing nothing. Trends Neurosci. 22:497-504.
Shields, C.R., Tran, M.N., Wong, R.O.L., and Lukasiewicz, P.D. 2000. Distinct ionotropic GABA receptors mediate presynatpic and postsynaptic inhibition in retinal bipolar cells. J. Neurosci. 20:2673-2682.
Shiells, R.A. and Falk, G. 1990. Glutamate receptors of rod bipolar cells are linked to a cyclic GMP cascade via a G-protein. Proc. R. Soc. Lond. B 242:91-94.
Shiells, R.A. and Falk, G. 1999. A rise in intracellular Ca^{2+} underlies light adaptation in dogfish retinal 'on' bipolar cells. J. Physiol. 514:343-350.
Singer, J.H., Mirotznik, R.R., and Feller, M.B. 2001. Potentiation of L-type calcium channels reveals nonsynaptic mechanisms that correlate spontaneous activity in the developing mammalian retina. J. Neurosci. 21:8514-8522.
Smallman, H.S., MacLeod, D.I.A., He, S., and Kentridge, R.W. 1996. Fine grain of the neural representation of human spatial vision. J. Neurosci. 16:1852-1859.
Smirnakis, S.M., Berry II, M.J., Warland, D.K., Bialek, W., and Meister, M. 1997. Adaptation of retinal processing to image contrast and spatial scale. Nature 386:69-73.
Smith, R.G. 1995. Simulation of an anatomically-defined local circuit: The cone-horizontal cell network in cat retina. Vis. Neurosci. 12:545-561.
Smith, R.G., Freed, M.A., and Sterling, P. 1986. Microcircuitry of the dark-adapted cat retina: functional architecture of the rod-cone network. J. Neurosci. 6:3505-3517.
Smith, R.G. and Sterling, P. 1990. Cone receptive field in cat retina computed from microcircuitry. Vis. Neurosci. 5:453-461.
Smith, R.G. and Vardi, N. 1995. Simulation of the AII amacrine cell of mammalian retina: Functional consequences of electrical coupling and regenerative membrane properties. Vis. Neurosci. 12:851-860.
Sokolov, M., Lyubarsky, A., Strissel, K.J., Savchenko, A.B., Govardovskii, V.I., and Pugh Jr., E.N. 2002. Massive light-driven translocation of transducin between the two major compartments of rod cells: a novel mechanism of light adaptation. Neuron 34:95-106.

Soucy, E., Nirenberg, S., Nathans, J., and Meister, M. 1998. A novel signaling pathway from rod photoreceptors to ganglion cells in mammalian retina. Neuron 21:481-493.
Srinivasan, M.V., Laughlin, S.B., and Dubs, A. 1982. Predictive coding: A fresh view of inhibition in the retina. Proc. R. Soc. Lond. B 216:427-459.
Stafford, D.K. and Dacey, D. 1997. Physiology of the A1 amacrine: a spiking, axon-bearing interneuron of the macaque monkey retina. Vis. Neurosci. 14:507-522.
Stein, J.J., Johnson, S.A., and Berson, D.M. 1996. Distribution and coverage of beta cells in the cat retina. J. Comp. Neurol. 372:597-617.
Steinberg, R.H. 1969. Rod and cone contributions to s-potenials from the cat retina. Vision Res. 9:1319-1329.
Sterling, P. 1983. Microcircuitry of the cat retina. Annu. Rev. Neurosci. 6:149-185.
Sterling, P. 1995. Tuning retinal circuits. Nature 377:676-677.
Sterling, P., Cohen, E., Freed, M.A., and Smith, R.G. 1987. Microcircuitry of the on-beta ganglion cell in daylight, twilight and starlight. Neurosci. Res. (Suppl)6:5269-5285.
Sterling, P., Cohen, E., Smith, R.G., and Tsukamoto, Y. 1992. Retinal circuits for daylight: why ballplayers don't wear shades. Analysis and modeling of neural systems. Edited by F.H. Eeckman. Kluwer Academic Publishers, Boston.
Sterling, P., Freed, M.A., and Smith, R.G. 1988. Architecture of the rod and cone circuits to the *On*-beta ganglion cell. J. Neurosci. 8:623-642.
Stevens, C.F. and Tsujimoto, T. 1995. Estimates for the pool size of releasable quanta at a single central synapse and for the time required to refill the pool. Proc. Natl. Acad. Sci. USA 92:846-849.
Stockman, A., Sharpe, L.T., Rüther, K., and Nordby, K. 1995. Two signals in the human rod visual system: a model based on electrophysiological data. Vis. Neurosci. 12:951-970.
Stone, J. and Fukuda, Y. 1974. Properties of cat retinal ganglion cells: a comparison of W-cells with X- and Y-cells. J. Neurophysiol. 37:722-748.
Stone, L.S. 1950. The role of retinal pigment cells in regenerating neural retinae of adult salamander eyes. J. Exp. Zool. 113:9-32.
Strettoi, E., Dacheux, R.F., and Raviola, E. 1990. Synaptic connections of rod bipolar cells in the inner plexiform layer of the rabbit retina. J. Comp. Neurol. 295:449-466.
Stryker, M.P. and Zahs, K.R. 1983. On and off sublaminae in the rlateral geniculate nucleus of the ferret. J. Neurosci. 3:1943-1951.
Szél, A., Diamanstein, T., and Röhlich, P. 1988. Identification of the blue sensitive cones in the mammalian retina by anti-visual pigment antibody. J. Comp. Neurol. 273:593-602.
Szél, A., Röhlich, P., Caffé, A.R., Juliusson, B., Aguirre, G., and Van Veen, T. 1992. Unique topographic separation of two spectral classes of cones in the mouse retina. J. Comp. Neurol. 325:327-342.
Tachibana, M. and Kaneko, A. 1984. Gamma-aminobutyric acid acts at axon terminals of turtle photoreceptors: Difference in sensitivity among cell types. Proc. Natl. Acad. Sci. USA 81:7961-7964.
Tachibanaki, S., Tsushima, S., and Kawamura, S. 2001. Low amplification and fast visual pigment phosphorylation as mechanisms characterizing cone photoresponses. Proc. Natl. Acad. Sci. USA 98:14044-14049.
Tamura, T., Nakatani, K., and Yau, K.-W. 1989. Light adaptation in cat retinal rods. Science 245:755-758.
Tamura, T., Nakatani, K., and Yau, K.-W. 1991. Calcium feedback and sensitivity regulation in primate rods. J. Gen. Physiol. 98:91-130.
Tauchi, M. and Masland, R.H. 1984. The shape and arrangement of the cholinergic neurons in the rabbit retina. Proc. R. Soc. Lond. B 223:101-119.
Taylor, W.R. 1999. TTX attenuates surround inhibition in rabbit retinal ganglion cells. Vis. Neurosci. 16:285-290.
Taylor, W.R. and Morgans, C. 1998. Localization and properties of voltage-gated calcium channels in cone photoreceptors of *Tupaia belangeri*. Vis. Neurosci. 15:541-552.
Taylor, W.R. and Wässle, H. 1995. Receptive field properties of starburst cholinergic amacrine cells in the rabbit retina. Eur. J. Neurosci. 7:2308-2321.
Teranishi, T., Negishi, K., and Kato, S. 1984. Regulatory effect of dopamine on spatial properties of horizontal cells in carp retina. J. Neurosci. 4:1271-1280.
Townes-Anderson, E., Dacheux, R.F., and Raviola, E. 1988. Rod photoreceptors dissociated from the adult rabbit retina. J. Neurosci. 8:320-331.
Townes-Anderson, E., MacLeish, P.R., and Raviola, E. 1985. Rod cells dissociated from mature salamander retina: ultrastructure and uptake of horseradish peroxidase. J. Cell Biol. 100:175-188.
Tsukamoto, Y., Masarachia, P., Schein, S.J., and Sterling, P. 1992. Gap junctions between the pedicles of macaque foveal cones. Vision Res. 32:1809-1815.
Tsukamoto, Y., Morigiwa, K., Ueda, M., and Sterling, P. 2001. Microcircuits for night vision in mouse retina. J. Neurosci. 21:8616-8623.
Tsukamoto, Y., Smith, R.G., and Sterling, P. 1990. "Collective coding" of correlated cone signals in the retinal ganglion cell. Proc. Natl. Acad. Sci. USA 87:1860-1864.
Tsukamoto, Y. and Sterling, P. 1991. Spatial summation by ganglion cells: Some consequences for the efficient encoding of natural scenes. Neurosci. Res. Suppl. 15:S185-S198.
Uchiyama, H. and Barlow, R.B. 1994. Centrifugal inputs enhance responses of retinal ganglion cells in the Japanese quail without changing their spatial coding properties. Vision Res. 34:2189-2194.
Uchiyama, Y. and Ito, H. 1993. Target cells for the isthmo-optic fibers in the retina of the Japanese quail. Neurosci. Lett. 154:35-38.
Van Essen, D.C., Anderson, C.H., and Felleman, D.J. 1992. Information processing in the primate visual system: An integrated systems perspective. Science 255:419-423.
van Hateren, J.H. 1992. A theory of maximizing sensory information. Biol. Cybern. 68:23-29.
van Hateren, J.H. 1993. Spatiotemporal contrast sensitivity of early vision. Vision Res. 33:257-267.
van Rossum, M.C.W. and Smith, R.G. 1998. Noise removal at the rod synapse of mammalian retina. Vis. Neurosci. 15:809-821.

Vaney, D.I. 1985. The morphology and topographic distribution of AII amacrine cells in the cat retina. Proc. R. Soc. Lond. B 224:475-488.
Vaney, D.I. 1986. Morphological identification of serotonin-accumulating neurons in the living retina. Science 233:444-446.
Vaney, D.I. 1990. The mosaic of amacrine cells in mammalian retina. Chapter 2 in Progress in retinal research. Edited by N. Osborne and J. Chader. Pergamon Press, Oxford UK.
Vaney, D.I. 1993. The coupling pattern of axon-bearing horizontal cells in the mammalian retina. Proc. R. Soc. Lond. B 252:93-101.
Vaney, D.I. 1994a. Patterns of neuronal coupling in the retina. Prog. Ret. & Eye Res. 13:301-355.
Vaney, D.I. 1994b. Territorial organization of direction-selective ganglion cells in rabbit retina. J. Neurosci. 14:6301-6316.
Vaney, D.I. 2002a. Retinal amacrine cells. Chapter 25 in The visual neurosciences. Edited by L. Chalupa and J.S. Werner. MIT Press.
Vaney, D.I. 2002b. Retinal neurons: cell types and coupled networks. Chapter 18 in Changing views of Cajal's neuron. Edited by E.C. Azmitia, J. DeFelipe, E.G. Jones, P. Rakic, and C.E. Ribak . Elsevier, Amsterdam.
Vaney, D.I., Collin, S.P., and Young, H.M. 1989a. Dendritic relationships between cholinergic amacrine cells and direction-selective retinal ganglion cells. Neurobiology of the Inner Retina. Edited by R. Weiler and N.N. Osborne. Springer-Verlag, Berlin.
Vaney, D.I., Gynther, I.C., and Young, H.M. 1991. Rod-signal interneurons in the rabbit retina: 2. AII amacrine cells. J. Comp. Neurol. 310:154-169.
Vaney, D.I., Nelson, J.C., and Pow, D.V. 1998. Neurotransmitter coupling through gap junctions in the retina. J. Neurosci. 18:10594-10602.
Vaney, D.I., Whitington, G.E., and Young, H.M. 1989b. The morphology and topographic distribution of substance-P-like immunoreactive amacrine cells in the cat retina. Proc. R. Soc. Lond. B 237:471-488.
Vaney, D.I. and Young, H.M. 1988. GABA-like immunoreactivity in cholinergic amacrine cells of the rabbit retina. Brain Res. 438:369-373.
Vardi, N. 1998. Alpha subunit of G_o localizes in the dendritic tips of ON bipolar cells. J. Comp. Neurol. 395:43-52.
Vardi, N. and Auerbach, P. 1995. Specific cell types in cat retina express different forms of glutamic acid decarboxylase. J. Comp. Neurol. 351:374-384.
Vardi, N., Duvoisin, R.M., Wu, G., and Sterling, P. 2000a. Localization of mGluR6 to dendrites of ON bipolar cells in primate retina. J. Comp. Neurol. 423:402-412.
Vardi, N., Masarachia, P., and Sterling, P. 1989. Structure of the starburst amacrine network and its association with alpha ganglion cells. J. Comp. Neurol. 288:601-611.
Vardi, N., Masarachia, P., and Sterling, P. 1992. Immunoreactivity to $GABA_A$ receptor in the outer plexiform layer of the cat retina. J. Comp. Neurol. 320:394-397.
Vardi, N., Matesic, D.F., Manning, D.R., Liebman, P.A., and Sterling, P. 1993. Identification of a G-protein in depolarizing rod bipolar cells. Vis. Neurosci. 10:473-478.
Vardi, N. and Morigiwa, K. 1997. ON cone bipolar cells in rat express the metabotropic receptor mGluR6. Vis. Neurosci. 14:789-794.
Vardi, N., Morigiwa, K., Wang, T.-L., Shi, Y.-J., and Sterling, P. 1998. Neurochemistry of the mammalian cone 'synaptic complex'. Vision Res. 38:1359-1369.
Vardi, N. and Smith, R.G. 1996. The AII amacrine network: coupling can increase correlated activity. Vision Res. 36:3743-3757.
Vardi, N. and Sterling, P. 1994. Subcellular localization of $GABA_A$ receptor on bipolar cells in macaque and human retina. Vision Res. 34:1235-1246.
Vardi, N., Zhang, L.-L., Payne, J.A., and Sterling, P. 2000b. Evidence that different cation chloride cotransporters in retinal neurons allow opposite responses to GABA. J. Neurosci. 20:7657-7663.
Vasilaki, A., Hatzilaris, E., Liapakis, G., Georgoussi, Z., and Thermos, K. 1996. Somatostatin receptor subtypes (SSTR2) in the rabbit retina. Soc. Neurosci. 22:180. [Abstract]
Velte, T.J. and Masland, R.H. 1999. Action potentials in the dendrites of retinal ganglion cells. J. Neurophysiol. 81:1412-1417.
Veruki, M.L. and Hartveit, E. 2002. AII (rod) amacrine cells form a network of electrically coupled interneurons in the mammalian retina. Neuron 33:935-946.
Veruki, M.L. and Wässle, H. 1996. Immunohistochemical localization of dopamine D_{1} receptors in rat retina. Eur. J. Neurosci. 8:2286-2297.
Victor, J.D. 1987. The dynamics of the cat retinal X cell centre. J. Physiol. 386:219-246.
Victor, J.D., Shapley, R.M., and Knight, B.W. 1977. Nonlinear analysis of cat retinal ganglion cells in the frequency domain. Proc. Natl. Acad. Sci. USA 74:3068-3072.
Viitala, J., Korpimäki, E., Palokangas, P., and Koivula, M. 1995. Attraction of kestrels to vole scent marks visible in ultraviolet light. Nature 373:425-427.
Vogel, M. 1978. Postnatal development of the cat's retina. Edited by M. Vogel. Springer-Verlag, Berlin.
Voight, T. and Wässle, H. 1987. Dopaminergic innervation of AII amacrine cells in mammalian retina. J. Neurosci. 7:4115-4128.
von Gersdorff, H. and Matthews, G. 1994. Dynamics of synaptic vesicle fusion and membrane retrieval in synaptic terminals. Nature 367:735-739.
von Gersdorff, H., Vardi, E., Matthews, G., and Sterling, P. 1996. Evidence that vesicles on the synaptic ribbon of retinal bipolar neurons can be rapidly released. Neuron 16:1221-1227.
Vu, T.Q., Payne, J.A., and Copenhagen, D. 2000. Localization and developmental expression patterns of the neuronal K-Cl cotransporter (KCC2) in the rat retina. J. Neurosci. 20:1414-1423.
Watanabe, M. and Rodieck, R.W. 1989. Parasol and midget ganglion cells of the primate retina. J. Comp. Neurol. 289:434-454.
Wässle, H. 2003. The cone pedicle, the first synapse in the retina. The neural basis of early vision Springer Verlag, Tokyo.
Wässle, H. and Boycott, B.B. 1991. Functional architecture of the mammalian retina. Physiol. Rev. 71:447-480.
Wässle, H., Boycott, B.B., and Illing, R.B. 1981a. Morphology and mosaic of on- and off-beta cells in the cat retina and some functional considerations. Proc. R. Soc. Lond. B 212:177-195.
Wässle, H., Boycott, B.B., and Peichl, L. 1978a. Receptor contacts of horizontal cells in the retina of the domestic cat. Proc. R. Soc. Lond. B 203:247-267.

Wässle, H. and Chun, M.-H. 1988. Dopaminergic and indoleamine-accumulating amacrine cells express GABA-like immunoreactivity in the cat retina. J. Neurosci. 8:3383-3394.
Wässle, H., Grünert, U., Chun, M.-H., and Boycott, B.B. 1995. The rod pathway of the macaque monkey retina: identification of AII-amacrine cells with antibodies against calretinin. J. Comp. Neurol. 361:537-551.
Wässle, H., Grünert, U., Martin, P.R., and Boycott, B.B. 1994. Immunocytochemical characterization and spatial distribution of midget bipolar cells in the macaque monkey retina. Vision Res. 34:561-579.
Wässle, H., Grünert, U., Röhrenbeck, J., and Boycott, B.B. 1989. Cortical magnification factor and the ganglion cell density of the primate retina. Nature 341:643-646.
Wässle, H., Peichl, L., and Boycott, B. 1981b. Dendritic territories of cat retinal ganglion cells. Nature 292:344-345.
Wässle, H., Peichl, L., and Boycott, B.B. 1978b. Topography of horizontal cells in the retina of the domestic cat. Proc. R. Soc. Lond. B 203:269-291.
Wässle, H., Peichl, L., and Boycott, B.B. 1981c. Morphology and topography of on- and off-alpha cells in the cat retina. Proc. R. Soc. Lond. B 212:157-175.
Wässle, H. and Riemann, H.J. 1978. The mosaic of nerve cells in the mammalian retina. Proc. R. Soc. Lond. B 200:441-461.
Wässle, H., Yamashita, M., Greferath, U., Grünert, U., and Müller, F. 1991. The rod bipolar cell of the mammalian retina. Vis. Neurosci. 7:99-112.
Weiler, R., Pottek, M., He, S., and Vaney, D.I. 2000. Modulation of coupling between retinal horizontal cells by retinoic acid and endogenous dopamine. Brain Res. 32:121-129.
Werblin, F.S. and Dowling, J.E. 1969. Organization of the retina of the mudpuppy, *Necturus maculosus*. II. Intracellular recording. J. Neurophysiol. 32:339-355.
White, C.A., Chalupa, L.M., Johnson, D., and Brecha, N.C. 1990. Somatostatin-immunoreactive cells in the adult cat retina. J. Comp. Neurol. 293:134-150.
Williams, D., Sekiguchi, N., and Brainard, D. 1993a. Color, contrast sensitivity, and the cone mosaic. Proc. Natl. Acad. Sci. USA 90:9770-9777.
Williams, D.R. 1992. Photoreceptor sampling and aliasing in human vision. Tutorials in Optics . Edited by D.T. Moore. Optical Society of America, Rochester, N.Y.
Williams, D.R., MacLeod, D.I.A., and Hayhoe, M.M. 1981. Punctate sensitivity of the blue-sensitive mechanism. Vision Res. 21:1357-1375.
Williams, R.W., Bastiani, M.J., Lia, B., and Chalupa, L.M. 1986. Growth cones, dying axons, and develpmental fluctuations in the fiber population of the cat's optic nerve. J. Comp. Neurol. 246:32-69.
Williams, R.W., Cavada, C., and Reinoso-Suárez, F. 1993b. Rapid evolution of the visual system: A cellular assay of the retina and dorsal lateral geniculate nucleus of the Spanish wildcat and the domestic cat. J. Neurosci. 13:208-228.
Williams, R.W. and Herrup, K. 1988. The control of neuron number. Annu. Rev. Neurosci. 11:423-453.
Wilson, M. 2002. Retinal processing: smaller babies thrown out with bathwater. Curr. Biol. 12:R625-R627.
Wilson, M. 2003. Retinal synapses. Chapter 19 in The Visual Neurosciences. Edited by L. Chalupa and J.S. Werner. MIT Press, Cambridge.
Witkovsky, P., Nicholson, C., Rice, M.E., and Bohmaker, K. 1993. Extracellular dopamine concentration in the retina of the clawed frog, *Xenopus laevis*. Proc. Natl. Acad. Sci. USA 90:5667-5671.
Wong, R.O.L., Herrmann, K., and Shatz, C.J. 1991. Remodeling of retinal ganglion cell dendrites in the absence of action potential activity. J. Neurobiol. 22(7):685-697.
Wong, R.O.L. and Oakley, D.M. 1996. Changing patterns of spontaneous bursting activity of On and Off retinal ganglion cells during development. Neuron 16:1087-1095.
Wu, S.M. 1992. Feedback connections and operation of the outer plexiform layer of the retina. Curr. Opinion Neurobiol. 2:462-468.
Xiang, M., Zhou, L., and Nathans, J. 1996. Similarities and differences among inner retinal neurons revealed by the expresion of reporter transgenes controlled by Brn-3a, Brn-3b, and Brn-3c promotor sequences. Vis. Neurosci. 13:955-962.
Xin, D. and Bloomfield, S.A. 1997. Tracer coupling pattern of amacrine and ganglion cells in the rabbit retina. J. Comp. Neurol. 383:512-528.
Xin, D. and Bloomfield, S.A. 1999. Comparison of the responses of AII amacrine cells in the dark- and light-adapted rabbit retina. Vis. Neurosci. 16:653-665.
Yau, K.-W. 1994. Phototransduction mechanism in retinal rods and cones. Invest. Ophthalmol. Vis. Sci. 35:9-32.
Young, H.M. and Vaney, D.I. 1991. Rod-signal interneurons in the rabbit retina: 1. Rod bipolar cells. J. Comp. Neurol. 310:139-153.
Zhang, L., Freed, M., Sterling, P., and Vardi, N. 2003. Developmental switch in the retina of chloride-cation cotransporters from NKCC to KCCC2 mediates the switch of GABA from excitatory to inhibitory. (Submitted) .
Zhou, L., Yoshioka, T., and Nathans, J. 1996. Retina-derived POU-domain factor-1: a complex POU-domain gene implicated in the development of retinal ganglion and amacrine cells. J. Neurosci. 16:2261-2274.
Zhou, Z.J. 2001a. A critical role of the strychnine-sensitive glycinergic system in spontaneous retinal waves of the developing rabbit. J. Neurosci. 21:5158-5168.
Zhou, Z.J. 2001b. The function of the cholinergic system in the developing mammalian retina. Prog. Brain Res. 131:599-613.
Zhou, Z.J. and Fain, G.L. 1995. Neurotransmitter receptors of starburst amacrine cells in rabbit retinal slices. J. Neurosci. 15:5334-5345.
Zucker, C.L. and Dowling, J.E. 1987. Centrifugal fibres synapse on dopaminergic interplexiform cells in the teleost retina. Nature 330:166-168.